

The role of oceanic lithosphere in inter- and intra-volcano geochemical  
heterogeneity at Maui Nui, Hawaii

Amy M. Gaffney

A dissertation submitted in partial fulfillment  
of the requirements for the degree of

Doctor of Philosophy

University of Washington

2004

Program Authorized to Offer Degree: Earth and Space Sciences

UMI Number: 3131156

### INFORMATION TO USERS

The quality of this reproduction is dependent upon the quality of the copy submitted. Broken or indistinct print, colored or poor quality illustrations and photographs, print bleed-through, substandard margins, and improper alignment can adversely affect reproduction.

In the unlikely event that the author did not send a complete manuscript and there are missing pages, these will be noted. Also, if unauthorized copyright material had to be removed, a note will indicate the deletion.

**UMI**<sup>®</sup>

---

UMI Microform 3131156

Copyright 2004 by ProQuest Information and Learning Company.

All rights reserved. This microform edition is protected against unauthorized copying under Title 17, United States Code.

ProQuest Information and Learning Company  
300 North Zeeb Road  
P.O. Box 1346  
Ann Arbor, MI 48106-1346

University of Washington

Graduate School

This is to certify that I have examined this copy of a doctoral dissertation by

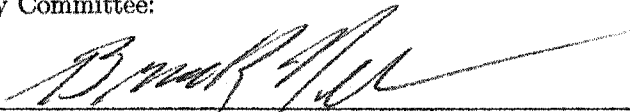
Amy M. Gaffney

and have found that it is complete and satisfactory in all respects,

and that any and all revisions required by the final

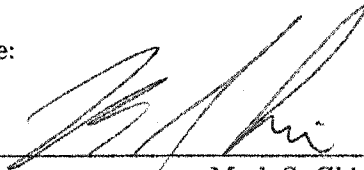
examining committee have been made.

Chair of Supervisory Committee:

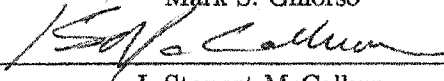


Bruce K. Nelson

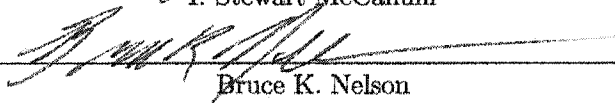
Reading Committee:



Mark S. Giorso



I. Stewart McCallum



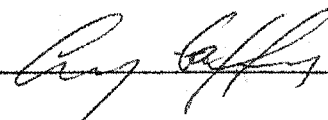
Bruce K. Nelson

Date:

June 3, 2004

In presenting this dissertation in partial fulfillment of the requirements for the Doctoral degree at the University of Washington, I agree that the Library shall make its copies freely available for inspection. I further agree that extensive copying of this dissertation is allowable only for scholarly purposes, consistent with "fair use" as prescribed in the U.S. Copyright Law. Requests for copying or reproduction of this dissertation may be referred to Bell and Howell Information and Learning, 300 North Zeeb Road, Ann Arbor, MI 48106-1346, to whom the author has granted "the right to reproduce and sell (a) copies of the manuscript in microform and/or (b) printed copies of the manuscript made from microform."

Signature



Date

June 4, 2002

University of Washington

Abstract

The role of oceanic lithosphere in inter- and intra-volcano geochemical heterogeneity  
at Maui Nui, Hawaii

Amy M. Gaffney

Chair of Supervisory Committee:  
Professor Bruce K. Nelson  
Earth and Space Sciences

The volcanoes of Maui Nui (West Molokai, East Molokai, Lanai, West Maui, Haleakala and Kahoolawe) record Hawaiian magmatism at  $\sim$ 1-2 Ma. These volcanoes nearly span the compositional range erupted from all the Hawaiian volcanoes over the past 5 My, and erupt lavas representing both the Kea and Koolau compositional endmembers of Hawaiian lavas. Using lavas from these volcanoes, we evaluate the role that oceanic lithosphere, both ancient recycled lithosphere in the Hawaiian plume and modern Pacific lithosphere, plays in the generation of geochemical variability on inter- and intra-volcano scales. We also present trace element models that explicitly address the petrologic complexities of melting eclogite (derived from ancient oceanic lithosphere) in the plume. Trace element, major element and isotope compositions of Lanai are consistent with the origin of these lavas in large degree ( $\sim$ 70%) melts of ancient upper oceanic crust (basalt + sediment) that mix with plume-derived Haleakala-type melts. Trace element and isotope compositions of West Maui and East Molokai are consistent with an origin in ancient depleted oceanic lithosphere that has been re-fertilized with moderate-degree melts (20-40%) of associated crustal gabbro. The physical mechanisms through which the oceanic lithospheric components melt and mix within the plume lead to the generation of isotopically homogeneous Kea-type lavas and isotopically heterogeneous Koolau-type lavas.

Stratigraphically-controlled sequences of late shield-building stage lavas from West Maui

volcano show age-dependent compositional variability distinct from that seen in shield-stage lavas from any other Hawaiian volcano. These distinctions are defined by  $^{206}\text{Pb}/^{204}\text{Pb}$ - $^{207}\text{Pb}/^{204}\text{Pb}$  variation as well as  $^{87}\text{Sr}/^{86}\text{Sr}$  correlation with  $^{206}\text{Pb}/^{204}\text{Pb}$ ,  $^{187}\text{Os}/^{188}\text{Os}$  and trace element compositions. The  $^{87}\text{Sr}/^{86}\text{Sr}$ - $^{206}\text{Pb}/^{204}\text{Pb}$  and  $^{87}\text{Sr}/^{86}\text{Sr}$ - $^{187}\text{Os}/^{188}\text{Os}$  variation in the deep lavas is orthogonal to the all-Hawaii variation, indicating that it is not the result of mixing between components normally sampled by Hawaiian shield-stage magmas. We compare our West Maui data to observed compositions of Pacific oceanic basaltic and gabbroic crust, and predicted compositions for 2 Ga basaltic and gabbroic oceanic crust. The observed fine-scale compositional variability in the stratigraphically deep West Maui lavas is consistent with 10-15% mixing of small degree (2%) partial melts of the Pacific gabbroic oceanic crust with plume-derived, Kea-type magmas.

## TABLE OF CONTENTS

<b>List of Figures</b>	<b>iii</b>
<b>List of Tables</b>	<b>v</b>
<b>Chapter 1: Geochemical constraints on the role of oceanic lithosphere in intra-volcano heterogeneity in West Maui, Hawaii</b>	<b>1</b>
1.1 Introduction . . . . .	1
1.2 Samples and Procedures . . . . .	3
1.3 Results . . . . .	5
1.4 Discussion . . . . .	10
1.5 Conclusions . . . . .	23
<b>Chapter 2: Oxygen-osmium isotopic compositions of West Maui lavas and the link to oceanic lithosphere</b>	<b>50</b>
2.1 Introduction . . . . .	50
2.2 Samples and Procedures . . . . .	51
2.3 Results . . . . .	53
2.4 Discussion . . . . .	54
2.5 Conclusions . . . . .	64
<b>Chapter 3: Melting in the Hawaiian plume at 1-2 Ma as recorded at Maui Nui: the role of eclogite, peridotite and source melting</b>	<b>75</b>
3.1 Introduction . . . . .	75
3.2 The Hawaiian endmembers, their compositions and sources - a review . . . . .	77
3.3 Data selection, normalization, filtering and assumptions . . . . .	78

3.4	Observations . . . . .	80
3.5	Geochemical evaluation of oceanic lithosphere in Maui Nui lavas . . . . .	84
3.6	Lanai source model . . . . .	87
3.7	West Maui/East Molokai source model . . . . .	91
3.8	Discussion of the source models . . . . .	93
3.9	Implications for structure and processes in the plume under Maui Nui . . . . .	97
3.10	Summary and relevance to the past 5 My of Hawaiian shield-stage magmatism	99
3.11	Conclusions . . . . .	101
	<b>Bibliography</b>	<b>136</b>
	<b>Appendix A: Sample locations</b>	<b>137</b>
	<b>Appendix B: Maui Nui data sources</b>	<b>141</b>



## LIST OF FIGURES

1.1	Map of Hawaii and West Maui . . . . .	25
1.2	Major element compositions of West Maui lavas . . . . .	26
1.3	Incompatible trace element compositions of West Maui lavas . . . . .	27
1.4	Compatible trace element compositions of West Maui lavas . . . . .	28
1.5	$^{87}\text{Sr}/^{86}\text{Sr}$ , $^{143}\text{Nd}/^{144}\text{Nd}$ and $^{176}\text{Hf}/^{177}\text{Hf}$ compositions of West Maui lavas . . . . .	29
1.6	$^{206}\text{Pb}/^{204}\text{Pb}$ , $^{207}\text{Pb}/^{204}\text{Pb}$ , and $^{208}\text{Pb}/^{204}\text{Pb}$ compositions of West Maui lavas . . . . .	30
1.7	$^{87}\text{Sr}/^{86}\text{Sr}$ - $^{206}\text{Pb}/^{204}\text{Pb}$ variation in West Maui lavas . . . . .	31
1.8	$^{176}\text{Hf}/^{177}\text{Hf}$ and $^{206}\text{Pb}/^{204}\text{Pb}$ stratigraphy for Papalaua Gulch and Mahinahina Well sections . . . . .	32
1.9	$^{87}\text{Sr}/^{86}\text{Sr}$ - $^{206}\text{Pb}/^{204}\text{Pb}$ mixing relationships in West Maui lavas . . . . .	33
1.10	$^{206}\text{Pb}/^{204}\text{Pb}$ - $^{176}\text{Hf}/^{177}\text{Hf}$ mixing relationships in West Maui lavas . . . . .	34
1.11	$^{87}\text{Sr}/^{86}\text{Sr}$ - trace element variation in West Maui lavas . . . . .	35
1.12	Modeled compositions of oceanic crustal gabbro melts . . . . .	36
1.13	MELTS models of gabbro crust assimilation . . . . .	37
2.1	$^{187}\text{Os}/^{188}\text{Os}$ compositions of West Maui lavas . . . . .	66
2.2	$\delta^{18}\text{O}$ compositions of West Maui lavas . . . . .	67
2.3	$^{187}\text{Os}/^{188}\text{Os}$ - $\delta^{18}\text{O}$ variation in Hawaiian and Icelandic lavas . . . . .	68
2.4	$^{187}\text{Os}/^{188}\text{Os}$ - $^{87}\text{Sr}/^{86}\text{Sr}$ variation in Hawaiian lavas and xenoliths . . . . .	69
2.5	$^{187}\text{Os}/^{188}\text{Os}$ and $\delta^{18}\text{O}$ compositions of mantle and crustal materials . . . . .	70
2.6	$^{187}\text{Os}/^{188}\text{Os}$ - $^{87}\text{Sr}/^{86}\text{Sr}$ mixing relationships in West Maui lavas . . . . .	71
2.7	Average $^{87}\text{Sr}/^{86}\text{Sr}$ , $^{143}\text{Nd}/^{144}\text{Nd}$ , $^{176}\text{Hf}/^{177}\text{Hf}$ and $^{206}\text{Pb}/^{204}\text{Pb}$ of Hawaiian shield-stage lavas . . . . .	72
2.8	$^{87}\text{Sr}/^{86}\text{Sr}$ - $^{206}\text{Pb}/^{204}\text{Pb}$ compositions of Hawaiian shield-stage lavas . . . . .	73

3.1	Map of Hawaii and ages of Maui Nui volcanoes . . . . .	103
3.2	$^{87}\text{Sr}/^{86}\text{Sr}$ - $^{143}\text{Nd}/^{144}\text{Nd}$ variation in Maui Nui lavas . . . . .	104
3.3	$^{143}\text{Nd}/^{144}\text{Nd}$ - $^{176}\text{Hf}/^{177}\text{Hf}$ variation in Maui Nui lavas . . . . .	105
3.4	$^{206}\text{Pb}/^{204}\text{Pb}$ , $^{207}\text{Pb}/^{204}\text{Pb}$ and $^{208}\text{Pb}/^{204}\text{Pb}$ isotope compositions of Maui Nui lavas . . . . .	106
3.5	$^{176}\text{Hf}/^{177}\text{Hf}$ - $^{206}\text{Pb}/^{204}\text{Pb}$ compositions of Maui Nui lavas . . . . .	107
3.6	Major element compositions of Maui Nui lavas . . . . .	108
3.7	Average $^{87}\text{Sr}/^{86}\text{Sr}$ -major element compositions of Maui Nui lavas . . . . .	109
3.8	$\text{TiO}_2$ - $^{206}\text{Pb}/^{204}\text{Pb}$ and $\text{SiO}_2$ - $^{206}\text{Pb}/^{204}\text{Pb}$ variation in Maui Nui lavas . . . . .	110
3.9	Rare earth element compositions of Maui Nui lavas . . . . .	111
3.10	$\text{La}/\text{Nb}$ - $^{87}\text{Sr}/^{86}\text{Sr}$ compositions of Maui Nui lavas . . . . .	112
3.11	Predicted $\text{Sm}/\text{Yb}$ vs. $F$ for MORB melting . . . . .	113
3.12	$\text{Sm}/\text{Yb}$ vs. $^{87}\text{Sr}/^{86}\text{Sr}$ in Maui Nui lavas . . . . .	114
3.13	$\text{MgO}-\text{TiO}_2$ constraints on mixing between eclogite melts and Haleakala lavas . . . . .	115
3.14	$\text{Hf}/\text{Zr}$ - $\text{Sm}/\text{Yb}$ variation in Maui Nui lavas . . . . .	116
3.15	$\text{Hf}/\text{Nb}$ - $\text{Hf}/\text{Zr}$ variation in Maui Nui lavas . . . . .	117

## LIST OF TABLES

1.1	Major and trace element compositions of West Maui lavas . . . . .	38
1.2	Sr, Nd and Hf isotope compositions of West Maui lavas . . . . .	43
1.3	Pb isotope compositions of West Maui lavas . . . . .	46
1.4	Calculated compositions of aged oceanic lithosphere . . . . .	49
2.1	Oxygen and osmium isotope compositions of West Maui lavas . . . . .	74
3.1	Pearson's correlation coefficients for Maui Nui lavas . . . . .	118
3.2	Modeled trace element compositions for oceanic lithosphere components . . .	119
3.3	Peridotite partition coefficients used in modeling . . . . .	120
3.4	Eclogite partition coefficients used in modeling . . . . .	121
A.1	West Maui sample locations . . . . .	138

## ACKNOWLEDGMENTS

Glenn Bauer provided the Mahinahina Well samples and logistical information, and David Sherrod was a collaborator in field efforts on West Maui. Janne Blichert-Toft, Laurie Reisberg and John Eiler graciously hosted me in their labs, where I did many of the isotope analyses. Jerry Hinn and Philippe Télouk always kept the mass spectrometers running smoothly. J. Bryce, A. Pietruszka and H.-J. Yang gave helpful and constructive journal reviews for Chapter 1, "Geochemical constraints on the role of oceanic lithosphere in intra-volcano heterogeneity in West Maui, Hawaii", which currently is in press with *Journal of Petrology*. Co-authors for this paper are Bruce K. Nelson and Janne Blichert-Toft. This work was supported by a Geological Society of America Harold T. Stearns grant, a DOSECC Internship grant and UW Graduate Research grants.

## Chapter 1

**GEOCHEMICAL CONSTRAINTS ON THE ROLE OF OCEANIC  
LITHOSPHERE IN INTRA-VOLCANO HETEROGENEITY IN WEST  
MAUI, HAWAII****1.1 Introduction**

Investigations of the role of oceanic lithosphere in the geochemistry of Hawaiian magma sources has generated two main families of hypotheses. One invokes ancient oceanic lithosphere that has been subducted, stored in the mantle for some length of time and recycled into the plume source where it contributes to compositional variation in the plume-generated lavas [e.g., Hauri, 1996a; Lassiter and Hauri, 1998; Blichert-Toft et al., 1999]. Alternatively, plume-generated magmas acquire geochemical characteristics of oceanic lithosphere by interacting with or assimilating it as they rise to the surface [e.g., Chen and Frey, 1985; Eiler et al., 1996]. Singly or together, these processes may contribute to the range of compositional variability expressed through the two primary compositional endmembers of Hawaiian shield-stage magmatism: the relatively enriched Koolau component and the relatively depleted Kea component.

Kea-type lavas show the most depleted Sr and Nd isotopic compositions of all Hawaiian shield-stage lavas, and thus the Kea source material has been interpreted as having an association with or derivation from ambient depleted mantle or oceanic lithosphere. To date, the Kea component has been well-described in late shield-stage lavas at only one volcano, Mauna Kea, where it has been thoroughly characterized through multi-disciplinary work on the Hawaii Scientific Drilling Project (HSDP) cores [e.g., Stolper et al., 1996; Blichert-Toft and Albarède, 1999; Abouchami et al., 2000; DePaolo et al., 2001; Blichert-Toft et al., 2003; Eisele et al., 2003; Huang and Frey, 2003]. From this characterization,

broad conclusions have been drawn about the compositional structure of the Hawaiian plume and the generation of the compositional variations within the plume feeding Mauna Kea. Currently-active Kilauea also has Kea-type compositions, and its historical summit lavas show rapid compositional changes [Pietruszka and Garcia, 1999]. Kilauea lavas provide a point of contrast with West Maui and Mauna Kea, as they sample a window of time earlier in the shield-building stage than that sampled at West Maui or Mauna Kea. Loihi, Mauna Loa and Koolau are not dominated by Kea-type compositions as are Mauna Kea, Kilauea and West Maui; however, these volcanoes do show, over specific time intervals, time-dependent shifts towards Kea-type compositions [Staudigel et al., 1984; Garcia et al., 1993, 1995; Kurz et al., 1995; Tanaka et al., 2002]. To date, the best characterizations of the Kea component over a large time window (i.e., over a significant stratigraphic section) are from the relatively young volcanoes Mauna Kea and Kilauea; there is so far no detailed characterization of the Kea component sampled over a comparably large time window at an older volcano.

Identification and characterization of oceanic lithosphere associations or other fine-scale compositional variations within Kea-type lavas require high-density sampling as well as stratigraphic (i.e., time) control. West Maui volcano samples Kea-type lavas throughout its sampled history, but there exist only few published geochemical data for this volcano [Macdonald and Katsura, 1964; Diller, 1982; Stille et al., 1986; Tatsumoto et al., 1987]. The goals of this study thus are to (1) characterize geochemically the compositional breadth of lavas sampled by a Kea-type volcano at 1.5 Ma, (2) compare characteristics of the Kea component as sampled at West Maui to that sampled at the younger volcanoes Mauna Kea and Kilauea, as well as Mauna Loa, Koolau and Loihi, (3) evaluate the oceanic lithosphere hypotheses as the probable cause of fine-scale compositional variations observed in West Maui lavas, and (4) determine the relationship, if any, of this variation to the Kea plume source.

## 1.2 Samples and Procedures

West Maui is one of six volcanoes which form Maui Nui, a bathymetric high comprising coalescing volcanoes (Haleakala, Kahoolawe, Lanai, West Maui, East and West Molokai) with a total area similar to that of the Big Island of Hawaii (Fig. 1.1). The K-Ar ages for shield-building activity in the Maui Nui volcanoes range from  $1.84 \pm 0.07$  Ma at West Molokai to  $0.83 \pm 0.17$  Ma at Haleakala [Naughton et al., 1980]. Most exposed lavas at West Maui volcano are from the shield-building stage, and in places are capped by a thin veneer of lavas transitional between the shield-stage tholeiitic (Wailuku Basalts) and post-shield alkalic (Honolua Volcanics) stages [Stearns and Macdonald, 1942; Diller, 1982]. There are several post-shield stage alkalic flows, and four mapped occurrences of rejuvenated stage lavas (Lahaina Volcanics). Published K-Ar ages are few and range from 1.27 to  $1.97 \pm 0.96$  Ma for the shield stage lavas (including transitional lavas), 1.15 to  $1.50 \pm 0.13$  Ma for post-shield lavas, and  $0.385 \pm 0.012$ ,  $0.388 \pm 0.009$ ,  $0.584 \pm 0.010$  and  $0.610 \pm 0.012$  Ma for the rejuvenated lavas [McDougall, 1964; Naughton et al., 1980; Tagami et al., 2003].

The sample set for this study comprises in part two stratigraphically-controlled sequences of lavas, the Papalaua Gulch section (260 m thick) and the Mahinahina Well section (345 m thick), that sample late shield-building stage West Maui lavas (Fig. 1.1). The shorter Papalaua Gulch section is more proximal to the caldera margin and samples a smaller window of time than the more distal Mahinahina Well section. In order to more completely characterize the compositional breadth of late shield-stage West Maui lavas, we also collected samples from a wide geographic distribution around the volcano. Based upon sample location, distance from the caldera rim and collection depth within the volcanic edifice, we have categorized all samples as either 'deep' or 'shallow'. These categories refer to the depths of samples within the volcanic edifice, relative to one another. Since these categories also have geochemical significance, we will use this terminology in the subsequent geochemical discussion. Figure 1.1 shows sampling locations for both deep and shallow samples. See Appendix A for detail on sample categorization procedure.

Samples are dark to light gray, fine-grained basalts. Olivine phenocrysts are commonly present and a few samples also contain plagioclase phenocrysts or microphenocrysts.

Clinopyroxene phenocrysts are only very rarely present. Some samples contain iddingsite-rimmed olivine phenocrysts. The samples from the Mahinahina Well cuttings show a higher degree of oxidation and Fe-staining than the surface-collected samples. Lithologically, the splits of cuttings are homogeneous, indicating little mixing between layers during drilling. For splits which showed some heterogeneity, we only used pieces that matched the dominant lithology of the split. For all isotopic analyses, we hand-picked 2-5 mm sample chips which were free of visible alteration.

Major (X-ray fluorescence; XRF) and trace (inductively-coupled plasma mass spectrometry; ICP-MS) element analyses were completed at the Washington State University Geo-Analytical Laboratory, according to procedures described by Johnson et al. [1999] (Table 1.1). Two-sigma analytical precision, based upon repeat analyses of the BCR-P standard and consistent with repeat analyses of samples and our UWBCR-1 internal standard, is as follows: SiO<sub>2</sub>-0.11%, Al<sub>2</sub>O<sub>3</sub>-0.29%, TiO<sub>2</sub>-0.79%, FeO-0.31%, MnO-1.09%, CaO-0.57%, MgO-2.8%, K<sub>2</sub>O-0.91%, Na<sub>2</sub>O-3.0%, P<sub>2</sub>O<sub>5</sub>-0.53%, Ni-11.8%, Cr-7.2%, Sc-15.4%, Ga-8.7%, Zn-3.2%, La-3.7%, Ce-0.2%, Pr-1.9%, Nd-3.5%, Sm-4.3%, Eu-4.7%, Gd-2.4%, Tb-1.7%, Dy-2.8%, Ho-2.8%, Er-3.0%, Tm-3.6%, Yb-1.8%, Lu-3.8%, Ba-3.9%, Th-4.9%, Nb-4.4%, Y-1.5%, Hf-3.0%, Ta-4.9%, U-7.3%, Pb-6.4%, Rb-2.9%, Cs-6.3%.

Pb, Sr and Nd isotope analyses were all made from the same initial sample dissolution. Prior to dissolution, we leached sample powders for 45 minutes in 6N HCl, using approximately 1 ml HCl per 100 mg sample. During leaching, we placed samples on a 100° C hotplate for 20 minutes, in an ultrasonic bath for 10 minutes, on the hotplate again for 10 minutes and in the ultrasonic bath for 5 more minutes. We rinsed samples in sub-boiling distilled H<sub>2</sub>O prior to dissolution. We completed all sample preparation for Sr, Nd and Pb isotope analysis at the University of Washington (UW), Seattle, according to procedures described by Nelson [1995] (Tables 1.3 and 1.2). We prepared Hf separations both at the Ecole Normale Supérieure in Lyon (ENSL), France, and at UW following the procedures described by Blichert-Toft et al. [1997]. TIMS (thermal ionization mass spectrometer) isotope analyses of Sr and Nd were carried out on the VG Sector at UW. MC-ICP-MS (multi-collector ICP-MS) isotope analyses of Pb and Hf were done on the VG Plasma 54 at ENSL [Blichert-Toft et al., 1997; White et al., 2000]. Strontium NBS 987 standards run over



the course of the West Maui analyses ( $n = 33$  over 2 years) have an average  $^{87}\text{Sr}/^{86}\text{Sr} = 0.710294 \pm 0.000019$  (2-sigma). Average composition of Nd La Jolla standards run during this same time period ( $n = 25$ ) is  $^{143}\text{Nd}/^{144}\text{Nd} = 0.511845 \pm 0.000020$  (2-sigma). This precision for the standard is similar to that obtained for multiple aliquots ( $n = 10$ ) and analyses of our internal UWBCR-1 basalt powder ( $^{143}\text{Nd}/^{144}\text{Nd} = 0.512617 \pm 0.000024$ , 2-sigma). Two-sigma external reproducibility for Pb isotopic compositions is determined from repeat analyses of the 98B internal standard ( $n = 28$  over two analytical sessions) and is 0.043%, 0.048% and 0.056% for  $^{206}\text{Pb}/^{204}\text{Pb}$ ,  $^{207}\text{Pb}/^{204}\text{Pb}$  and  $^{208}\text{Pb}/^{204}\text{Pb}$  respectively. The JMC 475 Hf standard gave  $^{176}\text{Hf}/^{177}\text{Hf} = 0.282160 \pm 0.000010$  (2-sigma) and was measured between every second or third sample to verify machine performance. Precision for  $^{176}\text{Hf}/^{177}\text{Hf}$  is determined from replicate aliquots ( $n = 10$ ) and analyses of our UWBCR-1 internal standard powder ( $^{176}\text{Hf}/^{177}\text{Hf} = 0.282865 \pm 0.000016$ ). Although our standard powder has been well-homogenized, the quoted precision represents a maximum value, given that it incorporates all procedural sources of error and any sample heterogeneity that may exist.

### 1.3 Results

Most samples have loss on ignition (LOI) < 0.4%, indicating minimal alteration. For most samples (21 of 27)  $\text{K}_2\text{O}/\text{P}_2\text{O}_5 > 1$ , likewise indicating that the samples have not undergone significant post-cooling alteration, which would mobilize K relative to P. All but one of the samples with  $\text{K}_2\text{O}/\text{P}_2\text{O}_5 < 1$  are shallow samples. The samples that exhibit K loss also show loss of the mobile incompatible elements U and Rb relative to immobile incompatible elements such as Nb, Th and Zr. Cerium, which is mobile when oxidized to  $\text{Ce}^{+4}$  during alteration, is well-correlated with immobile incompatible elements in all samples with one exception (LT 22), indicating that alteration has only affected some elements in some samples. Of the samples that exhibit K, U or Rb loss, none has anomalous isotopic or major element compositions, with the exception of two samples with anomalously low  $\text{SiO}_2$  (LT27 and WA13). None of the indicators of element mobility ( $\text{K}_2\text{O}/\text{P}_2\text{O}_5$ , K, U, Rb) correlates with  $^{87}\text{Sr}/^{86}\text{Sr}$  or  $^{206}\text{Pb}/^{204}\text{Pb}$ , compositions that are potentially susceptible to alteration.

Therefore, we include all samples in subsequent geochemical discussion.

### 1.3.1 Major elements

The West Maui shield-building stage samples are all tholeiitic basalts with 45-51 wt. %  $\text{SiO}_2$ , and 6-21 wt. %  $\text{MgO}$  (Fig. 1.2). We also sampled three transitional-stage lavas (between tholeiitic shield-stage and alkalic post-shield stage), identified through mapping and description by Diller [1982], and one each of post-shield alkalic and rejuvenated stage lavas. Data for these samples are included in the tables, but not in any figures or discussion. The major element variability for the deep and shallow groups have only partially overlapping fields. The systematics of the sample suite as a whole correspond for the most part to expected differentiation trends, and are analogous to well-documented differentiation trends at Kilauea [Garcia et al., 2003]. The two shallow West Maui samples (LT27 and WA13) with anomalously low  $\text{SiO}_2$  are also two of the most altered samples ( $\text{K}_2\text{O}/\text{P}_2\text{O}_5 = 0.72$  and  $0.47$ , respectively). It appears that, in general, the shallow samples either tend to be more evolved than the deep samples, or to have undergone a higher degree of olivine accumulation (e.g.,  $\text{MgO} > 15$  wt.%). The major element compositions of these lavas are broadly similar to tholeiites of the extensively-studied Kea-type volcanoes Mauna Kea [Yang et al., 1994; Rhodes, 1996] and Kilauea [Chen et al., 1996; Garcia et al., 1996, 2000]. Notably, the bend in  $\text{Al}_2\text{O}_3$ ,  $\text{CaO}$ ,  $\text{CaO}/\text{Al}_2\text{O}_3$ , and  $\text{TiO}_2$  vs.  $\text{MgO}$  variation for West Maui (Fig. 1.2) occurs at similar whole rock compositions in the Kilauea lavas, suggesting common differentiation processes, of olivine crystallization followed by clinopyroxene and plagioclase.

### 1.3.2 Trace elements

To account for variable amounts of olivine accumulation or fractionation, we adjusted all sample compositions to 13 wt.%  $\text{MgO}$  by either incrementally adding equilibrium olivine or by removing  $\text{Fo}_{87}$  olivine until the sample composition reached 13 wt.%  $\text{MgO}$ , and adjusted incompatible trace element compositions accordingly (assuming  $D_x^{\text{ol/liq}} = 0$ ). Because no olivine composition data exist for these samples, we chose  $\text{Fo}_{87}$  olivine as an equilibrium composition for our assumed parental magma. Although primitive Hawaiian magmas with

MgO up to 16 wt.% have been documented at other volcanoes (Haleakala- Chen et al. [1992]; Kilauea- Clague et al. [1995]), we have no samples in our West Maui collection in the 14-16 wt.% MgO range, and consequently we have chosen not to call upon a primitive composition that we did not observe. Samples with MgO < 7.0 wt.% have likely begun to fractionate clinopyroxene as well as olivine [Helz and Wright, 1992; Montierth et al., 1995], and therefore we exclude these samples from plots and discussion involving corrected trace elements.

Both the deep and shallow groups of samples show a similar absolute range in the rare earth element (REE) slope La/Yb, although the deep group generally has lower [La] (Fig. 1.3). Both groups also show the same positive correlation between La/Yb and [La]. This REE compositional variation is similar to, but encompasses a narrower range than, the variation observed in Mauna Kea tholeiites [Albarède, 1996; Feigenson et al., 1996; Yang et al., 1996; Huang and Frey, 2003]. Overall REE patterns are distinct between the deep and shallow groups of West Maui lavas. The samples within the shallow group have similar overall REE patterns, but the REE concentrations vary among the samples (Fig. 1.3). This is a common pattern of intra-volcano variation for Hawaiian tholeiites [e.g., Tilling et al., 1987; Frey et al., 1991]. These observations contrast with those for the deep samples as a group, which show less variability in H(heavy)REE compared to L(light)REE concentrations (Fig. 1.3); this variation pattern is similar to that observed in the historical Kilauea summit lavas [Pietruszka and Garcia, 1999]. The shallow West Maui samples generally have a steeper HREE slope (higher Sm/Yb) than the deep samples, for a similar range in [Sm]. As a group, the deep samples have lower average REE concentrations than the shallow samples.

Variation in ratios of incompatible trace elements, particularly HFSE (high field strength element)/HFSE and LILE (large ion lithophile element)/HFSE, such as, respectively, Nb/Zr and La/Nb, have only partially overlapping ranges for the deep and shallow groups (Fig. 1.3). This indicates variation in either the source compositions or the range of source melting sampled by the two families. The deep samples extend to lower [Nb] and Nb/Zr and to higher Sr/Nb than do the shallow samples (Fig. 1.3).

Uncorrected concentrations of the compatible trace elements Ni and Cr are well-correlated with MgO, and the Ni, Cr-MgO correlations define continuous trends that encompass both

the deep and shallow groups of samples (Fig. 1.4). Scandium (uncorrected)-MgO variation defines two distinct groups: a strong correlation that extends to high MgO and a weaker correlation that includes the lower-MgO samples and extends to the highest [Sc]. We take the first group to be the result of olivine accumulation. The poorly-defined bend at  $\sim 7.5$  wt.% MgO in the second group may reflect the onset of clinopyroxene crystallization. In Hawaiian tholeiites, initiation of clinopyroxene crystallization at 7-7.5 wt.% MgO has been observed experimentally as well as in nature [Helz and Wright, 1992; Montierth et al., 1995].

### 1.3.3 Sr, Nd, Hf and Pb isotopes

Comparison of the  $^{87}\text{Sr}/^{86}\text{Sr}$ - $^{143}\text{Nd}/^{144}\text{Nd}$ - $^{176}\text{Hf}/^{177}\text{Hf}$  variation in the West Maui samples to Hawaiian compositions as a whole shows that these lavas, along with lavas from the Kea-dominated volcano Mauna Kea, and in agreement with the few previously published West Maui data [Stille et al., 1986; Tatsumoto et al., 1987], have some of the most depleted isotopic compositions of all the Hawaiian islands (Fig. 1.5). In Sr-Nd-Hf isotope space, there is little overlap between the fields defined by the deep and shallow groups. The deep group has the more depleted compositions, and in  $^{87}\text{Sr}/^{86}\text{Sr}$ - $^{143}\text{Nd}/^{144}\text{Nd}$  space is displaced slightly towards less radiogenic  $^{87}\text{Sr}/^{86}\text{Sr}$ , and in the direction of Pacific mid-ocean ridge basalt (MORB), relative to typical Kea-type compositions (as defined by Mauna Kea and Kilauea). There is small overlap between the deep West Maui lavas and Mauna Kea and Kilauea (Fig. 1.5). The  $^{143}\text{Nd}/^{144}\text{Nd}$ - $^{176}\text{Hf}/^{177}\text{Hf}$  variation for these samples shows a similar distinction between the deep and shallow groups, with the deep samples being more depleted than the shallow samples (Fig. 1.5). There is also much more scatter in the compositions of the deep samples - they show nearly twice the variability in  $^{143}\text{Nd}/^{144}\text{Nd}$  as do the shallow samples. This contrasts with major and trace element compositions for the deep samples which tend to be less variable than in the shallow samples. The West Maui samples as a group fall slightly below the ocean island basalt (OIB) array, as has been observed for Mauna Kea but not Kilauea [Blichert-Toft et al., 1999]. The West Maui and Mauna Kea samples fall farther below the OIB array than any other measured Hawaiian shield-stage lava.

The sample suite as a whole shows variation in  $^{207}\text{Pb}/^{204}\text{Pb}$  of only 4 to 5 times analytical error, and there is no distinction in the  $^{206}\text{Pb}/^{204}\text{Pb}$ - $^{207}\text{Pb}/^{204}\text{Pb}$  trend between the deep and shallow groups (Fig. 1.6).  $^{208}\text{Pb}/^{204}\text{Pb}$  is strongly correlated with  $^{206}\text{Pb}/^{204}\text{Pb}$  in the set of samples as a whole, and the deep vs. shallow samples show separate correlations (Fig. 1.6). The shallow and deep samples were analyzed at ENSL in random order and over the same periods of time, thus the contrast in Pb isotope ratios between the two sample groups is not due to a shift in instrument performance between multiple analytical sessions. The shallow samples have a slightly lower degree of correlation than the deep samples, and also show slightly lower  $^{208}\text{Pb}/^{204}\text{Pb}$  for the same range of  $^{206}\text{Pb}/^{204}\text{Pb}$  exhibited by the deep samples. High-precision Pb isotope studies of Mauna Kea HSDP-1 lavas (680 m thick; Abouchami et al. [2000]) also identify two compositional groups, although these groups appear to lack any correlation with stratigraphy. Interestingly, the two groups identified in Mauna Kea lavas are distinct both in  $^{206}\text{Pb}/^{204}\text{Pb}$ - $^{207}\text{Pb}/^{204}\text{Pb}$  and  $^{206}\text{Pb}/^{204}\text{Pb}$ - $^{208}\text{Pb}/^{204}\text{Pb}$  space, whereas the two West Maui groups show no distinction in  $^{206}\text{Pb}/^{204}\text{Pb}$ - $^{207}\text{Pb}/^{204}\text{Pb}$  space. Eisele et al. [2003] used high-precision Pb isotope compositions, specifically  $^{206}\text{Pb}/^{204}\text{Pb}$ - $^{208}\text{Pb}/^{204}\text{Pb}$  variation, to define three distinct compositional groups in the HSDP-2 lavas (2790 m thick). All of our West Maui samples, as well as the HSDP-1 Mauna Kea samples, correspond to the HSDP-2 array with the lowest  $^{208}\text{Pb}/^{204}\text{Pb}$ .

The  $^{206}\text{Pb}/^{204}\text{Pb}$ - $^{87}\text{Sr}/^{86}\text{Sr}$  variation in the West Maui lavas shows a distinction between the deep and shallow lavas (Fig. 1.7). The deeper samples show a positive correlation that trends to less radiogenic  $^{206}\text{Pb}/^{204}\text{Pb}$  and  $^{87}\text{Sr}/^{86}\text{Sr}$  than shallow West Maui or Mauna Kea. Discussion of this trend is in the following section. This contrasts with the  $^{208}\text{Pb}/^{204}\text{Pb}$ - $^{87}\text{Sr}/^{86}\text{Sr}$  variation (not shown), where the shallow samples display a better correlation than the deep samples.

The  $^{176}\text{Hf}/^{177}\text{Hf}$  and  $^{206}\text{Pb}/^{204}\text{Pb}$  stratigraphy for the Papalaua Gulch and Mahinahina Well sections shows minimal correlation between the two isotope systems, or of either isotope ratio with depth (Fig. 1.8). The average  $^{206}\text{Pb}/^{204}\text{Pb}$  composition and standard deviation for the two sections is nearly identical. The average  $^{176}\text{Hf}/^{177}\text{Hf}$  of the deeper section (0.28312) is slightly more radiogenic than that of the shallower section (0.28311), and the range of values in these two sections show the same standard deviation. Although the av-

erage  $^{176}\text{Hf}/^{177}\text{Hf}$  of these two sections are within error of each other, they coincide in the expected sense to different average  $^{143}\text{Nd}/^{144}\text{Nd}$  compositions (0.51299 and 0.51301 for the deep and shallow sections, respectively), and therefore we believe that the  $^{176}\text{Hf}/^{177}\text{Hf}$  compositional difference between the two sections is real. Blichert-Toft et al. [1999] described the all-Hawaii  $^{176}\text{Hf}/^{177}\text{Hf}$ - $^{206}\text{Pb}/^{204}\text{Pb}$  variation as a mixing hyperbola between the Kea endmember with relatively radiogenic  $^{176}\text{Hf}/^{177}\text{Hf}$  and  $^{206}\text{Pb}/^{204}\text{Pb}$  and the Koolau endmember with relatively unradiogenic  $^{176}\text{Hf}/^{177}\text{Hf}$  and  $^{206}\text{Pb}/^{204}\text{Pb}$ . Not unexpectedly, our West Maui data fall on the upper limb of this hyperbola, near Mauna Kea.

#### 1.4 Discussion

At West Maui, we observe fine-scale geochemical variation defined by  $^{206}\text{Pb}/^{204}\text{Pb}$ - $^{87}\text{Sr}/^{86}\text{Sr}$ ,  $^{206}\text{Pb}/^{204}\text{Pb}$ - $^{208}\text{Pb}/^{204}\text{Pb}$  and  $^{87}\text{Sr}/^{86}\text{Sr}$ -trace element compositions. These correlations are present at West Maui only in lavas that erupted over a particular time interval. Studies of Pb isotope composition have identified fine-scale Pb isotope variability within other Kea-dominated volcanoes (Kilauea-Pietruszka and Garcia [1999]; Mauna Kea-Abouchami et al. [2000]; Eisele et al. [2003]), but the particular  $^{87}\text{Sr}/^{86}\text{Sr}$ -correlated trends we identify at West Maui have not been observed in shield-stage lavas of any other Hawaiian volcano. The  $^{206}\text{Pb}/^{204}\text{Pb}$ - $^{87}\text{Sr}/^{86}\text{Sr}$  trend in the deep West Maui lavas is oblique to the trend of pure mixing between Kea and Koolau components as they are typically sampled by Hawaiian shield-stage magmas. It is not uncommon to observe Hawaiian shield-stage lava compositions that deviate from the pure Kea-Koolau mixing trend, and in fact it is the rule rather than the exception that at least three endmember compositions are required to describe compositional variations within one volcano or across the whole chain. However, the specific signal that we have identified in the  $^{87}\text{Sr}/^{86}\text{Sr}$ - $^{206}\text{Pb}/^{204}\text{Pb}$ -trace element compositions is unique to this volcano both in its compositional range and in its stratigraphic dependency.

There exists a long history of associating Hawaiian magma source regions with oceanic lithosphere [e.g., Hofmann and White, 1982; Chen and Frey, 1985; Eiler et al., 1996; Hauri, 1996a; Lassiter and Hauri, 1998], and several studies associate oceanic lithosphere with both the Kea and Koolau endmembers. The Sr-Nd-Pb-O isotopic compositions of Kea-type mag-

mas have supported hypotheses for the origin of the Kea component in small-degree melts of ambient depleted MORB-source mantle [Chen and Frey, 1985] or hydrothermally-altered Pacific oceanic crust [Eiler et al., 1996] that mixes with plume-derived magmas. Blichert-Toft et al. [1999] used Pb-Hf isotopic correlations to argue against Pacific lithosphere as the source of the Kea component, and Lassiter and Hauri [1998] used O-Os isotope correlations to argue that the Kea source is the gabbro + harzburgite/dunite segment of ancient (>1 Ga) oceanic crust that has been subducted and recycled into the Hawaiian plume. Koolau-type magmas have been interpreted, on the basis of Hf-Pb isotopic correlation [Blichert-Toft et al., 1999] and O-Os compositions [Lassiter and Hauri, 1998], to have their source in recycled basaltic oceanic crust  $\pm$  pelagic sediment in the Hawaiian plume.

While mixing between the Kea and Koolau endmembers serves as a general framework to explain inter-volcano isotopic and elemental variability among Hawaiian volcanoes on the scale of the entire archipelago, it does not account for the fine-scale variability we observe in West Maui volcano. In the following, we examine the origin of the fine-scale, intra-volcano chemical trends in West Maui, and evaluate whether we can relate these variations to the hypotheses for involvement of oceanic crust discussed previously. Specifically, we compare the expected compositional variation for ambient vs. ancient upper (hydrothermally-altered basaltic) and lower (gabbroic) oceanic crust, and model the contributions of these compositional reservoirs to Kea-type lavas. In doing this, we evaluate whether the source of the fine-scale, intra-volcano West Maui variation is inherent to the Kea source or instead represents a distinct process or source that operates or exists independently of the origin or identity of the Kea source. Finally, we seek to identify similar trends in other volcanoes, and determine whether processes that we recognize at West Maui operate at other Hawaiian volcanoes as well.

#### *1.4.1 Sr-Pb-Hf isotope variation*

The  $^{206}\text{Pb}/^{204}\text{Pb}$ - $^{87}\text{Sr}/^{86}\text{Sr}$  variation observed in the shallow West Maui lavas is similar to that observed in shield-stage lavas in other Kea-dominated volcanoes [e.g., Anders and Nelson, 1996; Lassiter et al., 1996; Pietruszka and Garcia, 1999]. However, the deep lavas

are unique among Kea-type volcanoes in that they define a positive  $^{206}\text{Pb}/^{204}\text{Pb}$ - $^{87}\text{Sr}/^{86}\text{Sr}$  trend that extends to less radiogenic  $^{87}\text{Sr}/^{86}\text{Sr}$  than observed in shield-stage lavas from any other Kea-type volcano (Fig. 1.9). As mentioned above, this variation is oblique to the overall all-Hawaii shield-stage trend, and hence cannot be the result of mixing between Hawaiian plume components as they are represented at other volcanoes.

The two possibilities that we explore are contributions of very small-degree partial melts of ambient Pacific lithosphere ( $\sim 110$  Ma) or within-plume melts of ancient ( $\sim 2$  Ga) oceanic crust that was hydrothermally altered at a mid-ocean ridge, subducted, stored in the mantle, and recycled into the Hawaiian plume. On a global scale, the details of subduction zone processes and their effect on the chemical budget of the subducting slab are poorly quantified, and potentially can have highly variable effects [Stracke et al., 2003]. For this reason, we have chosen to make no assumptions about subduction zone processing and instead focus on the first-order chemical variations we would expect in aged oceanic crust, based on the range of available observations and data sets from the literature.

Different lithologic layers in the oceanic lithosphere develop distinct radiogenic isotope signals over time, and thus we specifically consider two different segments of oceanic crust: the hydrothermally-altered basaltic upper crust and the gabbroic cumulates in the lower crust. These, in combination with other lithologies (pelagic sediment + basalt; gabbro + depleted lithosphere), have been used to explain the genesis of Kea and Koolau compositional endmembers [Lassiter and Hauri, 1998; Blichert-Toft et al., 1999]. In our models, we investigate whether altered basalt and gabbro, independently or combined, can explain the fine-scale compositional variation distinct from Kea-Koolau mixing that we observe within just one Kea-type volcano.

For the 110 Ma Pacific upper oceanic crust endmember, we use  $^{87}\text{Sr}/^{86}\text{Sr}$  and  $^{206}\text{Pb}/^{204}\text{Pb}$  measured for upper oceanic crust from ODP site 843 [King et al., 1993], located 300 km from Maui. For the 110 Ma gabbroic endmember, we use  $^{87}\text{Sr}/^{86}\text{Sr}$  and  $^{206}\text{Pb}/^{204}\text{Pb}$  of gabbroic xenoliths from Hualalai volcano, interpreted to be Pacific oceanic crust, measured by Lassiter and Hauri [1998]. We use [Sr] and [Pb] measured in oceanic crust drill cores [Staudigel et al., 1995; Hart et al., 1999]. There currently exist no  $^{176}\text{Hf}/^{177}\text{Hf}$  measurements for oceanic crust of the appropriate age, so we calculated a possible range of compositions



based upon the  $^{176}\text{Hf}/^{177}\text{Hf}$  composition of modern East Pacific Rise MORB [Chauvel and Blichert-Toft, 2001]. We calculated the  $^{176}\text{Hf}/^{177}\text{Hf}$  composition of this depleted mantle MORB-source reservoir at 110 Ma, and then forward-modeled the  $^{176}\text{Hf}/^{177}\text{Hf}$  composition of the basaltic and gabbroic portions of oceanic crust generated from this depleted mantle reservoir, based upon Lu/Hf measured in oceanic crust drill-cores [Staudigel et al., 1995; Hart et al., 1999]. For the 2 Ga endmembers, we calculated the  $^{87}\text{Sr}/^{86}\text{Sr}$ ,  $^{206}\text{Pb}/^{204}\text{Pb}$  and  $^{176}\text{Hf}/^{177}\text{Hf}$  of the depleted mantle MORB-source reservoir at 2 Ga, again based upon modern compositions of East Pacific Ridge MORB [Chauvel and Blichert-Toft, 2001], and then forward-modeled the composition of basaltic and gabbroic crust derived from this reservoir at 2 Ga, in the same way as we did for the  $^{176}\text{Hf}/^{177}\text{Hf}$  composition of the 110 Ma gabbro crust. For calculating the elemental concentrations in the 2% gabbro melt, we use a gabbro mode of 20% orthopyroxene, 20% clinopyroxene, 20% plagioclase and 40% olivine, and partition coefficients from Hauri and Hart [1995] and McKenzie and O'Nions [1991]. These results are presented in Table 1.4.

Of the modeled 2 Ga source components, hydrothermally-altered upper oceanic crust has radiogenic  $^{87}\text{Sr}/^{86}\text{Sr}$  and  $^{206}\text{Pb}/^{204}\text{Pb}$  compositions, whereas gabbroic crust evolves to unradiogenic  $^{87}\text{Sr}/^{86}\text{Sr}$  and  $^{206}\text{Pb}/^{204}\text{Pb}$  compositions (Fig. 1.9). Neither of these components alone lies on a trajectory of mixing with the shallow lavas that could result in the observed variability in the deep samples. However, mixing between a melt from an approximately 25:75 upper oceanic crust:gabbro solid-solid mixture and plume-derived Kea-type magmas would reproduce the range of compositions in the deep lavas.

Alternatively, we consider the composition of ambient Pacific oceanic crust. Isotopic compositions of upper oceanic crust from the ODP site 843 [King et al., 1993], located 300 km from Maui, has unradiogenic  $^{87}\text{Sr}/^{86}\text{Sr}$ , but  $^{206}\text{Pb}/^{204}\text{Pb}$  too radiogenic to cause the variability observed in the deep West Maui samples (Fig. 1.9). Some gabbro xenoliths from Hualalai volcano, which have been interpreted to represent the oceanic crust beneath Hawaii [Clague and Chen, 1986], have unradiogenic  $^{87}\text{Sr}/^{86}\text{Sr}$  and  $^{206}\text{Pb}/^{204}\text{Pb}$  and Sr/Pb such that a mixing hyperbola between small-degree melts (2%) of these gabbros and average shallow West Maui lavas describes the compositional range in the deep West Maui lavas [Okano and Tatsumoto, 1996; Lassiter and Hauri, 1998]. Mixing of small-degree melts of this ocean

crust layer with plume-generated Kea-like magmas would result in hybrid magmas similar to what we observe at West Maui. The Sr/Pb as well as [Sr] and [Pb] of the gabbro melt depends upon the fraction of melt generated (F). Higher-F melts (>2-3%) will have lower [Sr] and [Pb] and therefore a larger proportion of this melt would be required to mix with the plume-generated magmas in order to produce the observed trends. A smaller-degree melt would also provide the observed mixing trend, but such a small-degree melt may not have sufficient melt connectivity to separate from the solid residue.

Within the range of  $^{176}\text{Hf}/^{177}\text{Hf}$  variability at West Maui, the deep samples tend to have only slightly higher-than-average compositions (Fig. 1.10). Thus the source of this variation in the deep samples must be close enough in composition to the shallow lavas so that the extent of mixing required by the  $^{87}\text{Sr}/^{86}\text{Sr}$  compositions of the deep samples does not result in dramatic shifts in  $^{176}\text{Hf}/^{177}\text{Hf}$ . Whatever caused the isotopic shift in the deep samples must have a  $^{176}\text{Hf}/^{177}\text{Hf}$  composition similar to or higher than Kea, rather than lower. Magma generated through mantle melting (i.e., MORB) will have Lu/Hf lower than its mantle source, such that  $\epsilon_{\text{Hf}}$  (as defined in the footnote of Table 1.2) of the melt will decrease relative to the residual source as it ages. The 110 Ma oceanic crust that we model has  $^{176}\text{Hf}/^{177}\text{Hf}$  higher than Kea-type lavas, but progressively older model crust will have  $^{176}\text{Hf}/^{177}\text{Hf}$  less radiogenic than the Kea-type lavas. Thus, both of the modeled 2 Ga endmembers, or any mixture of them, will have  $^{176}\text{Hf}/^{177}\text{Hf}$  significantly lower than Kea-type lavas. However, as with the  $^{206}\text{Pb}/^{204}\text{Pb}$ - $^{87}\text{Sr}/^{86}\text{Sr}$  variability, the  $^{206}\text{Pb}/^{204}\text{Pb}$ - $^{176}\text{Hf}/^{177}\text{Hf}$  variation in the deep samples is consistent with modeled contributions of small-degree melts from ambient Pacific gabbros, with the same mixing proportions as identified in the  $^{87}\text{Sr}/^{86}\text{Sr}$ - $^{206}\text{Pb}/^{204}\text{Pb}$  variation (Fig. 1.9).

#### 1.4.2 $^{87}\text{Sr}/^{86}\text{Sr}$ and trace element constraints on endmember compositions

The deep West Maui lavas show correlations of  $^{87}\text{Sr}/^{86}\text{Sr}$  with some trace elements (Fig. 1.11). Among the deep samples, those with less radiogenic  $^{87}\text{Sr}/^{86}\text{Sr}$  trend to higher La/Yb, Nb/Zr, Nb/Hf, Nb/La, [Nb] and [Sr]. Although these elemental indicators are dependent in part on degree of melting, the correlation with  $^{87}\text{Sr}/^{86}\text{Sr}$  indicates that the variations they describe

are fundamentally related to the source. The high degree of correlation for these parameters also implies that the melt endmembers involved are very homogeneous, and therefore there is only a small range in extent of melting of this endmember source as it contributes to the magmas. If this source melted over a wider range of  $F$  as it contributed to the West Maui lavas, then the melt endmember would have a wider range in elemental composition for a given isotopic composition, and there would be much more scatter in the West Maui trends. With  $^{87}\text{Sr}/^{86}\text{Sr}$  vs.  $\text{Nb}/\text{Zr}$  and  $\text{Nb}/\text{Hf}$ , the deep samples define a linear trend that is distinct from the trend defined by the shallow samples. Although the absolute spread in  $\text{Nb}/\text{Zr}$  of the deep samples is close to the analytical error for this ratio, the difference in this ratio between the two sample groups is greater than the analytical uncertainty. It appears that three endmembers (at least) are required to explain the observed trends. While one endmember has high  $^{87}\text{Sr}/^{86}\text{Sr}$  and two endmembers low  $^{87}\text{Sr}/^{86}\text{Sr}$ , they are distinct in trace element composition. In these mixing relationships, the deep samples form well-correlated arrays implying that, at least for the chemical signals under consideration, the contributing endmembers are homogeneous. It therefore follows that the larger range in compositions observed for the shallow compared to the deep samples stems from heterogeneity in the low- $^{87}\text{Sr}/^{86}\text{Sr}$  endmember that contributes to the array defined by the shallow samples.

For  $\text{La}/\text{Yb}$ ,  $\text{Nb}/\text{Zr}$ ,  $\text{Nb}/\text{Hf}$  and  $\text{Nb}/\text{La}$  vs.  $^{87}\text{Sr}/^{86}\text{Sr}$  the shallow West Maui samples fall within the range defined by Kilauea, Mauna Kea and Loihi [Garcia et al., 1993, 1995; Albarède, 1996; Chen et al., 1996; Hofmann and Jochum, 1996; Lassiter et al., 1996; Pietruszka and Garcia, 1999]. For these trace element ratios, Kilauea historical and prehistoric lavas together define a broader range and extend to higher values than West Maui, Mauna Kea or Loihi. Only for  $\text{Nb}/\text{La}$ - $^{87}\text{Sr}/^{86}\text{Sr}$  do the Kilauea historical lavas define a trend that is distinct from prehistoric Kilauea lavas. The deep West Maui lavas fall either on the edge or outside of the fields defined by Mauna Kea, Kilauea and Loihi. None of these volcanoes shows  $\text{La}/\text{Yb}$ ,  $\text{Nb}/\text{Zr}$ ,  $\text{Nb}/\text{Hf}$  or  $\text{Nb}/\text{La}$  vs.  $^{87}\text{Sr}/^{86}\text{Sr}$  trends as clearly defined as the deep West Maui lavas.

Placed in the context of the preceding discussion, we can consider whether any of the proposed isotopic reservoirs can also produce a unique trace element signature. Gabbros from the Gabal Gerf Ophiolite complex [Zimmer et al., 1995], as well as ODP site 735B

[Hart et al., 1999], show an extremely wide range in Nb/La (0.19-1.5), Nb/Zr (0.03-0.14), La/Yb (1.24-4.28) and Nb/Hf (0.5-5.22). Because in all of these ratios the element in the numerator is more incompatible than the element in the denominator, the ratios will be greater in the melt relative to its source. The absolute increase of the ratio in the melt relative to the source depends upon  $F$ , partition coefficients and the mineralogical mode of the source. Within the range of variability introduced by these parameters (see discussion below), it is possible to calculate small-degree melts of oceanic gabbro that have trace element ratios appropriate for endmembers in the mixing scheme proposed here.

Partial melting of a gabbro can also potentially generate magmas with Eu and Sr anomalies. Gabbro from oceanic crust drill cores as well as ophiolites [Zimmer et al., 1995; Hart et al., 1999] show both positive and absent Eu and Sr anomalies. As shown in Fig. 1.12, the predicted presence or absence of a Eu anomaly is dependent upon the starting gabbro composition and partition coefficients. We show REE compositions of two representative gabbros [Zimmer et al., 1995], and 2% melts derived there using two different sets of partition coefficients [McKenzie and O'Nions, 1991; Hauri and Hart, 1995; Schnetzler and Philpotts, 1970]. La/Yb in these melts ranges from 0.5 to 7.9. The range of resultant melts shows positive, negative or absent Eu anomalies, and therefore it is difficult to use absence or presence of a Eu anomaly in the West Maui lavas as an argument either for or against mixing with small-degree gabbro melts. The West Maui lavas do not show any Eu anomaly, and both deep and shallow groups of samples show approximately the same range of [Sr]. However, the low- $^{87}\text{Sr}/^{86}\text{Sr}$  endmember which contributes to the deep samples also has higher [Sr] than the high- $^{87}\text{Sr}/^{86}\text{Sr}$  endmember contributing to the deep samples. This is consistent with additions of small-degree gabbro melts to the deep West Maui lavas.

Perhaps the primary uncertainty in modeling isotopic and elemental compositions of the oceanic crust endmembers is the effect of variation in choice of partition coefficients. Wherever possible, we avoid introducing this uncertainty by using elemental concentrations as are actually observed in rocks (e.g., ODP cores, xenoliths, young MORB). However, this is not always possible, and in Fig. 1.12 we illustrate the range of effects of two different sets of partition coefficients on modeling small-degree gabbro melts. The effect of this uncertainty is especially enhanced at the low degrees of partial melt (2%) that we are considering here.

The second largest variability in endmember choice or calculation is the variation inherent to the composition of the rocks themselves. In some instances ( $^{87}\text{Sr}/^{86}\text{Sr}$  and  $^{206}\text{Pb}/^{204}\text{Pb}$  of 110 Ma gabbro and upper oceanic crust) we are able to use data from actual rocks that we believe represent the endmember compositions. In these cases, we use an average of multiple analyses for the endmember composition. In other cases, where modeling of the composition of aged components (e.g.,  $^{176}\text{Hf}/^{177}\text{Hf}$ ) amplifies variation introduced by starting composition, we show a range of possibilities for the modeled endmembers (Figs. 1.9 and 1.10, Table 1.4). In Fig. 1.12, we also show melts generated from two different gabbro starting compositions. It is evident that the combination of gabbro starting composition and choice of distribution coefficient can result in a wide range of melt compositions. Although not all compositions provide results that are consistent with our hypothesis and data, we do find that there are geologically reasonable combinations of partition coefficient and gabbro composition that are consistent with predictions from our hypothesis.

#### *1.4.3 Age-correlated compositional shifts in other Hawaiian volcanoes*

Several other Hawaiian volcanoes show age-correlated compositional shifts in isotopic and trace element composition of shield-stage, tholeiitic lavas [e.g., Kurz et al., 1995; Pietruszka and Garcia, 1999; Tanaka et al., 2002]. In Koolau and Mauna Loa, these shifts are evident as Sr-Nd-Pb isotopic compositions that lie on a trajectory towards Kea-type compositions, as defined by Mauna Kea and Kilauea [Kurz et al., 1995; Tanaka et al., 2002]. A subset of Koolau lavas overlaps with Kilauea and Mauna Kea fields (Fig. 1.9), whereas none of the Mauna Loa lavas show compositional shifts of this magnitude. In both of these volcanoes, lavas showing the Kea-like compositions are the oldest ones sampled for each volcano: from the submarine Nuuanu slide block for Koolau, and from the submarine SW Rift, Ninole and Kahuku Basalts of Mauna Loa.

Kilauea, which is dominated by Kea-type compositions in its historical lavas, has pre-historic lavas (Hilina) that extend to the most radiogenic  $^{206}\text{Pb}/^{204}\text{Pb}$  observed in any Hawaiian shield-stage lavas, but do not extend to significantly lower  $^{87}\text{Sr}/^{86}\text{Sr}$ . In the Kea-like lavas from Mauna Loa and Koolau, as well as in the entire range of lavas from Mauna

Kea and Kilauea, the compositional variation is expressed with a wide range for  $^{206}\text{Pb}/^{204}\text{Pb}$  ( $\sim 18.2-18.9$ ) which corresponds to very limited variation in  $^{87}\text{Sr}/^{86}\text{Sr}$  ( $\sim 0.70358-0.70367$ ). In contrast, the compositional shifts we see in the deep West Maui lavas are specifically defined by lower  $^{87}\text{Sr}/^{86}\text{Sr}$  for a given range in  $^{206}\text{Pb}/^{204}\text{Pb}$ . Although we see short-term compositional changes in other Hawaiian volcanoes that indicate a complexity in source components and the time periods over which they contribute to the magmas, none of the absolute senses of variation observed in Kilauea, Mauna Loa or Koolau is consistent with interaction of magmas with oceanic crust, using the endmembers that we define for the oceanic crust beneath West Maui.

Tholeiites from Loihi, which is still in its early stages of growth, have Sr-Nd-Pb isotopic compositions comparable to Mauna Kea and Kilauea [Staudigel et al., 1984; Garcia et al., 1993]. A subset of Loihi tholeiitic lavas shows a positive  $^{206}\text{Pb}/^{204}\text{Pb}$ - $^{87}\text{Sr}/^{86}\text{Sr}$  correlation similar to what we observe in West Maui. Although the Loihi compositions do not actually overlap with West Maui compositions, and do not extend to  $^{87}\text{Sr}/^{86}\text{Sr}$  as low as those we observe in West Maui deep lavas, these lavas may still reflect a process similar to what we propose for West Maui. Primarily, the lower magma fluxes at the early and late stages of shield growth allow for the preservation of the geochemical signals of interaction between plume-generated magmas and the oceanic crust.

As this low- $^{87}\text{Sr}/^{86}\text{Sr}$  endmember is sampled at West Maui, and possibly at Loihi, it does not constitute an identifiable endmember in Kea-type lavas as they are sampled at Mauna Kea or Kilauea, or in the variability in the compositional range of Hawaiian volcanoes as a whole. It therefore does not appear that this compositional endmember is a fundamental component of the Hawaiian plume, which otherwise would be sampled in a more regular or identifiable manner. Rather, it may reflect transitory processes related to early (Loihi) and late (West Maui) stages of Hawaiian volcano growth. The existence of this endmember at West Maui is only identifiable through dense sampling and stratigraphic control, and therefore lack of observation of this signal at other volcanoes does not necessarily preclude its existence.

Rejuvenated stage lavas, which erupt after a period of quiescence following the post-shield stages of volcano growth, occur on Kauai (Koloa volcanics), Koolau (Hololulu Vol-

canics), East Molokai (Kalaupapa Volcanics), West Maui (Lahaina Volcanics) and Haleakala (Hana Volcanics). These lavas have more depleted  $^{87}\text{Sr}/^{86}\text{Sr}$ ,  $^{143}\text{Nd}/^{144}\text{Nd}$  and  $^{176}\text{Hf}/^{177}\text{Hf}$  than observed in any Hawaiian shield-stage lavas, and are commonly interpreted as having a source external to the Hawaiian plume [e.g., Clague and Frey, 1982; Reiners and Nelson, 1998]. Although they are compositionally distinct from the local Pacific oceanic crust, both the asthenosphere and Pacific lithosphere beneath Hawaii are possible sources for the rejuvenated lavas [Lassiter et al., 2000]. The rejuvenated lavas have less radiogenic  $^{206}\text{Pb}/^{204}\text{Pb}$  and  $^{87}\text{Sr}/^{86}\text{Sr}$  relative to the Kea endmember, as we also observe in the deep West Maui lavas, but they are offset from the trajectory suggested by the  $^{206}\text{Pb}/^{204}\text{Pb}$  -  $^{87}\text{Sr}/^{86}\text{Sr}$  variation in the deep West Maui lavas, and have  $^{206}\text{Pb}/^{204}\text{Pb}$  that is too unradiogenic to share a source with the deep West Maui lavas.

#### 1.4.4 Constraints on contributions of Pacific oceanic lithosphere to West Maui lavas

The model that is most consistent with our observations from West Maui is that compositional variations measured in the deep samples are the result of mixing small-degree melts of Pacific oceanic crust with the primary, plume-generated West Maui magmas. Trace element ratios and Sr concentrations in the deep samples point to a contribution from the gabbroic layer of oceanic crust, and Sr-Pb-Hf isotope variations suggest this is the  $\sim 110$  Ma Pacific crust, rather than ancient recycled oceanic crust within the plume itself.

The generation and incorporation of these melts have implications for the heat budget and mass balance of the overall system. We used the MELTS algorithm [Ghiorso and Sack, 1995] to model isenthalpic assimilation of oceanic crust gabbro into a primitive West Maui magma (sample WA17). For all model runs, the pressure is 2 kbar, starting temperature of the assimilating magma is  $1325^\circ\text{C}$ , and starting temperature of the assimilant is either  $100^\circ\text{C}$  or  $200^\circ\text{C}$ . We modeled assimilation of three starting compositions with olivine:orthopyroxene:clinopyroxene:plagioclase proportions of 40:20:20:20, 30:0:40:30 and 20:20:20:40, in order to understand the influence of the initial mineralogical mode of the assimilant. For each model run we report  $r = \text{mass assimilated}/\text{mass crystallized}$ , and in Fig. 1.13 we show this parameter as a function of total mass assimilated. In all models, for

the first 16 wt. % assimilation (relative to initial mass of the assimilating magma) olivine is the only crystallizing phase. After 16 wt.% assimilation, clinopyroxene and eventually plagioclase join the crystallizing assemblage. However, the isotope and trace element data presented in the previous sections indicate involvement of only small-degree ( $\sim 2\%$ ) melts of oceanic gabbro, so we limit the following discussion exclusively to a system with low degrees of assimilation. Within the range of assimilant composition and starting temperature that we explored in these models,  $r$  ranges from 0.73 to 0.9 for small degrees of assimilation, which translates into a maximum decrease in the total volume of liquid in the system of 10% over the range of assimilation required to result in the geochemical shifts observed in the deep lavas. Therefore, the assimilation model supported by the geochemical data is also thermally plausible.

The major element changes that accompany assimilation are slight increases in  $\text{SiO}_2$ ,  $\text{Al}_2\text{O}_3$  and  $\text{CaO}$ , and decreases in  $\text{MgO}$  and  $\text{FeO}$ . These shifts are similar to those that accompany olivine fractionation without any assimilation of gabbro, making it difficult to use major element composition alone as an indicator of assimilation of oceanic crust. Ten-15% assimilation of a small-degree gabbro melt into a primitive West Maui magma ( $\sim 13$  wt.%  $\text{MgO}$ ) will produce a resultant melt with 8.5-10 wt.%  $\text{MgO}$ . Of the deep West Maui lavas, only one sample has  $\text{MgO} > 10$  wt.%. We do not observe any significant differences between the deep and shallow groups with respect to major element variability as a function of  $^{87}\text{Sr}/^{86}\text{Sr}$ . However, we would not necessarily expect to observe significant variation, as the major element changes with assimilation are small, and it is difficult to distinguish them from olivine control.

As the starting composition in these models we used the most primitive ( $\text{MgO} = 13.61$  wt.%) shallow West Maui composition that did not show significant olivine accumulation (i.e., high olivine abundance in hand sample). In other Hawaiian volcanoes, primary magmas with  $\text{MgO} \geq 15$  wt.% have been identified [Chen, 1993; Clague et al., 1995], and a hotter, more primitive starting composition may produce a different result in the assimilation calculations. However, we have not observed any primitive magmas such as these at West Maui, and although they may exist, we prefer to use the observed primitive composition in order to keep our model consistent with our observations at this volcano.



Generation of these geochemical signals requires extraction of small degrees (2%) of melt from the lower oceanic crust. Assuming that the West Maui total volume is  $6.4 \times 10^3$  km<sup>3</sup> [Bargar and Jackson, 1974], presence of this oceanic crust-derived geochemical signal throughout the volcano would require 640-1280 km<sup>3</sup> of small-degree melt of oceanic crust, which would in turn imply depleting nearly 50,000 km<sup>3</sup> of oceanic crust of a small degree of melt. When comparing this to the volume of gabbro underlying the entire volcano,  $\sim 3000$  km<sup>3</sup> (volcano radius = 20 km; gabbro thickness = 2.5 km), it is apparent that no more than 5% of the total volume of erupted lavas can exhibit this geochemical signal, which derives from 10-15% mixing of low-degree gabbro partial melt with plume-derived magmas. It is reasonable to envisage that this signal would be present during times when the magma pathways through the oceanic crust reconfigure in response to the motion of the Pacific plate over the Hawaiian hotspot. Then, as new magma pathways become established and conduit walls armored or reacted, the imprint of the gabbro geochemical signal decreases. The lavas we sampled represent the latest stages of volcano growth, which could imply that the oceanic crust signal may be a response to a decreasing magma flux from the plume. West Maui is also the least voluminous of all the major Hawaiian volcanoes [Bargar and Jackson, 1974], which may explain why the geochemical signals of this process are preserved at this particular volcano, whereas at other larger volcanoes, where the geochemical fingerprint is swamped or diluted by the relatively more substantial volumes of magma moving through the oceanic crust, they are missing. Also, because few tholeiitic shield-stage volcanoes have been sampled in this much stratigraphic detail, this process may be as yet unrecognized in other shields.

#### 1.4.5 *Is there still a requirement for 2 Ga recycled oceanic crust in Kea-type lavas?*

Because none of the trace element signals that we attribute to Pacific oceanic lithosphere are dependent on the age of the source, it is possible they could derive from an ancient subducted and recycled oceanic crust gabbro layer, as has been previously suggested for Hawaii and other ocean island volcano systems [Lassiter and Hauri, 1998; Chauvel and Hémond, 2000; Geldmacher and Hoernle, 2000; Sobolev et al., 2000]. So far, we have not

considered the possible role of 2 Ga lithospheric mantle (harzburgite/therzolite) that is residual to the process of MORB generation. We calculated the isotopic composition of 2 Ga residual lithosphere that would be complementary to the 2 Ga gabbro and basalt compositions calculated above. For parent/daughter ratios in the depleted lithosphere, we used the residue of a 20% batch melt of depleted mantle, using partition coefficients from Hauri and Hart [1995] and McKenzie and O'Nions [1991], initial element concentrations from Sun and McDonough [1989], and a starting mineralogical composition of 52% olivine, 30% orthopyroxene, and 18% clinopyroxene [Hirschmann and Stolper, 1996]. Variation in mineralogical mode of the depleted residue (e.g., clinopyroxene content) has only a minor effect relative to the magnitude of the modeled isotopic compositions, and therefore does not influence our conclusions. This reservoir will develop extreme isotopic compositions ( $^{176}\text{Hf}/^{177}\text{Hf} = 0.2836$ ,  $^{87}\text{Sr}/^{86}\text{Sr} = 0.7025$ ,  $^{206}\text{Pb}/^{204}\text{Pb} = 14.22$ ) as will the gabbroic and basaltic parts of the oceanic crust (modeling and results discussed previously). However, such depleted lithosphere will only sensibly affect bulk isotopic composition when present in 90-95% abundances. A hybrid source of 90-95% 2 Ga depleted lithosphere and 5-10% of a 2 Ga 25:75 basalt:gabbro mixture will produce a source that could give rise to the Sr-Pb-Hf isotopic variations seen in the deep West Maui samples. This source would have relatively depleted major element compositions, and we therefore would expect magmas derived from a source dominated by residual mantle to show major element-isotope variability distinct from the typical Kea-type magmas. As this is not apparent, we argue against contributions of an ancient, hybrid, depleted lithosphere-basalt-gabbro source as the cause of the fine-scale variations we observe in the deep West Maui lavas.

The differences in isotopic composition among the modeled ancient depleted lithosphere, basalt and gabbro endmembers are so great that minor variations in the relative mixing proportions could have significant effects on the bulk composition of the mixture. It is therefore conceivable that a mixture of depleted lithosphere:basalt:gabbro could act as the source of the Kea plume component as defined by its Hf-Pb-Sr-Nd isotopic composition. However, Kea-type magmas that are sampled during the  $\sim 1.5$  My time span over which Mauna Kea, Kilauea and West Maui erupted are very homogeneous in isotopic composition. If the Kea source is the result of mixing between recycled lithosphere, basalt, and gabbro components,

then the mixing processes that generate the Kea source have remained extraordinarily reproducible over this time period. This implies consistent processes of oceanic crust generation and alteration at the mid-ocean ridge as well as sampling of the recycled oceanic lithosphere package in the plume.

### **1.5 Conclusions**

In the West Maui lavas, we see contributions from three different components. Mixing between two of these components describes the variability inherent to Kea-type magmas. These two sub-components are defined by their  $^{87}\text{Sr}/^{86}\text{Sr}$  variability and a number of trace elements. They show only small distinctions in Hf, Pb or Nd isotope compositions, and therefore it is likely that they are closely related genetically. The third component is not required to account for the compositional variability of Mauna Kea, Kilauea or the shallow lavas at West Maui. Our interpretation of the source of this component, and also its apparent absence in the Mauna Kea, Kilauea and shallow West Maui lavas, indicates that it is not intrinsic to Kea-type lavas or to the genesis of their plume source.

In the deep West Maui lavas, we have identified the chemical fingerprint of Pacific oceanic crust gabbro overprinted onto the plume-derived Kea-type magma compositions. These compositional variations that we attribute to mixing with small-degree melts of oceanic gabbro are present only over short time scales, and, based on mass balance calculations, can be present in no more than  $\sim 5\%$  of the total volume of lavas erupted. These characteristic compositional trends have not been observed in shield-stage lavas at other Hawaiian volcanoes. Their absence at other volcanoes may be, in some cases, a consequence of less dense sampling or lack of stratigraphic control, or may indicate that this geochemical signal is not generally characteristic of Kea-type volcanoes or of the plume source that generates Kea-type magmas.

The process that we observe in the West Maui deep lavas, namely the overprinting with signals of partial melts from gabbroic oceanic crust, is unlikely to be unique to this volcano. It is the fundamental homogeneity of Kea-type lavas that enables the identification of variation from plume-derived Kea-type compositions. The geochemical signal of this

process is so subtle that it would be extremely difficult to resolve in the more heterogeneous Koolau-type volcanoes or even at more voluminous Kea-type volcanoes where this signal would be diluted by the higher magma flux.

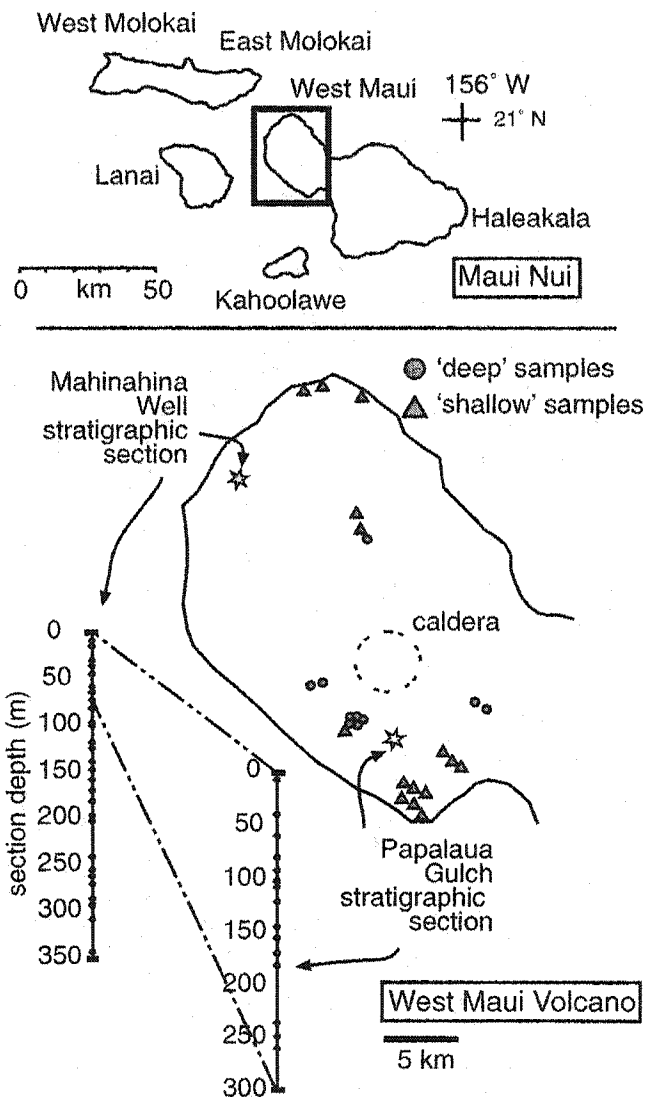


Figure 1.1: Location of Papalaua Gulch and Mahinahina Well stratigraphic sections, as well as deep and shallow samples. Section depths are given in meters. Caldera location from Stearns and Macdonald [1942].

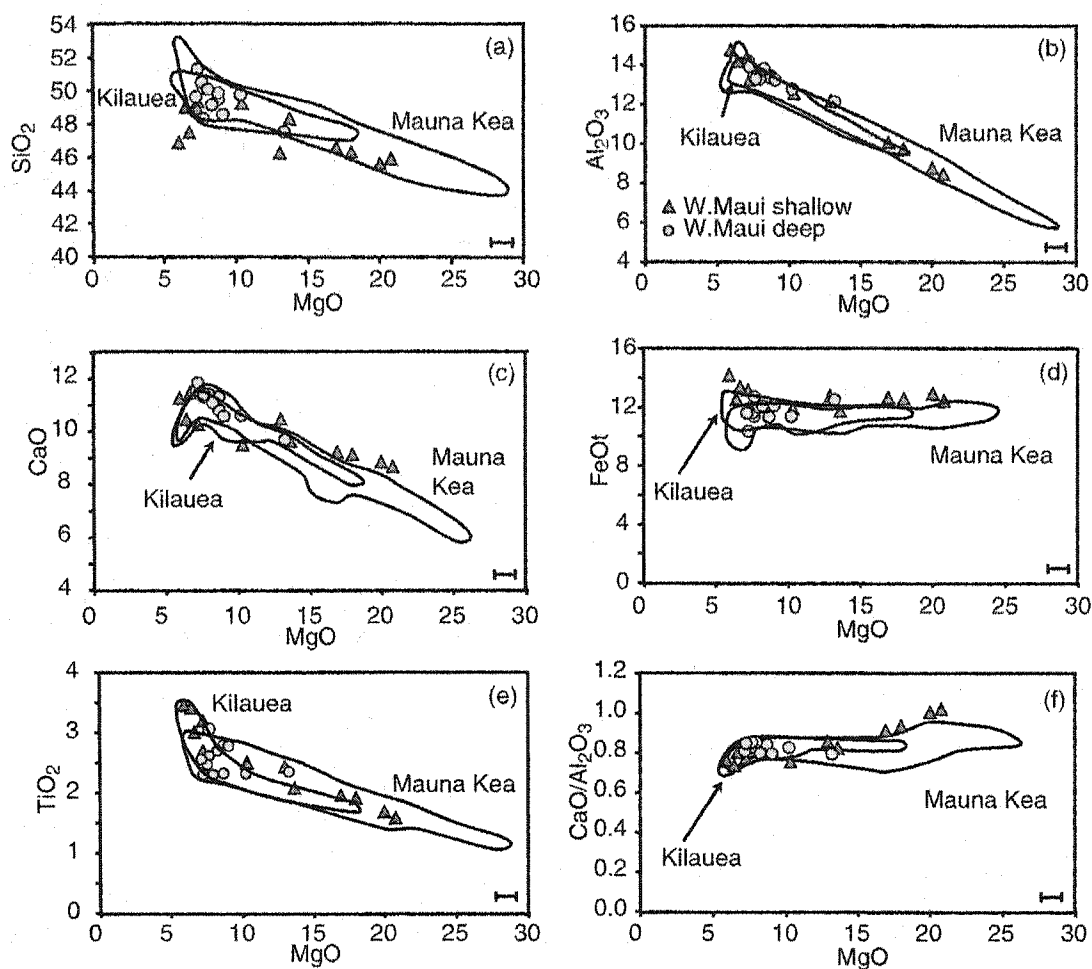


Figure 1.2: MgO variation diagrams for West Maui shield-stage lavas in 'deep' and 'shallow' sample categories. Oxides given in wt. %. Two-sigma external reproducibility is smaller than symbol size for all oxides except for MgO, for which 2-sigma error bar is shown. Also shown for comparison are compositions of Mauna Kea and Kilauea shield-stage lavas. Data sources: Garcia et al. [1992], Yang et al. [1994], Chen et al. [1996], Garcia et al. [1996], Rhodes [1996], Garcia et al. [2000].

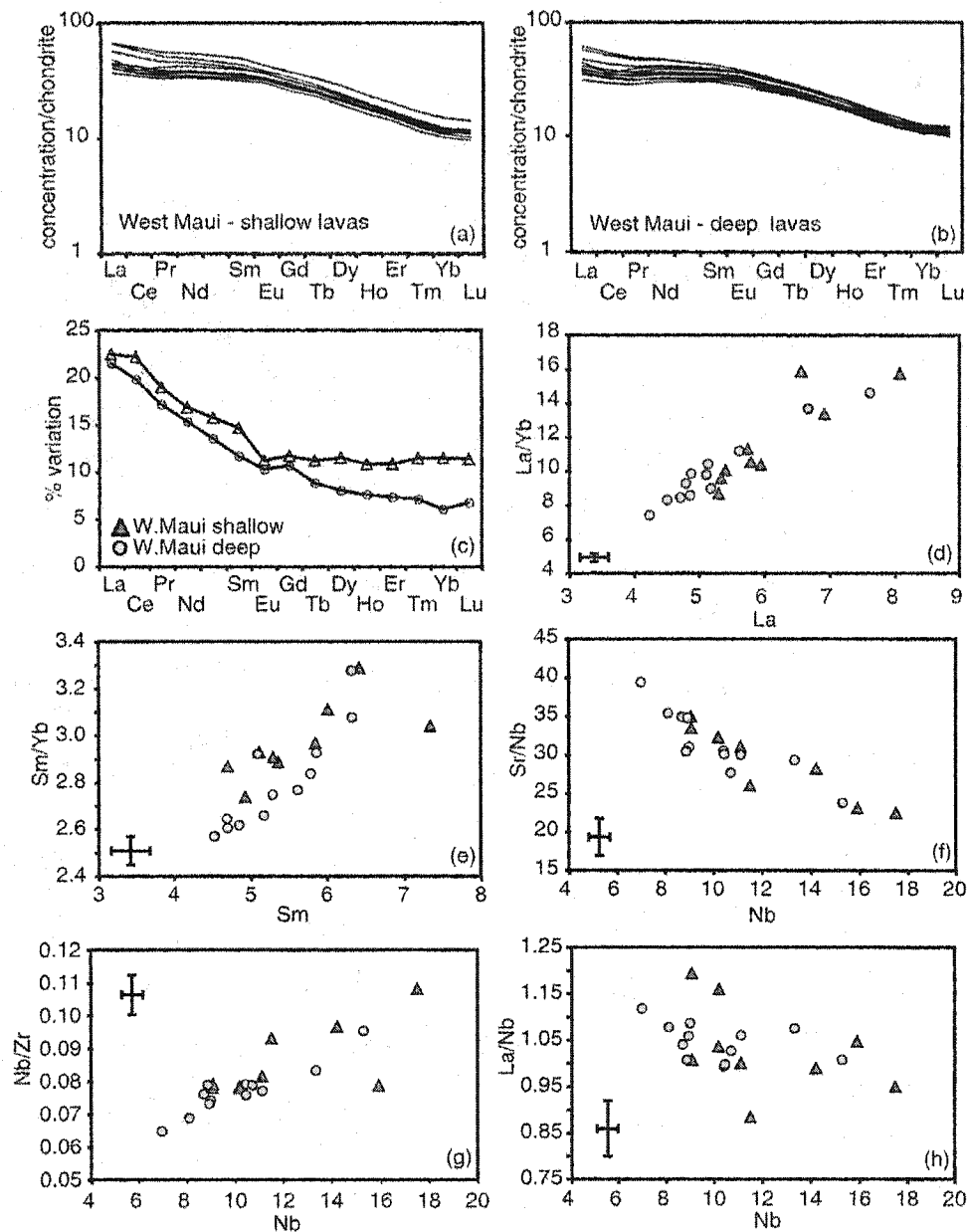


Figure 1.3: Rare earth element (REE) and incompatible trace element compositions for deep and shallow West Maui lavas. Trace element concentrations are corrected to 13 wt. % MgO. REE concentrations are chondrite-normalized using the values of Sun and McDonough [1989]. Error bars represent 2-sigma external reproducibility; percent variation =  $100 \times (\text{standard deviation}/\text{average})$ .

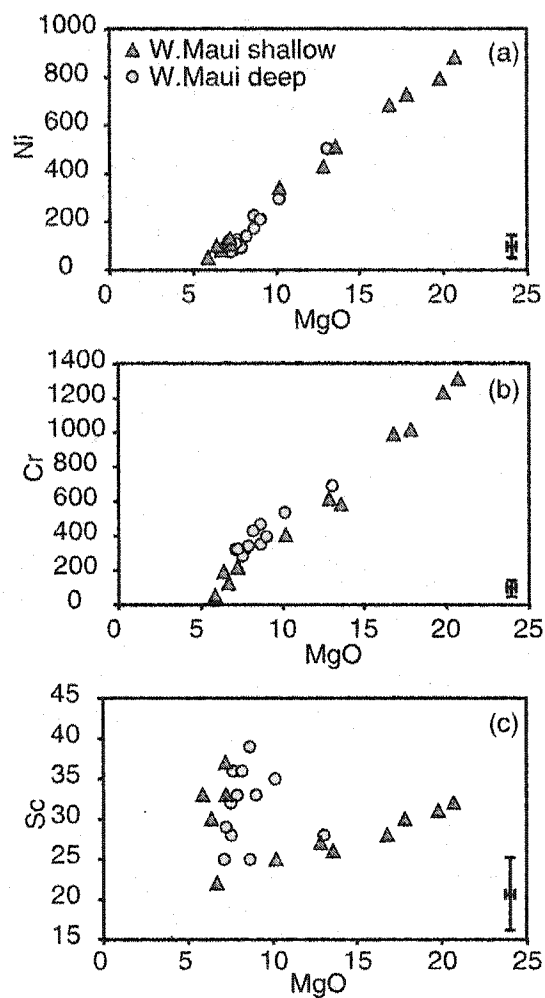


Figure 1.4: MgO-compatible trace element variation for West Maui shield-stage lavas. Trace element compositions are not corrected for olivine control. MgO composition is in wt. %, trace element composition is in ppm, and error bars represent 2-sigma external reproducibility.



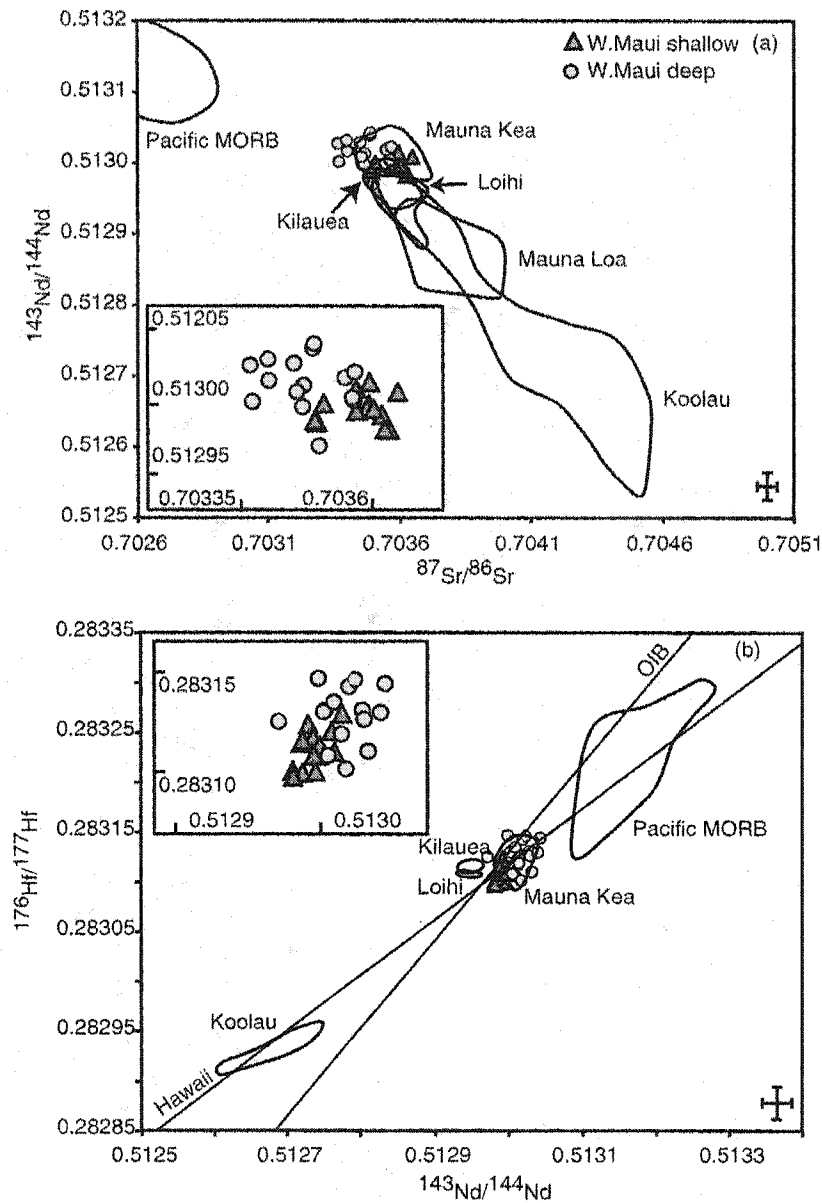


Figure 1.5: (a)  $^{87}\text{Sr}/^{86}\text{Sr}$  -  $^{143}\text{Nd}/^{144}\text{Nd}$  and (b)  $^{143}\text{Nd}/^{144}\text{Nd}$  -  $^{176}\text{Hf}/^{177}\text{Hf}$  variation in the West Maui lavas. Shown for comparison are the fields for shield-stage lavas from Koolau, Mauna Loa, Loihi, Mauna Kea and Kilauea. Insets show detail of compositional variation for West Maui lavas only. OIB and Hawaii correlation lines from Blichert-Toft et al. [1999]. Error bar represents 2-sigma external reproducibility. Data sources: Stille et al. [1986], Garcia et al. [1993], Roden et al. [1994], Garcia et al. [1995], Kurz et al. [1995], Chen et al. [1996], Lassiter et al. [1996], Blichert-Toft et al. [1999], Blichert-Toft and Albarède [1999], Pietruszka and Garcia [1999], Tanaka et al. [2002].

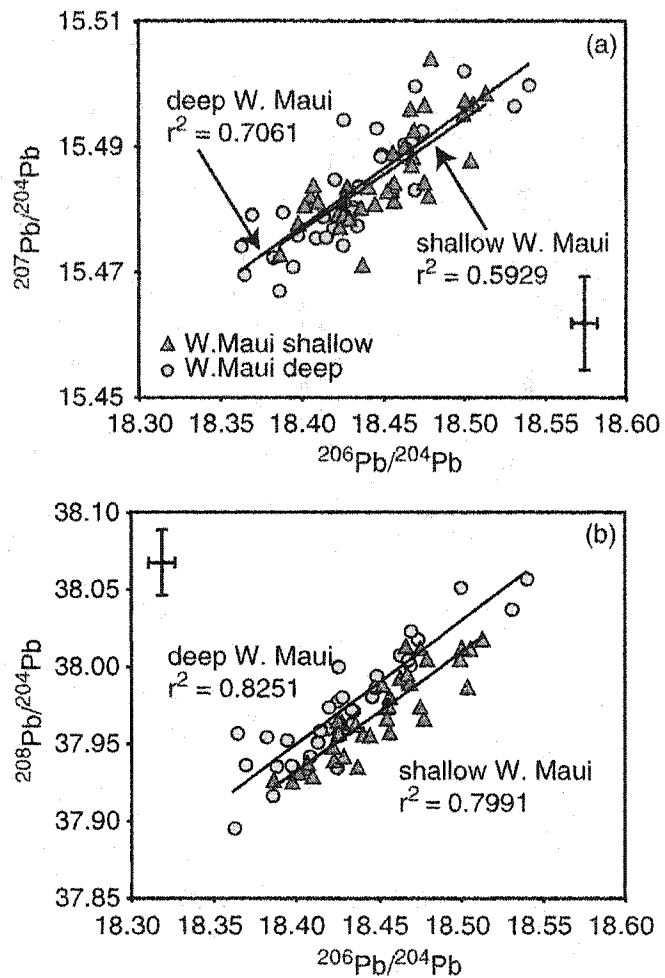


Figure 1.6: (a)  $^{206}\text{Pb}/^{204}\text{Pb}$ - $^{207}\text{Pb}/^{204}\text{Pb}$  and (b)  $^{206}\text{Pb}/^{204}\text{Pb}$ - $^{208}\text{Pb}/^{204}\text{Pb}$  variation in West Maui lavas. Error bar represents 2-sigma external reproducibility.

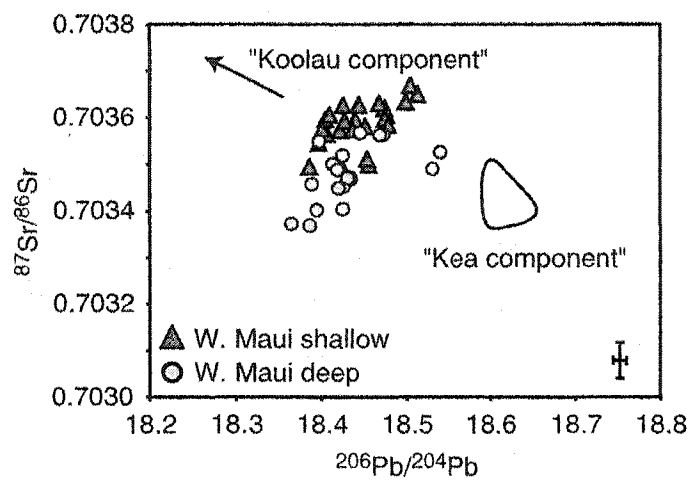


Figure 1.7:  $^{87}\text{Sr}/^{86}\text{Sr}$ - $^{206}\text{Pb}/^{204}\text{Pb}$  variation for West Maui lavas. Shown for reference are postulated compositions of the Kea and Koolau endmembers [Stille et al., 1986; West and Leeman, 1987; Eiler et al., 1998].

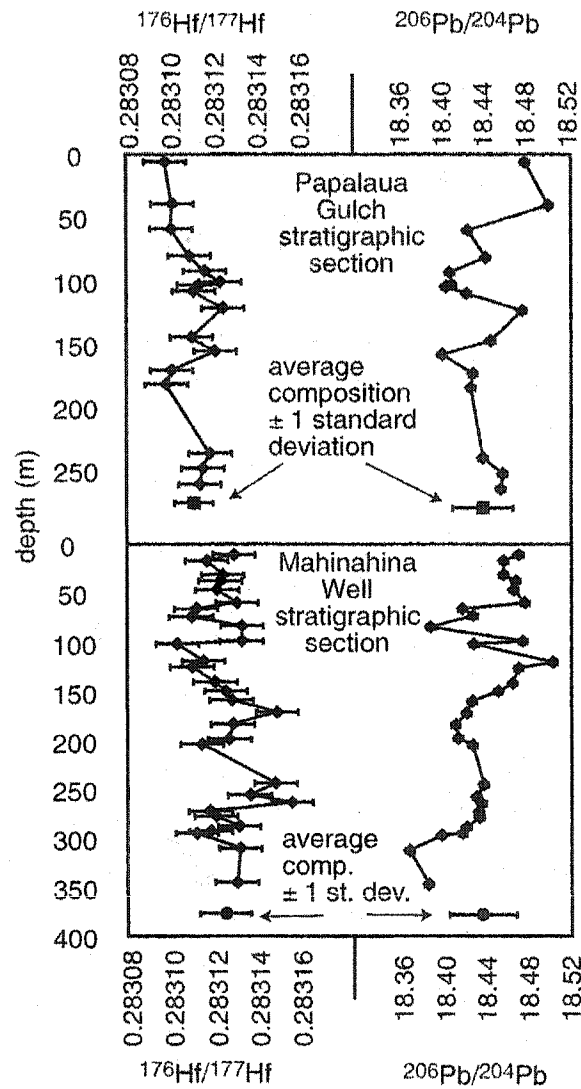


Figure 1.8:  $^{176}\text{Hf}/^{177}\text{Hf}$  and  $^{206}\text{Pb}/^{204}\text{Pb}$  stratigraphy for the Papalaua Gulch and Mahinahina Well stratigraphic sections. Also shown are the average compositions for each section,  $\pm$  one standard deviation

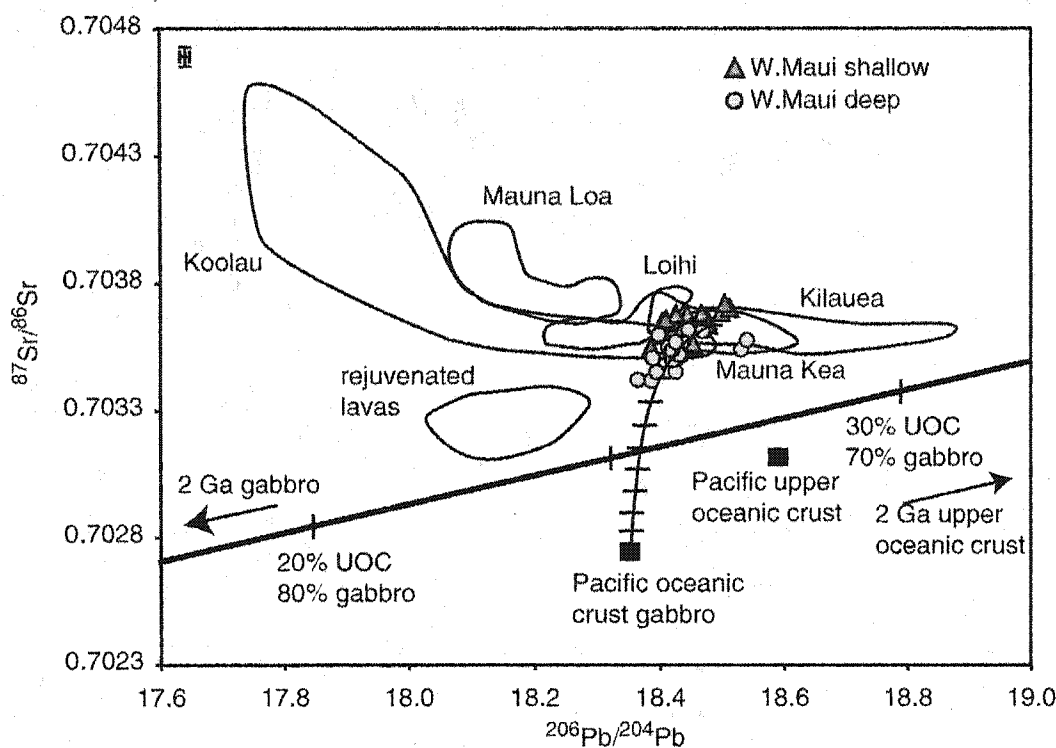


Figure 1.9:  $^{87}\text{Sr}/^{86}\text{Sr}$ - $^{206}\text{Pb}/^{204}\text{Pb}$  variation in West Maui lavas, with tholeiitic lava compositions from Koolau, Mauna Loa, Loihi, Mauna Kea, Kilauea and Hawaiian rejuvenated-stage lavas from Kauai, Koolau and Haleakala shown for comparison. Oceanic crustal endmember compositions are given in Table 1.4 and discussed in text. Mixing line between West Maui and Pacific oceanic crust gabbro represents mixing between 2% melt of oceanic gabbro and plume-derived Kea-type magma; tick marks indicate 10% mixing increments. Mixing line between 2 Ga gabbro and 2 Ga upper oceanic crust (UOC) is for solid-solid mixing between these endmembers; tick marks along this line indicate 5% increments of mixing. Data sources for other volcanoes: Stille et al. [1983], West et al. [1987], Reiners and Nelson [1998], Abouchami et al. [2000], Lassiter et al. [2000], Blichert-Toft et al. [2003].

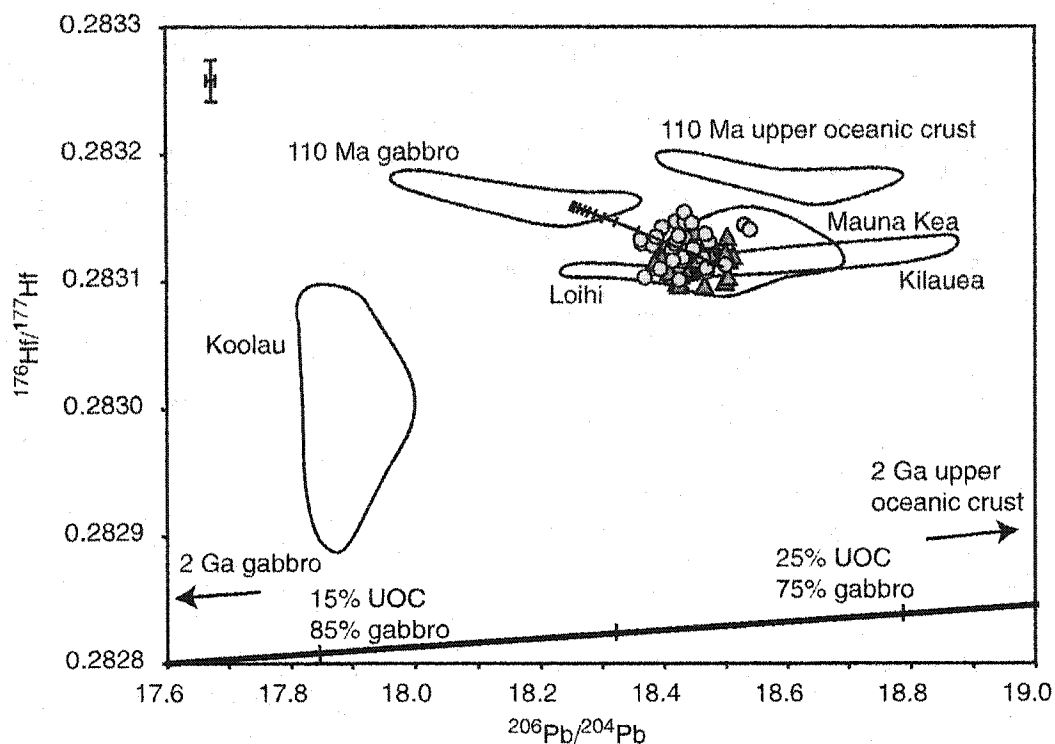


Figure 1.10:  $^{206}\text{Pb}/^{204}\text{Pb}$ - $^{176}\text{Hf}/^{177}\text{Hf}$  variation in West Maui lavas, with tholeiitic lava compositions from Koolau, Loihi, Mauna Kea and Kilauea. Oceanic crustal endmember compositions are given in Table 1.4 and discussed in text. Mixing line between West Maui and Pacific oceanic crust gabbro represents mixing between 2% melt of oceanic gabbro and plume-derived Kea-type magma; tick marks indicate 10% mixing increments. Mixing line between 2 Ga gabbro and 2 Ga upper oceanic crust (UOC) is for solid-solid mixing between these endmembers; tick marks along this line indicate 5% increments of mixing. Data sources for other volcanoes: Stille et al. [1983], West et al. [1987], Abouchami et al. [2000], Blichert-Toft et al. [2003].

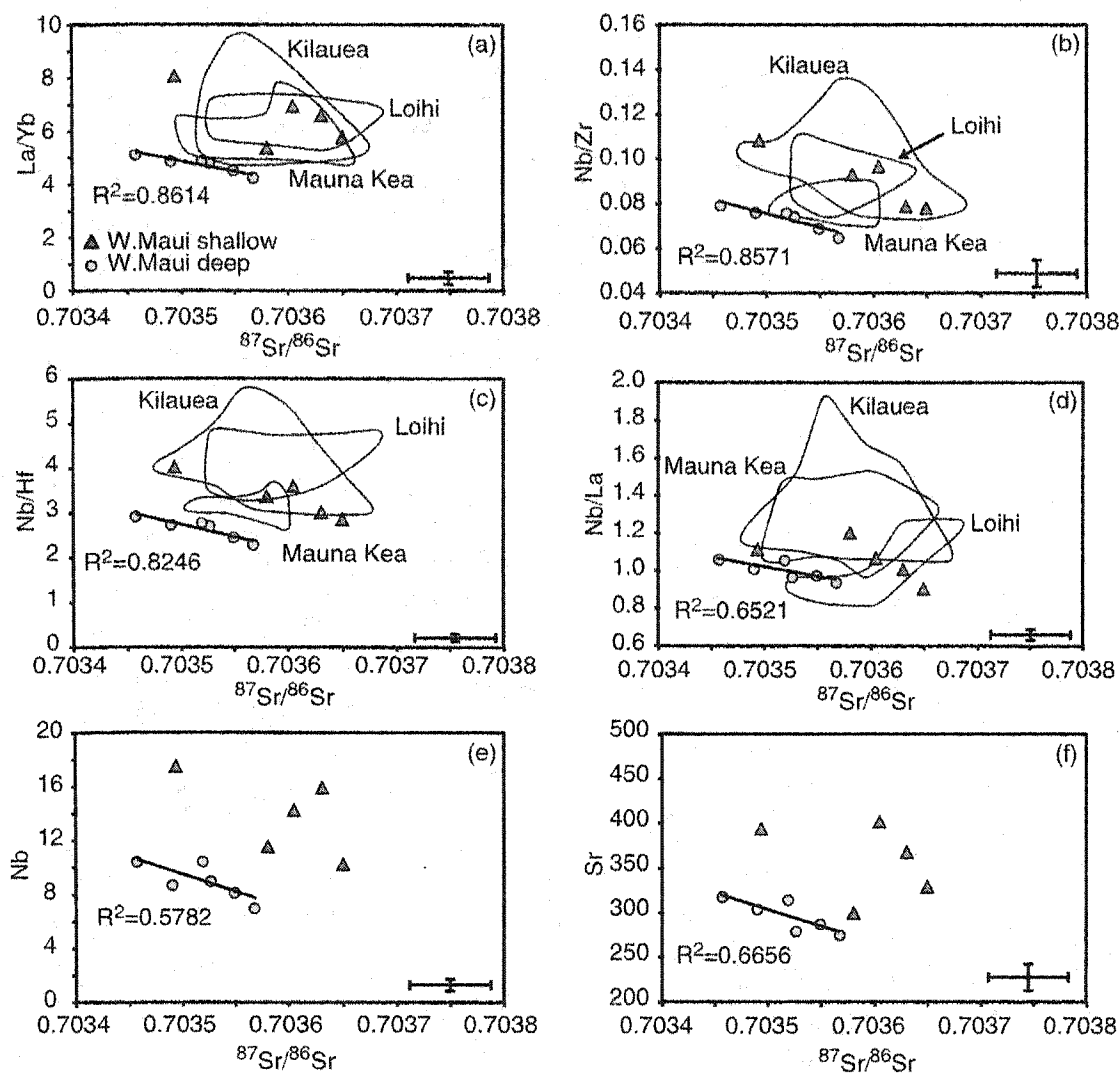


Figure 1.11: Trace element- $^{87}\text{Sr}/^{86}\text{Sr}$  variation diagrams. All trace element concentrations are normalized to 13 wt. % MgO. Error bar represents 2-sigma external reproducibility. Shown for comparison are fields for tholeiitic lavas from Mauna Kea, Kilauea and Loihi. Data sources: Garcia et al. [1993], Garcia et al. [1995], Albarède [1996], Chen et al. [1996], Hofmann and Jochum [1996], Lassiter et al. [1996], Pietruszka and Garcia [1999].

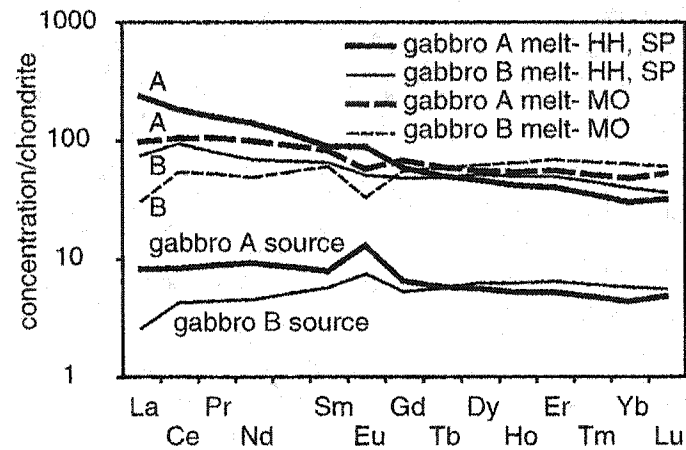


Figure 1.12: Range of possible REE concentrations for 2% melts of oceanic gabbro. Gabbro A and gabbro B represent typical range of ophiolite gabbro compositions (Zimmer et al. [1995], see text for discussion). Melts shown are for 2% melting of gabbro A and gabbro B using partition coefficients from Hauri and Hart [1995] for olivine, orthopyroxene, and clinopyroxene and Schnetzler and Philpotts [1970] for plagioclase (HH-SP) or from McKenzie and O'Nions [1991] for all minerals (MO).



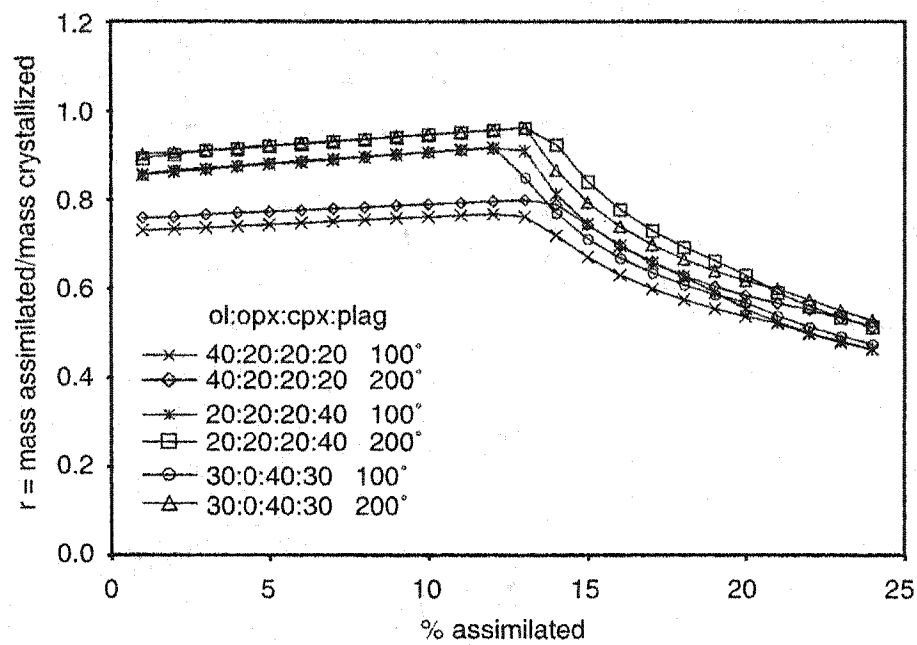


Figure 1.13: Results of MELTS [Ghiorso and Sack, 1995] models of assimilation of gabbro into primitive shallow West Maui magma. Different runs are labeled by mode of olivine : orthopyroxene : clinopyroxene : plagioclase and starting temperature of assimilant. See text for discussion of parameters.

Table 1.1: Major and trace element compositions of West Maui lavas

Sample:	OL28 deep	OL30 deep	OL31 deep	OL32 deep	OL33A deep	OL34 deep
<i>wt. %</i>						
SiO <sub>2</sub>	49.14	49.44	49.66	50.08	50.37	49.56
Al <sub>2</sub> O <sub>3</sub>	13.39	12.71	13.33	13.65	13.41	13.18
TiO <sub>2</sub>	2.786	2.311	2.321	2.619	2.470	2.282
FeO <sub>t</sub>	11.28	11.33	11.32	11.39	11.59	11.89
MnO	0.164	0.174	0.177	0.176	0.172	0.178
CaO	10.76	10.55	11.28	11.32	11.45	11.31
MgO	8.61	10.12	8.62	7.62	7.49	7.86
K <sub>2</sub> O	0.41	0.28	0.34	0.36	0.29	0.28
Na <sub>2</sub> O	2.45	2.15	2.28	2.37	2.16	2.15
P <sub>2</sub> O <sub>5</sub>	0.324	0.237	0.251	0.284	0.268	0.237
Total	99.32	99.30	99.58	99.87	99.67	98.93
LOI	-0.03	0.25	-0.11	-0.12	-0.09	0.05
<i>ppm: XRF</i>						
Ni	226	296	173	127	88	95
Cr	351	538	466	318	302	343
Sc	39	35	25	36	32	33
Ga	20	18	19	20	16	18
Zn	102	102	104	104	100	99
<i>ICP-MS</i>						
Cs	0.06	0.05	0.05	0.06	0.04	0.04
Rb	5.68	3.53	3.95	4.66	3.79	3.58
Ba	88.9	51.4	68.1	79.4	60.0	57.1
Th	0.84	0.57	0.63	0.77	0.66	0.62
U	0.26	0.18	0.19	0.24	0.21	0.19
Nb	12.6	8.7	9.8	12.2	10.5	10.3
Ta	0.90	0.62	0.67	0.82	0.73	0.69
La	12.7	9.0	9.7	11.5	10.9	9.8
Ce	30.0	21.8	23.2	27.5	24.9	23.0
Pb	0.92	0.73	0.73	0.93	0.73	0.70
Pr	4.32	3.18	3.32	3.93	3.81	3.40
Nd	21.5	16.1	16.8	19.8	19.2	17.0
Sr	377	310	344	372	327	313
Sm	6.62	5.23	5.29	6.18	6.05	5.44
Hf	4.53	3.57	3.59	4.17	3.88	3.60
Zr	163	127	129	153	141	130
Eu	2.34	1.90	1.92	2.24	2.16	1.96
Gd	7.20	5.87	5.82	6.81	6.62	6.15
Tb	1.16	0.97	0.96	1.10	1.08	1.00
Dy	6.68	5.73	5.73	6.40	6.35	5.87
Ho	1.22	1.08	1.05	1.18	1.19	1.11
Y	30.7	27.1	26.9	30.6	30.8	28.3
Er	3.00	2.65	2.61	2.96	2.98	2.80
Tm	0.39	0.35	0.34	0.39	0.39	0.36
Yb	2.26	2.00	2.00	2.25	2.27	2.09
Lu	0.33	0.29	0.28	0.32	0.33	0.30

Table 1.1, continued:

Sample:	WA09 deep	WA10 deep	WA12 deep	WA18 deep	WA21 deep	WA22 deep
<i>wt. %</i>						
SiO <sub>2</sub>	49.51	47.48	51.20	48.51	48.72	46.93
Al <sub>2</sub> O <sub>3</sub>	14.21	13.09	13.91	13.26	13.73	12.01
TiO <sub>2</sub>	2.562	3.014	2.312	2.784	2.687	2.328
FeO <sub>t</sub>	11.60	12.53	10.36	12.14	12.01	12.38
MnO	0.173	0.184	0.176	0.173	0.165	0.183
CaO	11.54	11.22	11.83	10.58	11.02	9.59
MgO	7.10	7.51	7.21	8.99	8.15	13.03
K <sub>2</sub> O	0.28	0.40	0.24	0.47	0.17	0.13
Na <sub>2</sub> O	2.49	2.49	2.29	2.60	2.23	1.88
P <sub>2</sub> O <sub>5</sub>	0.280	0.335	0.234	0.372	0.240	0.250
Total	99.75	98.26	99.76	99.87	99.12	98.71
LOI	-0.24	-0.35	0.09	-0.21	1.29	1.01
<i>ppm: XRF</i>						
Ni	120	112	75	211	141	505
Cr	322	284	324	397	429	691
Sc	25	28	29	33	36	28
Ga	20	19	21	20	19	16
Zn	104	113	94	104	103	103
<i>ICP-MS</i>						
Cs	0.02	0.05	0.03	0.11	0.05	0.01
Rb	2.88	4.15	2.90	5.11	2.09	1.33
Ba	73.0	139.3	51.7	122.9	60.1	50.4
Th	0.68	1.19	0.55	0.98	0.81	0.66
U	0.19	0.28	0.18	0.28	0.23	0.17
Nb	10.6	17.9	8.2	14.9	12.3	10.4
Ta	0.73	1.21	0.56	0.99	0.83	0.71
La	10.7	17.1	8.8	15.3	12.0	9.9
Ce	25.7	38.5	21.4	35.2	25.4	22.3
Pb	0.75	1.00	0.54	1.04	0.68	0.60
Pr	3.74	5.32	3.15	4.91	4.20	3.44
Nd	19.0	25.5	16.4	24.2	21.4	17.8
Sr	370	426	325	439	341	314
Sm	6.05	7.38	5.34	7.08	6.65	5.61
Hf	4.01	5.15	3.59	4.82	4.27	3.75
Zr	145	187	127	179	156	137
Eu	2.14	2.52	1.87	2.42	2.34	2.05
Gd	6.46	7.74	5.92	7.57	7.62	6.31
Tb	1.05	1.21	0.98	1.18	1.21	1.00
Dy	6.00	6.89	5.76	6.89	6.92	5.87
Ho	1.15	1.26	1.10	1.27	1.33	1.09
Y	28.4	31.9	27.6	32.7	35.8	27.8
Er	2.77	3.01	2.67	3.12	3.23	2.71
Tm	0.36	0.40	0.36	0.41	0.42	0.35
Yb	2.07	2.25	2.08	2.30	2.34	2.03
Lu	0.31	0.32	0.30	0.34	0.35	0.30

Table 1.1. continued:

Sample:	OL29	LT24	LT18	LT21	LT22	LT27
	shallow	shallow	shallow	shallow	shallow	shallow
<i>wt. %</i>						
SiO <sub>2</sub>	48.64	45.19	45.75	45.90	46.26	45.98
Al <sub>2</sub> O <sub>3</sub>	12.41	8.72	8.45	9.66	10.01	12.12
TiO <sub>2</sub>	2.471	1.673	1.580	1.896	1.949	2.423
FeO <sub>t</sub>	11.78	12.82	12.42	12.50	12.57	12.71
MnO	0.180	0.185	0.217	0.183	0.178	0.185
CaO	9.38	8.77	8.64	9.05	9.16	10.42
MgO	10.20	19.83	20.73	17.87	16.83	12.87
K <sub>2</sub> O	0.77	0.25	0.25	0.25	0.34	0.23
Na <sub>2</sub> O	2.56	1.50	1.48	1.62	1.75	2.16
P <sub>2</sub> O <sub>5</sub>	0.391	0.198	0.191	0.225	0.234	0.319
Total	98.79	99.14	99.71	99.15	99.28	99.42
LOI	-0.30	-0.61	-0.13	-0.40	-0.30	0.21
<i>ppm: XRF</i>						
Ni	340	793	882	727	684	429
Cr	404	1232	1312	1016	988	613
Sc	25	31	32	30	28	27
Ga	19	11	13	11	15	19
Zn	120	100	101	103	103	107
<i>ICP-MS</i>						
Cs	0.11	0.01	0.01	0.00	0.10	0.01
Rb	10.61	1.97	2.39	1.31	5.25	0.57
Ba	143.1	61.0	93.4	70.1	73.1	127.6
Th	1.18	0.44	0.44	0.53	0.57	0.90
U	0.42	0.13	0.13	0.15	0.19	0.15
Nb	17.2	7.6	7.4	8.9	9.2	14.2
Ta	1.16	0.53	0.52	0.62	0.63	0.99
La	17.1	7.3	8.5	8.8	10.2	13.4
Ce	40.3	17.7	18.6	21.0	21.5	31.2
Pb	1.25	0.54	0.55	0.68	0.65	1.01
Pr	5.58	2.55	2.73	3.03	3.47	4.28
Nd	26.9	12.9	13.9	15.1	17.4	20.8
Sr	397	253	260	288	296	402
Sm	7.93	3.92	4.19	4.71	5.27	6.01
Hf	5.72	2.67	2.62	3.11	3.22	3.96
Zr	218	96	95	114	118	147
Eu	2.60	1.42	1.47	1.64	1.85	2.06
Gd	8.06	4.28	4.65	5.13	5.63	6.31
Tb	1.29	0.70	0.73	0.81	0.90	0.99
Dy	7.56	3.96	4.26	4.71	5.21	5.59
Ho	1.38	0.74	0.80	0.88	0.98	1.05
Y	35.5	18.6	21.6	22.5	26.2	26.4
Er	3.47	1.87	1.98	2.20	2.44	2.57
Tm	0.45	0.23	0.25	0.29	0.31	0.33
Yb	2.61	1.37	1.43	1.63	1.78	1.93
Lu	0.38	0.20	0.20	0.24	0.25	0.28

Table 1.1, continued:

Sample:	WA05 shallow	WA13 shallow	WA14 shallow	WA16 shallow	WA17 shallow	WA19 shallow
<i>wt. %</i>						
SiO <sub>2</sub>	47.53	46.24	48.64	49.19	48.21	48.67
Al <sub>2</sub> O <sub>3</sub>	14.27	14.59	14.09	13.95	11.65	13.18
TiO <sub>2</sub>	3.015	3.416	3.384	2.693	2.080	3.183
FeO	13.38	14.00	12.47	11.85	11.71	13.09
MnO	0.194	0.205	0.185	0.179	0.195	0.191
CaO	11.48	11.10	10.38	11.61	9.62	10.22
MgO	6.70	5.87	6.39	7.25	13.61	7.22
K <sub>2</sub> O	0.29	0.19	0.46	0.31	0.34	0.65
Na <sub>2</sub> O	2.89	2.65	2.84	2.40	2.15	2.70
P <sub>2</sub> O <sub>5</sub>	0.356	0.408	0.443	0.305	0.245	0.394
Total	100.11	98.67	99.28	99.73	99.81	99.50
LOI	-0.26	0.92	0.25	-0.06	-0.65	-0.36
<i>ppm: XRF</i>						
Ni	81	50	100	106	511	132
Cr	122	50	190	218	582	213
Sc	22	33	30	33	26	37
Ga	21	24	24	18	18	22
Zn	122	128	118	102	104	117
<i>ICP-MS</i>						
Cs	0.01	0.02	0.06	0.03	0.04	0.12
Rb	0.80	0.47	5.86	3.26	4.99	10.24
Ba	130.3	121.6	122.9	83.7	77.3	168.3
Th	0.94	1.23	1.25	0.82	0.60	1.39
U	0.19	0.18	0.31	0.20	0.21	0.41
Nb	15.0	19.6	19.2	13.1	11.3	20.8
Ta	1.02	1.30	1.27	0.87	0.68	1.39
La	14.7	17.7	18.5	12.5	9.4	18.7
Ce	34.2	42.3	42.6	30.3	22.0	42.4
Pb	0.97	1.12	1.16	0.83	0.67	1.18
Pr	5.02	5.78	5.87	4.20	3.14	5.65
Nd	25.5	28.0	28.5	20.8	15.7	26.8
Sr	513	525	472	408	294	469
Sm	7.85	8.21	8.30	6.25	4.83	7.64
Hf	4.90	5.54	5.75	4.40	3.36	5.18
Zr	176	210	218	161	121	193
Eu	2.76	2.78	2.86	2.22	1.76	2.56
Gd	8.56	8.50	8.76	6.81	5.35	8.05
Tb	1.33	1.35	1.40	1.10	0.87	1.24
Dy	7.82	7.80	7.97	6.25	5.07	7.07
Ho	1.46	1.44	1.45	1.17	0.96	1.30
Y	36.9	36.2	37.4	29.6	24.4	33.2
Er	3.59	3.55	3.55	2.86	2.36	3.17
Tm	0.47	0.46	0.46	0.37	0.31	0.40
Yb	2.67	2.63	2.63	2.15	1.76	2.32
Lu	0.40	0.38	0.38	0.31	0.27	0.35

Table 1.1, continued:

Sample:	WA03	WA04	WA06	HO36	LA35
	transitional	transitional	transitional	post-shield	rejuvenated
<i>wt. %</i>					
SiO <sub>2</sub>	48.24	47.46	48.24	58.22	44.56
Al <sub>2</sub> O <sub>3</sub>	14.72	13.60	14.15	17.88	12.53
TiO <sub>2</sub>	2.809	3.360	3.176	1.145	2.235
FeO <sub>t</sub>	11.95	13.80	13.25	6.39	12.26
MnO	0.172	0.197	0.192	0.237	0.198
CaO	10.94	10.86	10.81	3.20	9.83
MgO	7.06	6.96	5.80	1.64	11.47
K <sub>2</sub> O	0.60	0.34	0.51	2.72	1.37
Na <sub>2</sub> O	2.88	2.83	2.89	7.03	4.15
P <sub>2</sub> O <sub>5</sub>	0.394	0.419	0.412	0.633	0.475
Total	99.77	99.82	99.43	99.09	99.07
LOI	-0.16	-0.40	-0.09	0.29	-0.30
<i>ppm: XRF</i>					
Ni	124	123	46	5	304
Cr	225	126	56	0	522
Sc	30	30	28	7	25
Ga	22	21	22	21	20
Zn	122	127	118	161	119
<i>ICP-MS</i>					
Cs	0.08	0.02	0.10	0.21	0.45
Rb	9.17	2.15	8.32	49.04	39.67
Ba	162.1	130.8	147.9	722.3	633.8
Th	1.07	1.04	1.13	6.14	5.30
U	0.37	0.23	0.35	1.66	1.25
Nb	17.5	16.5	18.1	88.4	51.0
Ta	1.17	1.12	1.22	5.70	3.10
La	31.8	16.3	17.2	77.4	39.4
Ce	79.8	38.2	39.3	145.9	70.3
Pb	1.03	1.01	1.12	4.85	2.77
Pr	10.53	5.43	5.41	18.72	7.76
Nd	50.7	27.4	26.3	77.7	31.8
Sr	513	458	497	1072	796
Sm	13.96	8.16	7.68	17.33	7.35
Hf	4.94	5.51	5.23	16.83	4.85
Zr	190	200	192	736	201
Eu	4.90	2.80	2.64	5.36	2.45
Gd	15.33	8.76	8.06	14.72	6.93
Tb	2.49	1.37	1.27	2.29	1.02
Dy	14.82	7.85	7.30	12.91	5.54
Ho	2.95	1.44	1.35	2.49	0.98
Y	93.3	36.7	33.7	76.9	25.1
Er	7.60	3.62	3.33	6.41	2.32
Tm	1.01	0.47	0.42	0.88	0.30
Yb	5.65	2.58	2.44	5.19	1.69
Lu	0.83	0.38	0.36	0.78	0.24

Table 1.2: Sr, Nd and Hf isotope compositions of West Mati lavas

<i>Papalaua Gulch Section</i>		$^{87}\text{Sr}/^{86}\text{Sr}$	$^{143}\text{Nd}/^{144}\text{Nd}$	$\epsilon_{\text{Nd}}$	$^{176}\text{Hf}/^{177}\text{Hf}$	$\epsilon_{\text{Hf}}$
<b>Shallow</b>						
UP50	5	0.703604			0.283131	12.7
UP47	38	0.703634	0.512982	6.7	0.283100	11.6
UP46	58	0.703497	0.512988	6.8	0.283099	11.6
UP43	79	0.703596	0.512999	7.0	0.283108	11.9
UP41	91	0.703596			0.283115	12.1
UP40	100	0.703565			0.283122	12.4
UP39	102	0.703574			0.283112	12.0
UP37	107	0.703572	0.513010	7.3	0.283110	11.9
LP16	121	0.703620	0.512992	6.9	0.283123	12.4
LP14	144	0.703627			0.283109	11.9
LP13	155	0.703545			0.283119	12.3
LP11	170	0.703593	0.512997	7.0	0.283100	11.6
LP10	181	0.703626	0.512982	6.7	0.283097	11.5
LP05	236	0.703574	0.512995	7.0	0.283117	12.2
LP03	248	0.703499	0.512987	6.8	0.283114	12.1
LP01	260	0.703511	0.513000	7.1	0.283113	12.0

Table 1.2, continued:

<i>Mahinahina Well Section</i>		$^{87}\text{Sr}/^{86}\text{Sr}$	$^{143}\text{Nd}/^{144}\text{Nd}$	$\epsilon_{\text{Nd}}$	$^{176}\text{Hf}/^{177}\text{Hf}$	$\epsilon_{\text{Hf}}$
<b>Shallow</b>						
MA30	9				0.283128	12.6
MA50	15				0.283115	12.1
MA100	30				0.283123	12.4
MA120	36				0.283121	12.4
MA150	45				0.283120	12.3
MA190	58	0.703598	0.513015	7.4	0.283129	12.6
MA210	64				0.283110	12.0
MA240	73				0.283108	11.9
<b>Deep</b>						
MA270	82	0.703368	0.513028	7.6	0.283131	12.7
MA320	97	0.703565	0.513003	7.1	0.283131	12.7
MA330	100	0.703404	0.513017	7.4	0.283102	11.7
MA390	118				0.283114	12.1
MA410	124	0.703563	0.513005	7.2	0.283108	11.9
MA460	139				0.283119	12.3
MA490	148				0.283124	12.4
MA520	158	0.703452	0.513029	7.6	0.283127	12.5
MA560	170	0.703449			0.283148	13.3
MA600	182				0.283127	12.6
MA650	197	0.703500	0.512971	6.5	0.283125	12.5
MA670	203				0.283113	12.0
MA800	242	0.703468	0.512999	7.0	0.283147	13.3
MA840	255				0.283135	12.8
MA865	262	0.703472			0.283155	13.5
MA895	271				0.283117	12.2
MA910	276	0.703470	0.513014	7.3	0.283119	12.3
MA945	286	0.703488	0.513040	7.8	0.283130	12.7
MA965	292				0.283117	12.2
MA970	294	0.703402	0.513032	7.7	0.283110	12.0
MA1020	309	0.703372	0.513002	7.1	0.283130	12.7
MA1135	344				0.283129	12.6



Table 1.2, continued:

	$^{87}\text{Sr}/^{86}\text{Sr}$	$^{143}\text{Nd}/^{144}\text{Nd}$	$\epsilon_{\text{Nd}}$	$^{176}\text{Hf}/^{177}\text{Hf}$	$\epsilon_{\text{Hf}}$
<b>'Breadth' samples - shallow</b>					
LT18				0.283117	12.2
LT21				0.283135	12.8
LT22	0.703650	0.513008	7.2	0.283120	12.3
LT24				0.283123	12.4
LT27	0.703605	0.512996	7.0	0.283108	11.9
OL29	0.703631	0.513004	7.1	0.283118	12.2
WA05				0.283117	12.2
WA13	0.703584			0.283119	12.3
WA14				0.283097	11.5
WA16				0.283106	11.8
WA17	0.703581			0.283139	13.0
WA19	0.703494	0.512988	6.8	0.283116	12.1
<b>'Breadth' samples - deep</b>					
OL28				0.283135	12.8
OL30	0.703549	0.513019	7.4	0.283143	13.1
OL31	0.703490	0.513043	7.9	0.283145	13.2
OL32	0.703457	0.513009	7.2	0.283135	12.8
OL33A	0.703526			0.283141	13.0
OL34				0.283111	12.0
WA09				0.283104	11.7
WA10				0.283133	12.8
WA12	0.703567	0.513023	7.5	0.283146	13.2
WA18				0.283126	12.5
WA21				0.283138	12.9
WA22	0.703519			0.283136	12.9
<b>Transitional</b>					
WA03				0.283110	12.0
WA04	0.703669	0.512998	7.0	0.283104	11.7
WA06				0.283088	11.2
<b>Post-Shield</b>					
HO36	0.703549	0.512972	6.5	0.283129	12.6
<b>Rejuvenated</b>					
LA35	0.703289	0.513023	7.5	0.283172	14.2

$\epsilon_{\text{Hf}}$  and  $\epsilon_{\text{Nd}}$  describe deviation from chondritic  $^{176}\text{Hf}/^{177}\text{Hf}$  and  $^{143}\text{Nd}/^{144}\text{Nd}$  and are defined as  $10,000 * ((^{176}\text{Hf}/^{177}\text{Hf}_{\text{meas}}/0.282772) - 1)$  and  $10,000 * ((^{143}\text{Nd}/^{144}\text{Nd}_{\text{meas}}/0.512638) - 1)$ , respectively.

Table 1.3: Pb isotope compositions of West Maui lavas

		Depth (m)	$^{206}\text{Pb}/^{204}\text{Pb}$	$^{207}\text{Pb}/^{204}\text{Pb}$	$^{208}\text{Pb}/^{204}\text{Pb}$
<i>Papalaua Gulch Section</i>					
<b>Shallow</b>					
UP50	5	18.477	15.482	37.966	
UP47	38	18.500	15.495	38.005	
UP46	58	18.423	15.477	37.939	
UP43	79	18.440	15.484	37.956	
UP41	91	18.405	15.482	37.934	
UP40	100	18.407	15.484	37.937	
UP39	102	18.402	15.481	37.931	
UP37	107	18.422	15.479	37.948	
LP16	121	18.475	15.484	37.974	
LP14	144	18.444	15.481	37.955	
LP13	155	18.398	15.478	37.925	
LP11	170	18.428	15.484	37.964	
LP10	181	18.426	15.482	37.957	
LP05	236	18.437	15.471	37.935	
LP03	248	18.456	15.481	37.980	
LP01	260	18.454	15.483	37.973	

Table 1.3, continued:

	Depth (m)	$^{206}\text{Pb}/^{204}\text{Pb}$	$^{207}\text{Pb}/^{204}\text{Pb}$	$^{208}\text{Pb}/^{204}\text{Pb}$
<b>Mahinahina Well Section</b>				
<b>Shallow</b>				
MA30	9	18.468	15.488	37.991
MA50	15	18.455	15.489	37.974
MA100	30	18.455	15.484	37.966
MA120	36	18.466	15.496	38.013
MA150	45	18.463	15.490	37.992
MA190	58	18.475	15.497	38.011
MA210	64	18.436	15.480	37.962
MA240	73	18.425	15.479	37.965
<b>Deep</b>				
MA270	82	18.386	15.467	37.916
MA320	97	18.473	15.493	38.018
MA330	100	18.425	15.480	37.978
MA390	118	18.500	15.502	38.051
MA410	124	18.469	15.500	38.023
MA460	139	18.462	15.490	38.007
MA490	148	18.448	15.489	37.994
MA520	158	18.426	15.480	37.956
MA560	170	18.420	15.485	37.974
MA600	182	18.408	15.475	37.942
MA650	197	18.413	15.479	37.951
MA670	203	18.425	15.494	38.000
MA800	242	18.434	15.484	37.971
MA840	255	18.428	15.480	37.980
MA865	262	18.433	15.480	37.972
MA895	271	18.430	15.480	37.961
MA910	276	18.431	15.480	37.960
MA945	286	18.419	15.477	37.960
MA965	292	18.415	15.476	37.959
MA970	294	18.395	15.471	37.952
MA1020	309	18.365	15.470	37.957
MA1135	344	18.382	15.472	37.954

Table 1.3. continued:

	$^{206}\text{Pb}/^{204}\text{Pb}$	$^{207}\text{Pb}/^{204}\text{Pb}$	$^{208}\text{Pb}/^{204}\text{Pb}$
<b>'Breadth' samples - shallow</b>			
LT18	18.506	15.497	38.011
LT21	18.504	15.488	37.987
LT22	18.513	15.498	38.018
LT24	18.501	15.497	38.012
LT27	18.410	15.481	37.929
OL29	18.469	15.493	37.989
WA05	18.456	15.484	37.957
WA13	18.479	15.504	38.005
WA14	18.467	15.487	37.995
WA16	18.429	15.478	37.941
WA17	18.452	15.483	37.988
WA19	18.387	15.473	37.926
<b>'Breadth' samples - deep</b>			
OL28	18.433	15.477	37.963
OL30	18.397	15.476	37.936
OL31	18.531	15.497	38.037
OL32	18.388	15.480	37.935
OL33A	18.540	15.500	38.057
OL34	18.469	15.483	38.001
WA09	18.369	15.479	37.936
WA10	18.363	15.474	37.895
WA12	18.445	15.493	37.980
WA18	18.448	15.488	37.987
WA21	18.467	15.491	38.004
WA22	18.425	15.474	37.934
<b>Transitional</b>			
WA03	18.838	15.564	38.264
WA04	18.505	15.494	38.013
WA06	18.467	15.494	37.992
<b>Post-Shield</b>			
HO36	18.508	15.483	38.023
<b>Rejuvenated</b>			
LA35	18.181	15.446	37.792

Pb isotope compositions are normalized to NIST  
 SRM-981  $^{206}\text{Pb}/^{204}\text{Pb}=36.7006$ ,  $^{207}\text{Pb}/^{204}\text{Pb}=15.4891$   
 and  $^{208}\text{Pb}/^{204}\text{Pb}=16.9356$  (Todt et al., 1996).

Table 1.4: Calculated compositions of aged oceanic lithosphere

	$^{87}\text{Sr}/^{86}\text{Sr}$	[Sr] ppm	$^{206}\text{Pb}/^{204}\text{Pb}$	[Pb] ppm	$^{177}\text{Hf}/^{177}\text{Hf}$	[Hf] ppm
<b>110 Ma endmembers</b>						
upper oceanic crust	0.7031	118	18.59	0.7	0.28317-0.28320	1.8
gabbroic lower oceanic crust, 2% melt	0.7027	479	18.35	6.6	0.28315-0.28318	28.8
<b>2 Ga endmembers</b>						
upper oceanic crust	0.7071-0.7088	118	23.5-25.8	0.7	0.2829-0.2832	1.8
gabbroic lower oceanic crust	0.7009-0.7027	158	14.6-17.1	0.6	0.2826-0.2829	2.1

## Chapter 2

**OXYGEN-OSMIUM ISOTOPIC COMPOSITIONS OF WEST MAUI  
LAVAS AND THE LINK TO OCEANIC LITHOSPHERE****2.1 Introduction**

Combined  $^{187}\text{Os}/^{188}\text{Os}$  -  $\delta^{18}\text{O}$  systematics are sensitive tracers of important geologic processes through which OIB sources are formed. Oxygen isotopic fractionation occurs during low-temperature processes at the Earth's surface, whereas the most significant perturbations in the Re-Os system occur during mantle melting processes. Thus, the combination of  $^{187}\text{Os}/^{188}\text{Os}$  and  $\delta^{18}\text{O}$  tracers with lithophile element isotopic tracers (Sr-Nd-Hf-Pb) presents a powerful tool for distinguishing among processes that may ultimately shape the geochemical characteristics of mantle-derived magmas.

In Hawaiian shield basalts, the observed isotopic (Sr-Nd-Pb-Hf-Os-O) compositional variability is broadly described by mixing between two compositional endmembers: the relatively enriched Koolau component and the relatively depleted Kea component [Stille et al., 1986]. Kilauea, Mauna Kea, West Maui and East Molokai are the volcanoes most dominated by the Kea component. These volcanoes are characterized by greater Sr-Nd-Hf isotopic homogeneity, on both intra- and inter-volcano scales, than volcanoes dominated by Koolau-type compositions, and this homogeneity reflects the processes that lead to the formation and eruption of Kea-type lavas. Of these volcanoes, previously-published  $^{187}\text{Os}/^{188}\text{Os}$  and  $\delta^{18}\text{O}$  data exist only for Kilauea and Mauna Kea. These data, combined with  $^{187}\text{Os}/^{188}\text{Os}$  and  $\delta^{18}\text{O}$  data for other Hawaiian volcanoes, have been used to argue that the range of source material in the Hawaiian plume derives from oceanic lithosphere that has been subducted, stored in the mantle and recycled into the Hawaiian plume [Lassiter and Hauri, 1998]. In this scenario, the Koolau endmember represents the upper basaltic + pelagic sediment segments of oceanic lithosphere, and the Kea endmember represents the

lower gabbroic + harzburgite/lherzolite segments of the same package of oceanic lithosphere [Lassiter and Hauri, 1998]. Eiler et al. [1996] and Wang et al. [2003] use  $\delta^{18}\text{O}$  data and major element differentiation trends to argue that the source of the Kea compositional end-member is the local Pacific lithosphere or the volcanic edifice itself. Recently, Gaffney et al. [2004] used  $^{87}\text{Sr}/^{86}\text{Sr}$ - $^{206}\text{Pb}/^{204}\text{Pb}$ -trace element correlations to identify small degree melts of the gabbroic layer of ambient Pacific oceanic crust as the source of fine-scale compositional trends observed in a subset of West Maui lavas. Thus, there are several scenarios in which oceanic lithosphere, both ancient recycled lithosphere and local Pacific lithosphere, could play a significant role in generating the compositional range of Hawaiian lavas.

West Maui is a  $\sim 1.8$  Ma expression of Kea-type magma generation. Analysis of West Maui lavas serves to both expand the existing data set for Kea-type lavas, and to evaluate variability in the Kea component over a  $\sim 1.8$  Ma time window. With this study, we a) describe the  $^{187}\text{Os}/^{188}\text{Os}$  and  $\delta^{18}\text{O}$  variability in late shield-building stage West Maui lavas, b) evaluate the oceanic lithosphere hypotheses for the origin of  $^{187}\text{Os}/^{188}\text{Os}$  and  $\delta^{18}\text{O}$  compositional variation and, c) discuss the West Maui isotopic variability in terms of implications for the origin of the Kea component.

## **2.2 Samples and Procedures**

The samples are late shield-stage tholeiites from West Maui volcano, Hawaii, and are a subset of the samples discussed by Gaffney et al. [2004]. They are all fine-grained, olivine-phyric basalts, and a few samples contain very rare plagioclase and clinopyroxene grains. For Os-O isotope analysis, we chose samples that were both Mg-rich and contained olivine phenocrysts. Of the samples for which we have MgO composition data, only one sample has  $\text{MgO} > 13$  wt.%, and therefore may have accumulated olivine which was not in equilibrium with the host magma. On the basis of stratigraphic relationships and field observations (sample distance from caldera and collection depth within volcanic edifice) we have classified samples as deep (relatively older) and shallow (relatively younger). Additional detail on sample location and classification criteria is presented in Gaffney et al. [2004]. These stratigraphic groupings have geochemical significance, evident in many isotopic and trace

element indicators, so we use these categories in subsequent geochemical discussion. Major and trace element and Sr-Pb-Hf-Nd isotopic data for these samples are presented in Gaffney et al. [2004].

We analyzed  $\delta^{18}\text{O}$  compositions on olivine phenocrysts from 15 samples. We prepared samples by crushing and hand-picking olivine under binocular microscope, washing the olivine in  $\sim 1$  N HCl, rinsing in ultrapure- $\text{H}_2\text{O}$ , ultrasonicing in an ethanol bath, and drying. After washing the olivine separates, we re-examined them under the binocular microscope and removed any fragments that contained visible inclusions or alteration. We analyzed the olivine by laser fluorination at the California Institute of Technology, using the procedure described by Eiler et al. [2000a,b]. We ran GMG garnet standards and San Carlos olivine secondary silicate standards interspersed with the sample analyses. All samples analyzed on any given day were normalized to GMG = 5.75‰, based upon the GMG standards run on that same day. Daily average standard deviation (1-sigma) for both standards is typically  $< 0.08\text{‰}$ . All samples were measured in duplicate, and average standard deviation (1-sigma) for GMG-normalized sample replicate analyses is  $\pm 0.09\text{‰}$ .

We prepared samples for Os isotopic analysis using powder ground with an agate mortar and pestle, and standard Carius-tube dissolution and HBr microdistillation techniques [Shirey and Walker, 1995; Reisberg et al., 1997] for Os separation. We measured Os isotopic composition by N-TIMS at CRPG/CNRS, Vandœuvre-les-Nancy, France [Creaser et al., 1991; Volkening et al., 1991]. We ran the Os standard between every 3 samples. The Os standards run over the course of these analyses gave  $^{187}\text{Os}/^{188}\text{Os} = 0.17377 \pm 0.00040$  (2-sigma,  $n=9$ ). Osmium concentrations for the samples were determined through isotope dilution analyses on the same aliquot for which the isotopic compositions were determined. Error on Os concentrations is determined through duplicate dissolutions, chemical separations and analyses of four samples, and ranges from 0 to 44%. This wide range likely reflects the high degree of control that very small amounts of sulfides can have on the Os concentrations.



### 2.3 Results

The deep West Maui samples have  $^{187}\text{Os}/^{188}\text{Os} = 0.1316\text{-}0.1327$  and  $[\text{Os}] = 61\text{-}399$  ppt; with one exception, the shallow samples have  $^{187}\text{Os}/^{188}\text{Os} = 0.1331\text{-}0.1346$  and  $[\text{Os}] = 41\text{-}273$  ppt (Table 1). One shallow sample has extremely low  $[\text{Os}]$  (20 ppt) and extremely high  $^{187}\text{Os}/^{188}\text{Os}$  (0.158), which we believe reflects shallow-level contamination. Otherwise, Os concentrations are generally above the threshold ( $\sim 50$  ppt) below which Os crustal contamination may affect isotopic compositions. Within the deep sample group, there is a strong negative correlation between  $^{187}\text{Os}/^{188}\text{Os}$  and  $[\text{Os}]$ . Both stratigraphic groups have similar absolute ranges in  $\delta^{18}\text{O}$ , 4.53-4.88‰ in the deep samples and 4.73-5.21‰ in the shallow samples, although the deep samples extend to slightly lower values, and the shallow samples extend to slightly higher values (Figs. 2.1, 2.2). MgO data exist for 9 of the 14 samples for which we have Os data (MgO compositions reported in Gaffney et al. [2004]), and for these 9 samples, there is no significant correlation of either  $[\text{Os}]$  or  $^{187}\text{Os}/^{188}\text{Os}$  with MgO.

The West Maui lavas have  $^{187}\text{Os}/^{188}\text{Os}$  compositions that generally reflect their Kea-like affinity. They fall near the unradiogenic  $^{187}\text{Os}/^{188}\text{Os}$  end of the all-Hawaii range, although Kea-type lavas from the younger Mauna Kea volcano extend to the most unradiogenic compositions of all Hawaiian shield-stage lavas (Fig. 2.3) [Lassiter and Hauri, 1998]. The deep West Maui lavas overlap with the field defined by Kea-type lavas from Kilauea and Mauna Kea, and the shallow West Maui lavas have more radiogenic  $^{187}\text{Os}/^{188}\text{Os}$  than observed at either of these volcanoes.

With one exception, the West Maui samples fall within the  $\delta^{18}\text{O}$  range of Kea-type lavas as defined by Mauna Kea and Kilauea [Eiler et al., 1996; Wang et al., 2003]. Together, these three volcanoes have the lightest  $\delta^{18}\text{O}$  compositions of all Hawaiian shield stage lavas. In contrast with the  $^{187}\text{Os}/^{188}\text{Os}$  composition of these lavas, the deep and shallow West Maui sample groups do not show any distinction in their  $\delta^{18}\text{O}$  composition. Although both sample groups show subtle, sub-parallel  $\delta^{18}\text{O}$ - $^{187}\text{Os}/^{188}\text{Os}$  trends, the range in  $\delta^{18}\text{O}$  is close to the limit of analytical uncertainty. In contrast, the whole suite of Hawaiian shield-stage lavas shows a significant positive  $\delta^{18}\text{O}$ - $^{187}\text{Os}/^{188}\text{Os}$  correlation (Fig. 2.3). This trend is not

apparent within lavas from any individual volcano.

The deep West Maui samples show a negative  $^{187}\text{Os}/^{188}\text{Os}$ - $^{87}\text{Sr}/^{86}\text{Sr}$  correlation which contrasts with the positive  $^{187}\text{Os}/^{188}\text{Os}$ - $^{87}\text{Sr}/^{86}\text{Sr}$  correlation in the overall Hawaii shield-stage trend (Fig. 2.4). An analogous trend is not evident in the shallow samples, or in the lavas from other individual volcanoes. No trends between either  $^{187}\text{Os}/^{188}\text{Os}$  or  $\delta^{18}\text{O}$  and  $^{143}\text{Nd}/^{144}\text{Nd}$   $^{176}\text{Hf}/^{177}\text{Hf}$  or  $^{206}\text{Pb}/^{204}\text{Pb}$  isotopic compositions are apparent. In part, this may reflect the smaller sample set presented in this paper, compared to the larger West Maui sample set discussed by Gaffney et al. [2004], for which they observe a positive  $^{206}\text{Pb}/^{204}\text{Pb}$ - $^{87}\text{Sr}/^{86}\text{Sr}$  trend. Although the subset of deep samples discussed here do show  $^{187}\text{Os}/^{188}\text{Os}$ - $^{87}\text{Sr}/^{86}\text{Sr}$  correlations, these samples do not show an analogous  $^{187}\text{Os}/^{188}\text{Os}$ - $^{206}\text{Pb}/^{204}\text{Pb}$  trend.

## 2.4 Discussion

West Maui lavas have generally Kea-like  $^{187}\text{Os}/^{188}\text{Os}$  and  $\delta^{18}\text{O}$  compositions, although the Kea-type lavas from Mauna Kea and Kilauea extend to lower  $^{187}\text{Os}/^{188}\text{Os}$  values than observed in West Maui.  $\delta^{18}\text{O}$ - $^{187}\text{Os}/^{188}\text{Os}$  and  $^{87}\text{Sr}/^{86}\text{Sr}$ - $^{187}\text{Os}/^{188}\text{Os}$  variations among all Hawaiian shield-stage lavas together delineate general positive correlations, yet trends within individual volcanoes tend to be less well-defined. This may be related to the generally reconnaissance nature of most Hawaiian  $^{187}\text{Os}/^{188}\text{Os}$  data sets, but may also represent a lack of coherence of  $^{187}\text{Os}/^{188}\text{Os}$  with other isotopic systems on the relatively short time and length scales represented by single volcanoes. The deep West Maui lavas are unique among Hawaiian volcanoes in that they define a negative  $^{87}\text{Sr}/^{86}\text{Sr}$ - $^{187}\text{Os}/^{188}\text{Os}$  correlation, which contrasts with the positive correlation observed across the Hawaiian trend as a whole [Lassiter and Hauri, 1998]. The trends that we observe both within the deep West Maui samples and among Kea-type lavas in general may reflect a combination of the variation in Hawaiian magma sources, Os behavior during magma-generation processes in the plume, and secondary processes that act upon plume-generated magmas.

#### 2.4.1 Controls on $^{187}\text{Os}/^{188}\text{Os}$ and $\delta^{18}\text{O}$ of mantle-derived magmas

Os isotopic variability in these geochemical systems typically is the result of Re/Os fractionation during mantle melting. Os is compatible in mantle lithologies, whereas Re is incompatible. This leads, over relatively short periods of time compared to lithophile element isotopic systems, to significant variability in  $^{187}\text{Os}/^{188}\text{Os}$ . Partitioning of Re and Os among phases in the mantle and during melting processes is understood at only a basic level, and estimates of partition coefficients vary by orders of magnitude [Hart and Ravizza, 1996; Crocket et al., 1997; Roy-Barman et al., 1998]. Because of the highly compatible nature of Os, melts and complementary residues have [Os] and Re/Os that show extreme variation. Furthermore, recent studies show that Re may be mobile in a variety of processes including hydrothermal alteration at the mid-ocean ridge, dewatering of the slab during subduction, and shallow magmatic degassing [Becker, 2000; Lassiter, 2003].

The  $^{187}\text{Os}/^{188}\text{Os}$  and Os concentrations of mantle-derived magmas are fundamentally dependent on the distribution of Re and Os in the source, and the mechanism for transfer of Os out of the source and into the melt. Os is generally considered to be a compatible element during mantle melting. This apparent compatibility reflects sulfide control on Os concentrations and mobility [e.g. Fleet et al., 1996; Hart and Ravizza, 1996; Burton et al., 1999]. Therefore, an understanding of the sulfide saturation state of the sources and melts in question is important.

Sulfur contents assumed for the mantle OIB and MORB source and observed Os concentrations of OIB and MORB are not consistent with equilibrium partitioning of Os between melt and residual sulfide or PGE(platinum group element)-alloy [Hart and Ravizza, 1996]. If both OIB- and MORB-melting residue contain residual sulfide, and Os undergoes equilibrium partitioning between melt and residual sulfide, then OIB and MORB should have much lower Os concentrations than are observed [Hart and Ravizza, 1996; Roy-Barman et al., 1998]. Bennett et al. [2000] used PGE concentrations in Hawaiian lavas to show that the Hawaiian plume contains residual sulfide. Hart and Ravizza [1996] propose that Os concentrations are controlled by sulfide dissolution but not sulfide partitioning, whereby diffusive Os partitioning does not keep pace with partial melting of sulfides. As sulfides

melt, the Os released to the melt does not partition back into the residual sulfide. A numerical modeling approach to this problem also suggests that diffusion is the dominant control on the composition of sulfide droplets, rather than instantaneous equilibrium partitioning [Mungall, 2002]. This model predicts that Os undergoes the slowest diffusion between sulfide and silicate melts, relative to the rest of the PGEs. Roy-Barman and Allègre [1995] explain the apparent compatible Os behavior in OIB through scavenging of Os by chromite crystallization and sulfide unmixing in the magma chamber during differentiation. Sulfur solubility is dependent on T, P, and compositional parameters ( $f_{O_2}$ ,  $f_{S_2}$ ). Mavrogenes and O'Neill [1999] investigated the relationship between T, P and sulfur saturation in basaltic melts. They show that sulfur content in a melt at the point of sulfide saturation increases exponentially as pressure decreases. Thus, if a melt is sulfide saturated at the time that it separates from the melting residue, it will become undersaturated in sulfide as it rises. In this case, this melt could assimilate, scavenge or otherwise incorporate sulfide from the rock through which it subsequently travels. Such processes as described above could have significant implications for [Os] and  $^{187}\text{Os}/^{188}\text{Os}$  of a melt that interacts with lithosphere on its way to the surface.

In contrast to  $^{187}\text{Os}/^{188}\text{Os}$ ,  $\delta^{18}\text{O}$  variability is introduced primarily through low-temperature processes at or near the Earth's surface. Hydrothermal alteration of oceanic crust, both on and off ridge axes, leads to  $\delta^{18}\text{O}$  values that deviate from typical mantle  $\delta^{18}\text{O}$  compositions ( $\sim 5.4\text{-}5.7\text{‰}$ ). Observations of both ophiolites and oceanic crust drill cores show a progressive change in the  $\delta^{18}\text{O}$  of the oceanic lithosphere with depth. The upper segments of crust (basalts) are characterized by  $\delta^{18}\text{O}$  heavier than typical mantle (up to  $15\text{-}20\text{‰}$ ), whereas the lower gabbroic crustal segments have  $\delta^{18}\text{O}$  lighter than typical mantle (down to  $0\text{-}3\text{‰}$ ) [Gregory and Taylor Jr., 1981; Stakes, 1991; Hart et al., 1999; Miller et al., 2001].  $\delta^{18}\text{O}$  of any of these given components or compositional reservoirs will not vary with aging, thus this parameter is a useful discriminant for process rather than time. Although  $\delta^{18}\text{O}$  is useful for determining whether or not oceanic lithosphere has contributed to Hawaiian magmas, it is the correlation of  $\delta^{18}\text{O}$  with other chemical tracers that is important for determining the process through which this contribution happens.

### 2.4.2 Possible source components for Hawaiian lavas

Several components have been called upon as sources that contribute to Kea-type compositions in Hawaiian magmas, including ambient depleted lithosphere or asthenosphere, metasomatized depleted lithosphere, recycled oceanic lithosphere in the Hawaiian plume, Pacific oceanic crust, and the volcanic edifice itself [e.g. Chen and Frey, 1985; Eiler et al., 1996; Lassiter and Hauri, 1998; Blichert-Toft et al., 1999; Norman and Garcia, 1999; Wang et al., 2003]. Each of these possible source components delineates a range in  $^{187}\text{Os}/^{188}\text{Os}$ - $\delta^{18}\text{O}$ - $^{87}\text{Sr}/^{86}\text{Sr}$  composition which we can use to evaluate as possible contributors to West Maui lavas (Fig. 2.5). Variability in  $^{187}\text{Os}/^{188}\text{Os}$  and  $\delta^{18}\text{O}$  is introduced by very different geologic processes, so together they present a powerful tool for differentiating among the possible magma sources and processes that may have influenced magma compositions.

The generally depleted Sr-Nd-Hf isotope composition of Kea-type magmas has led to interpretations that ambient MORB-source lithosphere and asthenosphere is a source of Hawaiian, and particularly Kea-type, magmas [Chen and Frey, 1985; Hauri, 1996a]. Modern mid-ocean ridge basalts, which sample depleted lithosphere and asthenosphere, have limited ranges in  $\delta^{18}\text{O}_{\text{glass}}$  (5.4-5.8‰; Eiler et al. [2000b]),  $^{187}\text{Os}/^{188}\text{Os}$  (0.1268-0.1316; Roy-Barman et al. [1998]) and  $^{87}\text{Sr}/^{86}\text{Sr}$  ( $\sim$ 0.7015-0.7025, Zindler and Hart [1986]). The MORB-source compositional reservoir does not lie on a mixing trajectory with the  $^{87}\text{Sr}/^{86}\text{Sr}$ - $^{187}\text{Os}/^{188}\text{Os}$  variation of the deep West Maui lavas (Fig. 2.4). It also has  $\delta^{18}\text{O}$  too high to be the primary source of Kea-type compositions in general (Fig. 2.4).

Depleted lithosphere of either continental or oceanic affinity that has been metasomatized or refertilized by small-degree melts is a possible source of Hawaiian magmas [Bennett et al., 1996; Norman and Garcia, 1999]. The effects of refertilization are most apparent in incompatible element tracers, which are disproportionately concentrated in the refertilized lithosphere relative to the depleted major element composition. The  $\delta^{18}\text{O}$ - $^{187}\text{Os}/^{188}\text{Os}$  of such a source would depend upon the origin of both the depleted lithosphere and the metasomatizing melt, as well as the time interval between metasomatism and subsequent melting in the Hawaiian plume. As discussed above, oceanic lithosphere will have unradiogenic  $^{187}\text{Os}/^{188}\text{Os}$  and light  $\delta^{18}\text{O}$ . Mantle-derived metasomatic melt (the product of small

degrees of melting) should contribute little or no Os to the depleted lithosphere. However, this metasomatic melt may have elevated Re/Os, which over time can generate radiogenic  $^{187}\text{Os}/^{188}\text{Os}$ . Metasomatized depleted lithosphere has incompatible trace element patterns and lithophile element isotopes indicative of refertilization-related enrichment, but the  $^{187}\text{Os}/^{188}\text{Os}$  will only reflect the metasomatism if enough time passes between the metasomatic event and melting in the plume. Refertilization will only have a significant effect on the bulk  $\delta^{18}\text{O}$  if the metasomatic melt  $\delta^{18}\text{O}$  is dramatically different from mantle values, and if it contributes in amounts greater than a few percent. A light  $\delta^{18}\text{O}$ , low  $^{187}\text{Os}/^{188}\text{Os}$  metasomatized component may contribute to Kea-type magma compositions, but this component does not have the correct sense of variability to be a source of the deep West Maui compositional trend.

Recycled oceanic lithosphere may contain compositionally distinct sections derived from its basaltic, gabbroic and harzburgite layers [Lassiter and Hauri, 1998]. If this complete recycled lithosphere package is sampled in the Hawaiian plume, the mafic section will dominate the lithophile isotope compositions of the derivative melts, whereas the ultramafic section will dominate the  $^{187}\text{Os}/^{188}\text{Os}$  composition of the derivative melts. Based on the apparent compatibility of Os relative to Re during mantle melting, the mafic parts of ancient recycled oceanic crust will have radiogenic  $^{187}\text{Os}/^{188}\text{Os}$  and low [Os], whereas the ultramafic segments will have unradiogenic  $^{187}\text{Os}/^{188}\text{Os}$  and high [Os].  $\delta^{18}\text{O}$  in the oceanic crust and lithosphere profile is controlled by temperatures and extent of hydrothermal alteration, such that the basaltic layer will have heavier  $\delta^{18}\text{O}$  ( $>5.3\text{‰}$ ) and the gabbroic segments will have lighter  $\delta^{18}\text{O}$  ( $\sim 3\text{--}6\text{‰}$ ) [Gregory and Taylor Jr., 1981; Stakes, 1991; Hart et al., 1999]. The ultramafic segment may have  $\delta^{18}\text{O}$  that may be lighter than or similar to typical depleted mantle [Cocker et al., 1982; Miller et al., 2001]. Gaffney et al. [2004] evaluated the role of recycled oceanic lithosphere in the genesis of the fine-scale compositional trends in the deep West Maui lavas. They calculated that a recycled lithosphere component comprising a solid-solid mixture of  $\sim 95\%$  harzburgite/lherzolite mantle residue and  $\sim 5\%$  basalt+gabbro is consistent with the lithophile element isotopic compositions. Such a mixture would be dominated by the unradiogenic  $^{187}\text{Os}/^{188}\text{Os}$  of the mantle residue, and this is not consistent with the  $^{187}\text{Os}/^{188}\text{Os}$ - $^{87}\text{Sr}/^{86}\text{Sr}$  trend apparent in the deep West Maui lavas. In contrast, the

unradiogenic  $^{187}\text{Os}/^{188}\text{Os}$  and potentially light  $\delta^{18}\text{O}$  of such a mixture could be a possible source for the Kea endmember [Lassiter and Hauri, 1998].

Recent work by Wang et al. [2003] on Mauna Kea shield-stage samples from the HSDP-2 drill core identified a distinct and abrupt change in the  $\delta^{18}\text{O}$  composition between the submarine and subaerial sections of the core. They interpret the higher  $\delta^{18}\text{O}$  (average:  $5.01 \pm 0.07\text{‰}$ , 1 sigma) of the submarine section as representing the pure plume source of the magmas. They conclude that the lavas of the subaerial section, which have lower  $\delta^{18}\text{O}$  compositions (average:  $4.79 \pm 0.13\text{‰}$ , 1 sigma), are plume-derived magmas that have interacted with or assimilated hydrothermally-altered, low  $\delta^{18}\text{O}$  material in the Pacific lithosphere or Mauna Kea volcanic edifice during magma fractionation or differentiation. This process is reflected in correlations among submarine and subaerial sample sets of  $\delta^{18}\text{O}$  with major and trace element indicators of progressive magmatic differentiation. The  $\delta^{18}\text{O}$  compositions of all the West Maui lavas are similar to the subaerial Mauna Kea lavas, and the general range of  $\delta^{18}\text{O}$  compositions in the West Maui lavas could result from processes described by Wang et al. [2003]. At West Maui, where the samples are probably all subaerial, we observed no lavas that would correspond to the  $\delta^{18}\text{O}$  compositions from the HSDP-2 Mauna Kea submarine samples. Thus, if such a process is responsible for the low  $\delta^{18}\text{O}$  in West Maui, then this process is occurring over the entire time range represented by our complete sample set, and we do not observe the transition from magmas sampling only the normal plume to magmas that have been affected by interaction with hydrothermally-altered lithosphere or the volcanic edifice.

The  $^{87}\text{Sr}/^{86}\text{Sr}$ - $^{176}\text{Hf}/^{177}\text{Hf}$ - $^{206}\text{Pb}/^{204}\text{Pb}$ -trace element correlations in the deep West Maui samples are consistent with the overprinting of plume-derived, Kea-type lavas with geochemical signals of small-degree melts of Pacific oceanic crust gabbros [Gaffney et al., 2004]. Both  $^{187}\text{Os}/^{188}\text{Os}$  and  $\delta^{18}\text{O}$  isotope compositions of oceanic crust gabbros show very wide ranges ( $^{187}\text{Os}/^{188}\text{Os} = 0.14\text{-}0.54$ : Lassiter and Hauri [1998]; Blusztajn et al. [2000];  $\delta^{18}\text{O} \sim 3\text{-}7$ : Gregory and Taylor Jr. [1981]; Stakes [1991]; Hansteen and Troll [2003]); oceanic crust gabbros also have low Os concentrations, typically 1-30 ppt [Lassiter and Hauri, 1998; Blusztajn et al., 2000]. This compositional component could contribute to the observed variation in the deep West Maui samples, and is consistent with the [Os] -  $^{187}\text{Os}/^{188}\text{Os}$  and  $^{87}\text{Sr}/^{86}\text{Sr}$

-  $^{187}\text{Os}/^{188}\text{Os}$  trends, as well as the  $\delta^{18}\text{O}$  compositions, of these lavas. If this process also operates on the shallow West Maui lavas, then it is evident only in elevated  $^{187}\text{Os}/^{188}\text{Os}$  of these samples, and not in any other geochemical tracers. This Pacific oceanic crustal component also has  $^{187}\text{Os}/^{188}\text{Os}$  too radiogenic to be the source of Kea-type magmas.

#### 2.4.3 *Pacific oceanic lithosphere in West Maui lavas*

The interpretation by Gaffney et al. [2004] for the  $^{87}\text{Sr}/^{86}\text{Sr}$ - $^{176}\text{Hf}/^{177}\text{Hf}$ - $^{206}\text{Pb}/^{204}\text{Pb}$ -trace element variability in the deep West Maui lavas implicates small-degree melts of oceanic crust gabbro that mix with ascending plume-generated magmas. The [Os] and  $^{187}\text{Os}/^{188}\text{Os}$  of this mixed magma reflects the abundance and stability of sulfides in the gabbroic crust, and the saturation state of sulfide in the small degree gabbro melts and the plume-generated magmas with which they interact. The solubility of sulfur in a small degree gabbro melt (at near-constant P) will depend upon  $f\text{O}_2$  and  $f\text{S}_2$  as well as bulk composition [Wallace and Carmichael, 1992]. However, these parameters are poorly constrained for this setting. The Os concentration observed in oceanic crust gabbros is generally 1-30 ppt, although mafic cumulate lithologies (e.g., troctolite) have higher [Os] ( $\sim 380$  ppt) [Lassiter and Hauri, 1998; Blusztajn et al., 2000]. Furthermore, estimates of Os partitioning between sulfide and silicate melt vary by orders of magnitude [Hart and Ravizza, 1996; Crocket et al., 1997; Roy-Barman et al., 1998]. Because of the uncertainty involved in all of the above parameters, and the potential large effect of this uncertainty on calculated stability of sulfide or Os partitioning between sulfide and silicate melt, we will discuss three possible scenarios for [Os] of small-degree gabbro melt, and the qualitative geochemical trends associated with each.

In the case that a small degree gabbro melt is sulfide undersaturated and could effectively dissolve all the sulfides from the melt residue, the melt would contain a significant fraction of the Os budget of the gabbroic oceanic crust. Assuming that the concentration of Os in gabbro is  $\sim 20$  ppt [Blusztajn et al., 2000; Lassiter and Hauri, 1998], and that the Os is all contained in sulfide, if all the sulfide in a melting region dissolves into a small degree ( $\sim 2\%$ ) silicate melt, then the melt would have [Os] on the order of 1000 ppt. This represents the



upper limit on the concentration of Os in a small-degree gabbro melt.

In the case that the small-degree gabbroic melt is sulfide saturated, the Os content of the gabbroic partial melt will depend upon partitioning of Os between residual sulfide and the melt. If partitioning processes operate in equilibrium, then most Os liberated from sulfide during melting would repartition back into residual sulfide, and subsequently the partial melt would have low [Os], effectively 0 ppt. However, observations of Os contents in co-existing phases in peridotite xenoliths [Hart and Ravizza, 1996; Burton et al., 1999] point to a disequilibrium partitioning process of Os between sulfide and melt during melting. In this event, most Os liberated by sulfide melting would remain in the melt, and hence the melt would have higher [Os], and could approach concentrations predicted by the previous scenario. Melts resulting from partial dissolution of sulfide could range in Os concentration from 0 for complete equilibrium partitioning to the upper limit of 1000 ppt with disequilibrium partitioning and near complete sulfide solubility.

The third scenario is not related to melting of the gabbro oceanic crust, but rather to scavenging of sulfide by an undersaturated basaltic, plume-derived melt. A sulfide-undersaturated magma could scavenge sulfide (and the Os which it contains) from the oceanic crust through which it passes, until the melt again is sulfide saturated. The melt will reach its sulfide saturation point either through dissolution of additional sulfide, or through crystallization which will effectively raise the sulfur content of the magma. Furthermore, melting initiates along grain boundaries, where the bulk of sulfide globules are located, so a modally disproportionately large amount of sulfides will be exposed to the melting regions.

Chemical changes in  $^{87}\text{Sr}/^{86}\text{Sr}$ ,  $^{206}\text{Pb}/^{204}\text{Pb}$  and trace elements will accompany the first two scenarios, but not necessarily the third. In Figure 2.6, we show a range of mixing curves between gabbro partial melts and primitive Kea-type magma that illustrate scenarios discussed above: mixing of gabbroic melts, with 1, 20 and 1000 ppt Os and  $^{187}\text{Os}/^{188}\text{Os} = 0.23$  and  $0.54$ , with a plume-derived, primitive Kea-type magma, with 1000 ppt Os and  $^{187}\text{Os}/^{188}\text{Os} = 0.1312$  [Bennett et al., 1996; Lassiter and Hauri, 1998]. It is evident that none of the discussed endmember processes alone ([Os] = 1 or 1000 ppt) can replicate the trends observed in the West Maui samples. However, assuming that the process which results in the variation in the lithophile element isotopic compositions of the deep West Maui lavas

(mixing with small-degree melts of Pacific oceanic crust gabbros) is the same process that results in the variation in  $^{187}\text{Os}/^{188}\text{Os}$  of these samples, we can constrain the composition of the gabbro melt to  $[\text{Os}] \sim 20$  ppt, given that its  $^{187}\text{Os}/^{188}\text{Os} = 0.23 - 0.54$  (Fig. 2.6). This in turn implies that not all of the sulfide in oceanic crust gabbro dissolves into the small degree partial melt, but also that Os does not undergo equilibrium partitioning. This also assumes that the bulk of the Os budget of the oceanic lithosphere is housed in sulfide. The degree of curvature of these mixing trends also depends upon the composition of the Kea-type magma. For this, we use the average  $^{187}\text{Os}/^{188}\text{Os}$  of Mauna Kea and Kilauea, and chose  $[\text{Os}] = 1000$  ppt, to represent the presumed primitive nature of a plume-derived magma, prior to extensive differentiation, and consistent with observations of primitive Mauna Kea magmas [Lassiter and Hauri, 1998]. If we choose  $[\text{Os}]$  as low as 500 ppt, the curvature of the mixing lines for the range in gabbro  $^{187}\text{Os}/^{188}\text{Os}$  composition would be less exaggerated, but still bracket the compositions of the deep West Maui samples.

#### 2.4.4 *Implications for the Kea component*

Lavas erupted from any individual Kea-dominated volcano are much more homogeneous in isotopic composition than lavas erupted from any individual Koolau-dominated volcano. This homogeneity is evident both within individual volcanoes as well as among volcanoes that erupted over the past 2 Ma (Fig. 2.7). It is not possible to define the absolute composition of the Kea or Koolau endmembers as they exist within the Hawaiian plume, as there is no way to evaluate whether any given lava has sampled any one component exclusively. However, it is apparent that the processes that result in the eruption of Kea type lavas, from the formation of the source, to the sampling of the source, to mixing with magmas from other sources, has been remarkably constant and reproducible over a 1.5-2 Ma time span. These processes result in the 'common Kea eruptive composition', which we can use to evaluate variation in the source and processes that lead to the generation and eruption of Kea-type lavas.

We use the area of compositional overlap in lithophile element isotope systems from Mauna Kea and Kilauea volcanoes, both younger than West Maui, to define the 'common

Kea eruptive composition'. The shallow West Maui lavas tend to lie closer to and within the common Kea eruptive composition, and the deep West Maui lavas tend to deviate from this common Sr-Nd-Pb-Hf isotope composition towards lower  $^{87}\text{Sr}/^{86}\text{Sr}$  and  $^{206}\text{Pb}/^{204}\text{Pb}$  and higher  $^{143}\text{Nd}/^{144}\text{Nd}$  and  $^{176}\text{Hf}/^{177}\text{Hf}$  (Fig. 2.8) [Gaffney et al., 2004]. Based upon this, we would expect the  $^{187}\text{Os}/^{188}\text{Os}$  of the shallow West Maui lavas to coincide with the common Kea eruptive composition and that the deep West Maui lavas would deviate from this. However, this relationship is reversed;  $^{187}\text{Os}/^{188}\text{Os}$  in the West Maui deep lavas overlap with the common Kea eruptive composition and the shallow lavas tend to deviate from this compositional baseline, towards higher  $^{187}\text{Os}/^{188}\text{Os}$ . This is a strong and previously unidentified indication of temporal heterogeneity in either the source or processes contributing to Kea-type lavas. This distinction in  $^{187}\text{Os}/^{188}\text{Os}$  of the common Kea eruptive composition relative to the lithophile element isotopic variation also points to a higher sensitivity of the Re-Os isotopic system to processes that lead to the generation of Kea-type lavas. Re/Os fractionation is highly sensitive to melt generation processes. It can vary by orders of magnitude during melting, and subsequent  $^{187}\text{Os}$  radiogenic ingrowth can lead to wide variability in the resultant  $^{187}\text{Os}/^{188}\text{Os}$ .

The  $\delta^{18}\text{O}$  compositions of the West Maui samples show a range similar to that observed in other Kea-type lavas. The range coincides nearly identically with the subaerial section of the HSDP-2 core [Wang et al., 2003]. In the Wang et al. [2003] study, the range in  $\delta^{18}\text{O}$  was attributed to post-magma-generation processes in the volcanic edifice or oceanic lithosphere. Wang et al. [2003] define the 'normal', plume-derived  $\delta^{18}\text{O}$  as  $\sim 5.0\text{‰}$ . If this value was consistent for Kea-type lavas erupted at West Maui, then the lower  $\delta^{18}\text{O}$  values ( $> 4.5\text{‰}$ ) observed for West Maui also implies that the crustal assimilation processes are taking place in all the West Maui lavas, not just the deep ones. Again, this process is not evident in the lithophile element isotope compositions of shallow West Maui lavas. Perhaps this indicates that all lavas at West Maui assimilated the hydrothermally-altered volcanic edifice which affects  $\delta^{18}\text{O}$  but not Sr-Nd-Hf-Pb isotope compositions, whereas the deep West Maui lavas record an additional interaction with the oceanic crust.

$^{187}\text{Os}/^{188}\text{Os}$  and  $\delta^{18}\text{O}$  correlations in Hawaiian lavas have been used to argue for ancient recycled lower oceanic lithosphere as the plume source of the Kea component [Lassiter and

Hauri, 1998]. Qualitative trends in isotopic systems tend to support this model. However, reconciling the mass balance in all isotope, major and trace element systems in a consistent way is at this point not resolved. Still at issue with this model is the mechanism for mixing and sampling of recycled oceanic lithosphere melts in the plume. Solid-solid mixing of gabbro-derived eclogite and peridotite and subsequent melting, mixing of eclogite-melts with peridotite-melts, and refertilization of solid peridotite by eclogite melts and subsequent melting of the fertilized peridotite are three distinct possibilities [Yaxley and Green, 1998; Takahashi and Nakajima, 2002; Pertermann and Hirschmann, 2003a]. Either solid-solid mixing or refertilization/metasomatism models include an event of 'pre-mixing' prior to generation of the erupted magmas, which may be a mechanism for homogenization of the Kea plume source. Also, both of these models predict major element compositions in equilibrium with residual lherzolite or harzburgite, consistent with observations [Wagner and Grove, 1998; Herzberg and O'Hara, 2002], rather than melts that have equilibrated with gabbro-derived eclogite.

The  $^{87}\text{Sr}/^{86}\text{Sr}$ - $^{143}\text{Nd}/^{144}\text{Nd}$ - $^{176}\text{Hf}/^{177}\text{Hf}$  homogeneity of Kea-type lavas indicates that consistent processes result in the formation of the Kea plume source and its subsequent sampling by magmas. In contrast, temporal heterogeneity in the  $^{187}\text{Os}/^{188}\text{Os}$  of the common Kea eruptive component suggests that  $^{187}\text{Os}/^{188}\text{Os}$  is perturbed independently of the lithophile isotopic systems. This sensitivity may stem from depletion or enrichment events early in the formation processes of the Kea magma sources, for example during subduction or metasomatism/refertilization events in the mantle, or may result from much more recent events, such as scavenging of sulfides from the oceanic lithosphere by plume generated magmas, as the magmas pass through on the way to the surface.

## 2.5 Conclusions

The  $^{187}\text{Os}/^{188}\text{Os}$  and  $\delta^{18}\text{O}$  compositions of the West Maui lavas are consistent with the Kea-type nature of these lavas, as identified through lithophile element (Sr-Pb-Hf-Nd) isotopic compositions. However, we identify a fine-scale  $^{87}\text{Sr}/^{86}\text{Sr}$ - $^{187}\text{Os}/^{188}\text{Os}$  correlation in the deep West Maui lavas which is distinct from that which characterizes the overall Hawaii

trend. This is the result of the superposition of the geochemical signals of Pacific oceanic lithosphere on plume-derived magmas.

$^{187}\text{Os}/^{188}\text{Os}$  of the shallow West Maui lavas deviates from the common Kea eruptive composition, as defined by lithophile element isotopic compositions (Sr-Nd-Pb-Hf) for Mauna Kea and Kilauea. This defines a component of temporal heterogeneity in either the sources or melt generation transport processes of Kea-type lavas, as they are sampled over the past  $\sim 1.8$  My. This heterogeneity may stem from processes of formation of the Kea plume source, or interaction of the plume-generated magmas with overlying lithosphere.

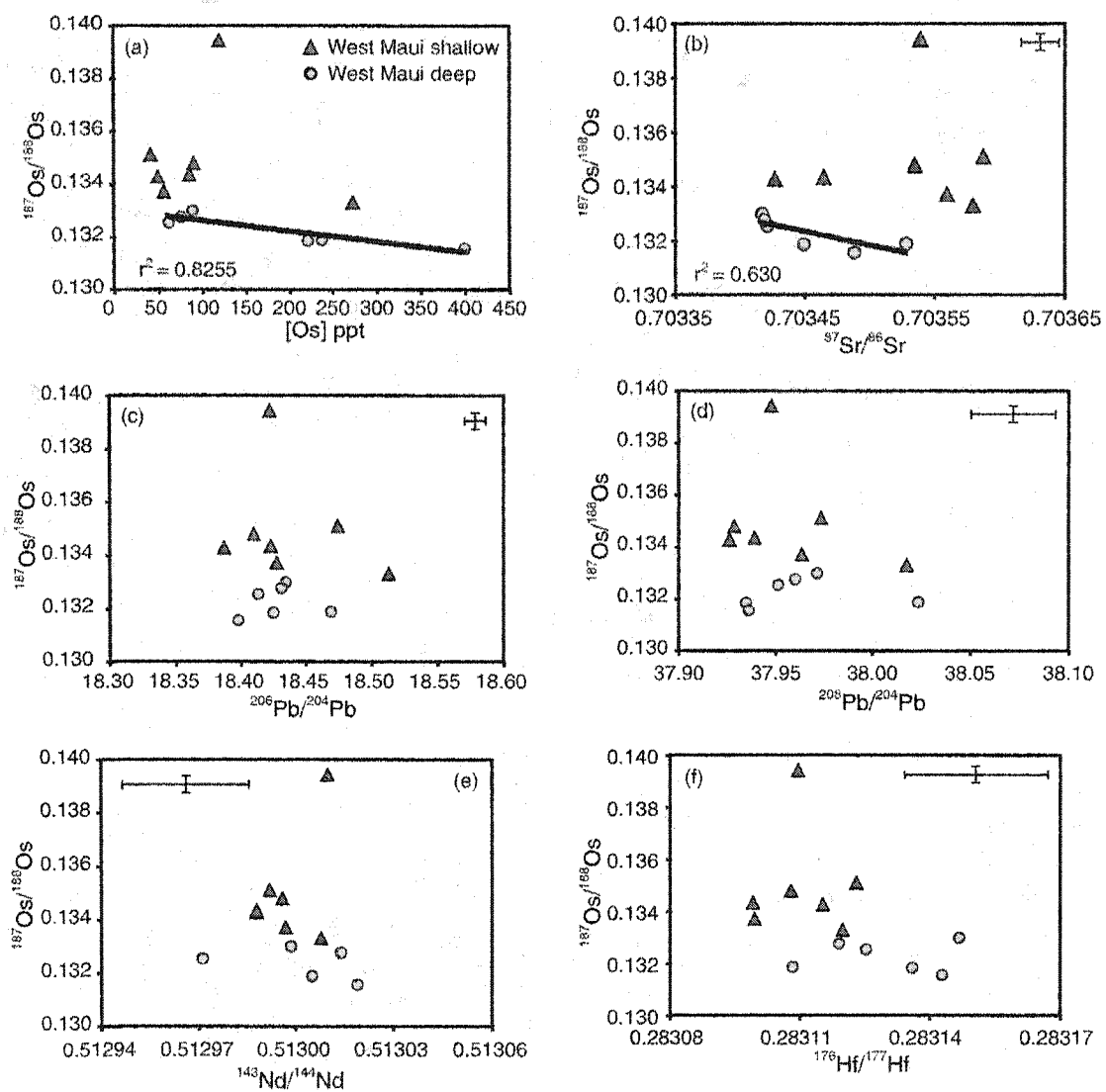


Figure 2.1:  $^{187}\text{Os}/^{188}\text{Os}$  compositions of deep and shallow West Maui lavas.

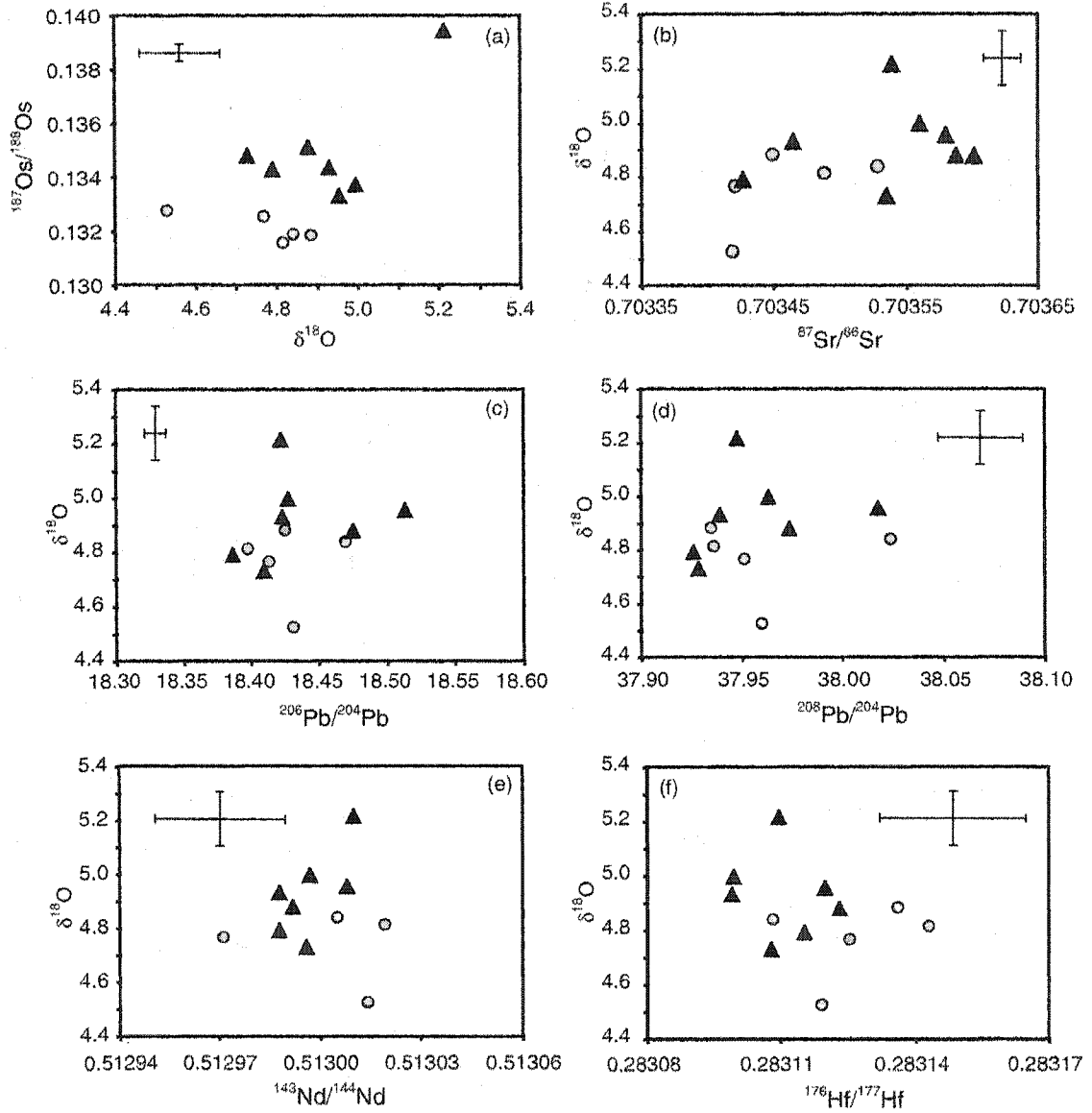


Figure 2.2:  $\delta^{18}\text{O}$  compositions of deep and shallow West Maui lavas.

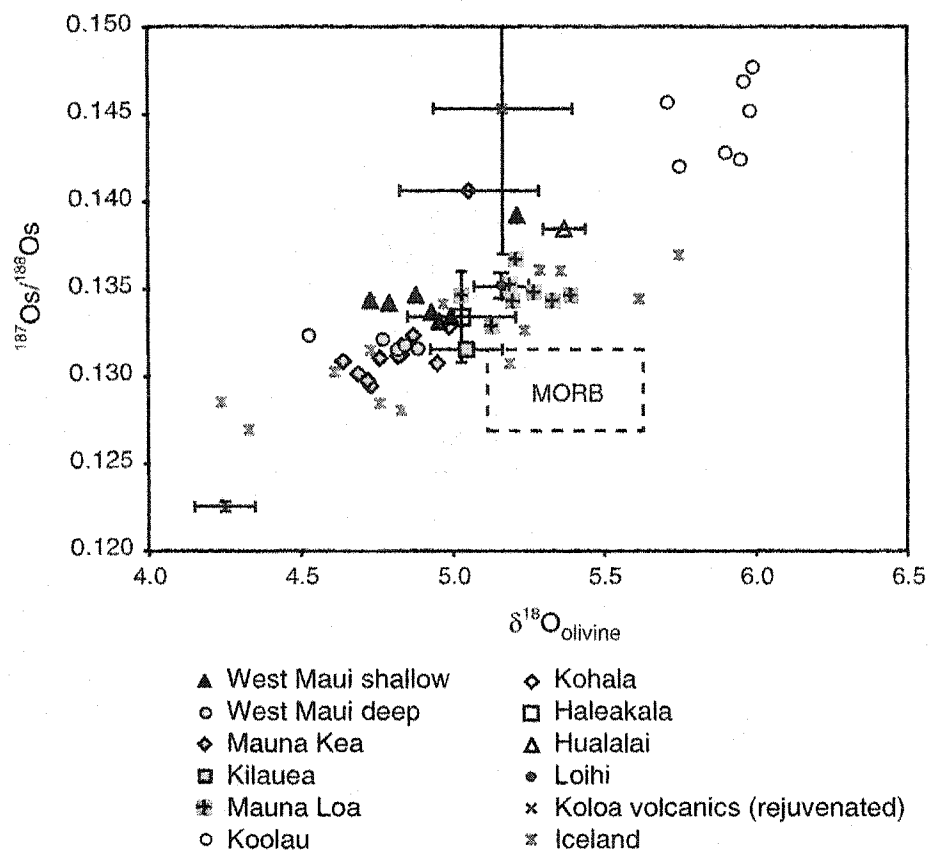


Figure 2.3:  $^{187}\text{Os}/^{188}\text{Os}$  -  $\delta^{18}\text{O}$  composition of Hawaiian and Icelandic lavas. Volcanoes for which  $^{187}\text{Os}/^{188}\text{Os}$  and  $\delta^{18}\text{O}$  data do not exist for the same samples are represented by average compositions  $\pm 1$  standard deviation. Data sources: this study, Martin et al. [1994], Eiler et al. [1996], Bennett et al. [1996], Hauri [1996b], Lassiter and Hauri [1998], Lassiter et al. [2000], Skovgaard et al. [2001].



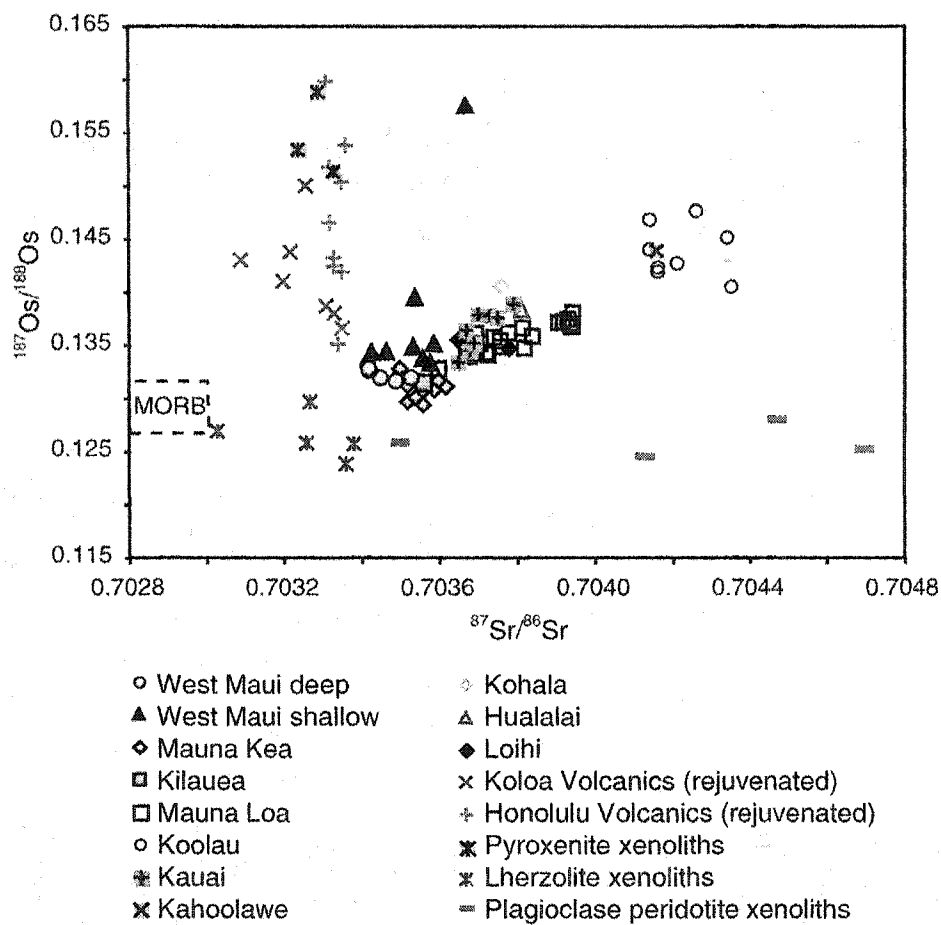


Figure 2.4:  $^{187}\text{Os}/^{188}\text{Os}$  -  $^{87}\text{Sr}/^{86}\text{Sr}$  compositions of Hawaiian shield- and rejuvenated-stage lavas and Hawaiian lithospheric xenoliths. Data sources: this study, Martin et al. [1994], Bennett et al. [1996], Hauri [1996b], Lassiter et al. [1996], Hauri [1997], Lassiter and Hauri [1998], Lassiter et al. [2000], Mukhopadhyay et al. [2003], Sen et al. [2003].

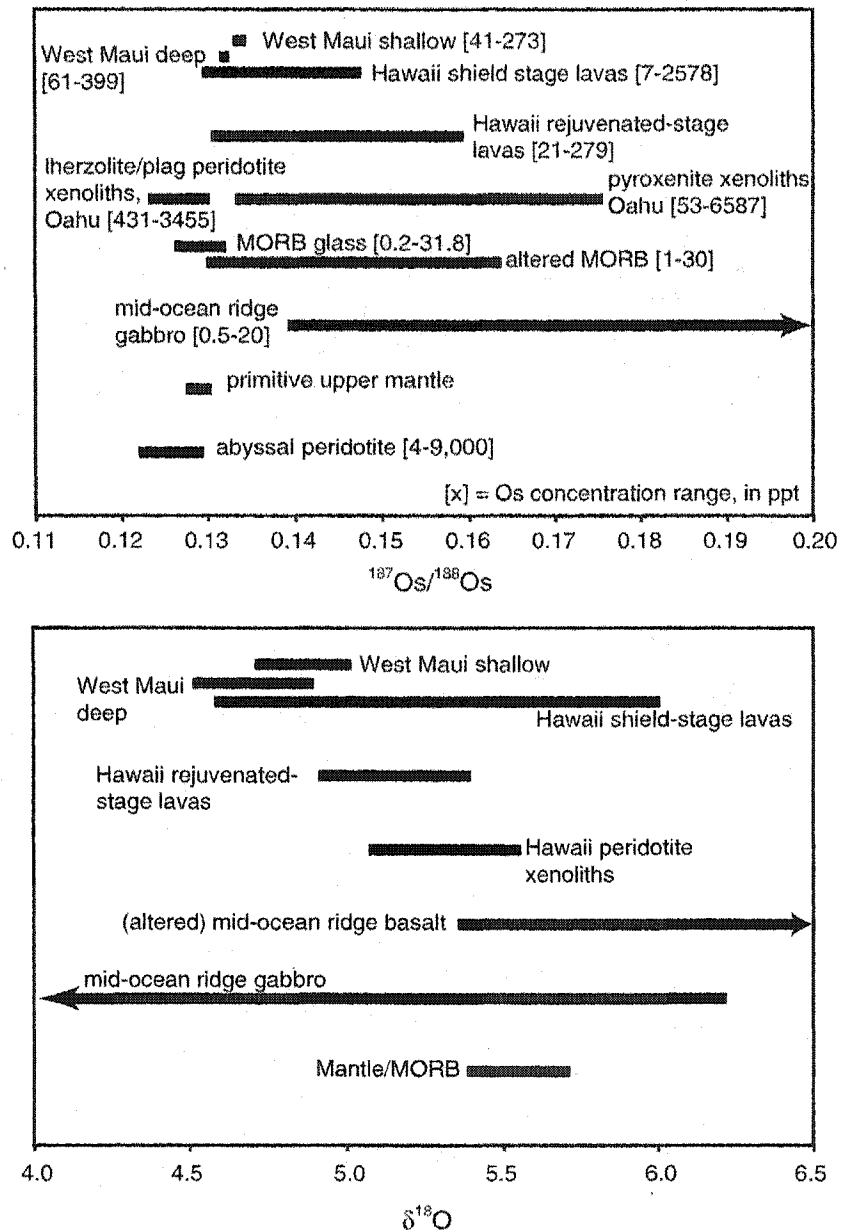


Figure 2.5: Ranges in (a)  $^{187}\text{Os}/^{188}\text{Os}$  and (b)  $\delta^{18}\text{O}$  compositions of mantle, oceanic lithosphere and Hawaiian materials. Data sources: this study, Gregory and Taylor Jr. [1981], Martin et al. [1994], Roy-Barman and Allègre [1994], Eiler et al. [1996], Meisel et al. [1996], Schiano et al. [1997], Lassiter and Hauri [1998], Roy-Barman et al. [1998], Blusztajn et al. [2000], Brandon et al. [2000], Eiler et al. [2000b], Lassiter et al. [2000], Meisel et al. [2001], Ducea et al. [2002], Peucker-Ehrenbrink et al. [2003], Sen et al. [2003], Wang et al. [2003].

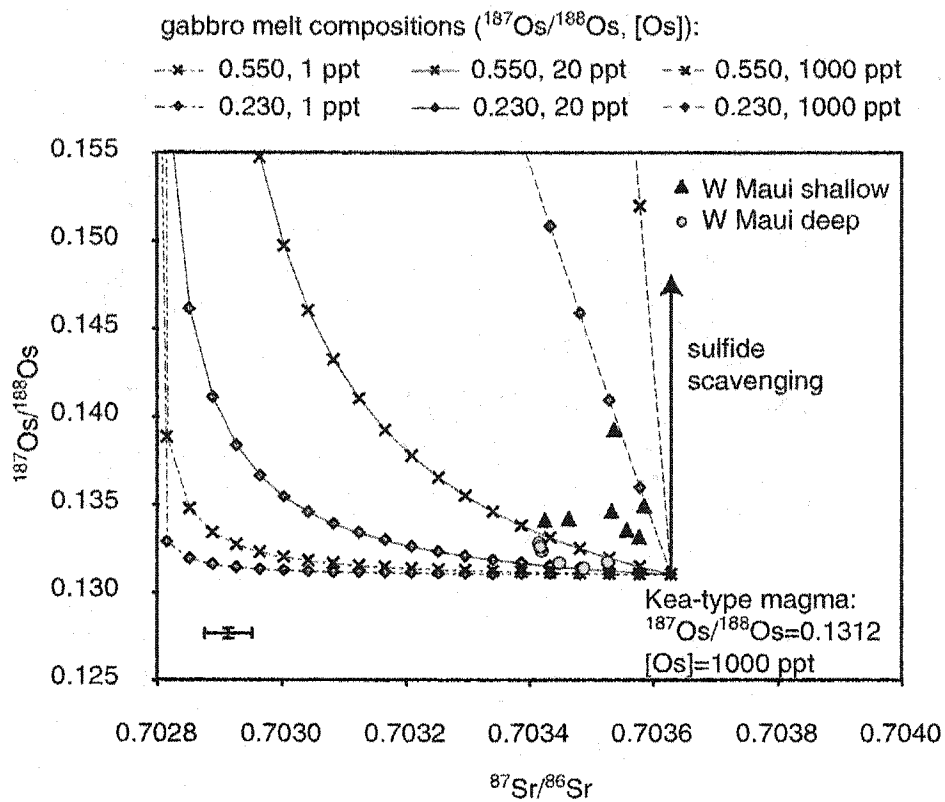


Figure 2.6: Range of curves for mixing between Kea-type magmas (black square) and small-degree melts of oceanic crust gabbro of variable  $^{187}\text{Os}/^{188}\text{Os}$  and [Os]. Analytical errors are approximately the same as symbol size.

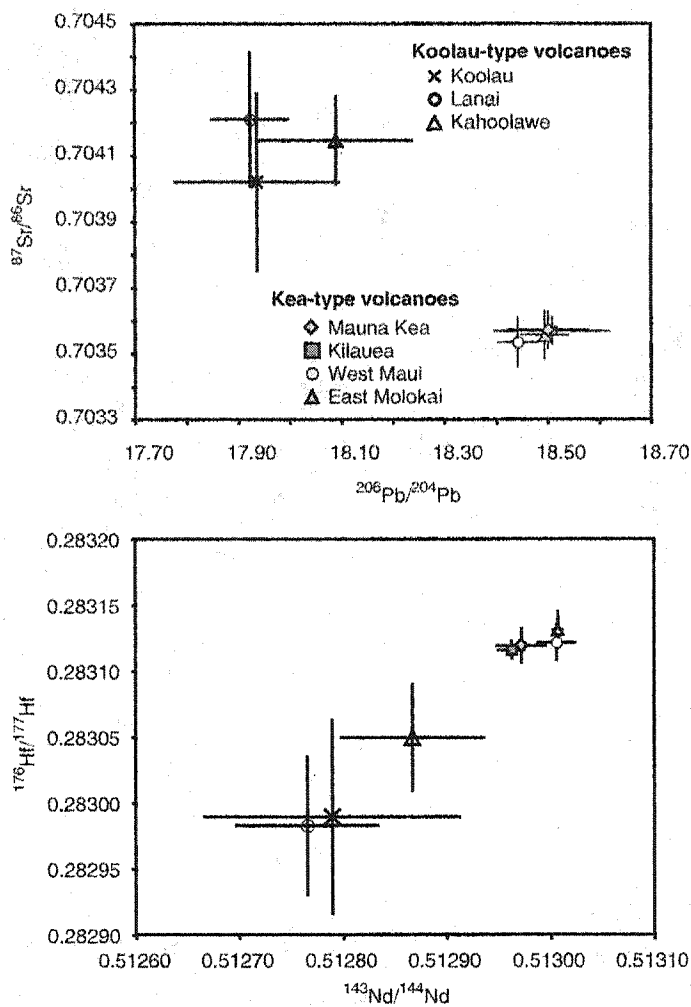


Figure 2.7: Average compositions of shield-building stage lavas for Kea-type and Koolau-type volcanoes. Error bars indicate  $\pm 1$  standard deviation about the average. Data sources: Lanphere and Clague [1980]; Stille et al. [1983]; Hofmann et al. [1984]; West et al. [1987]; Hart [1988]; Frey et al. [1994]; Leeman et al. [1994]; Roden et al. [1994]; Yang et al. [1994]; Anders and Nelson [1996]; Basu and Faggart Jr. [1996]; Chen et al. [1996]; Garcia et al. [1996]; Lassiter et al. [1996]; Lassiter and Hauri [1998]; Blichert-Toft et al. [1999]; Pietruszka and Garcia [1999]; Abouchami et al. [2000]; Garcia et al. [2000]; Tanaka et al. [2002]; Blichert-Toft et al. [2003]; Eisele et al. [2003]; Gaffney et al. [2004].

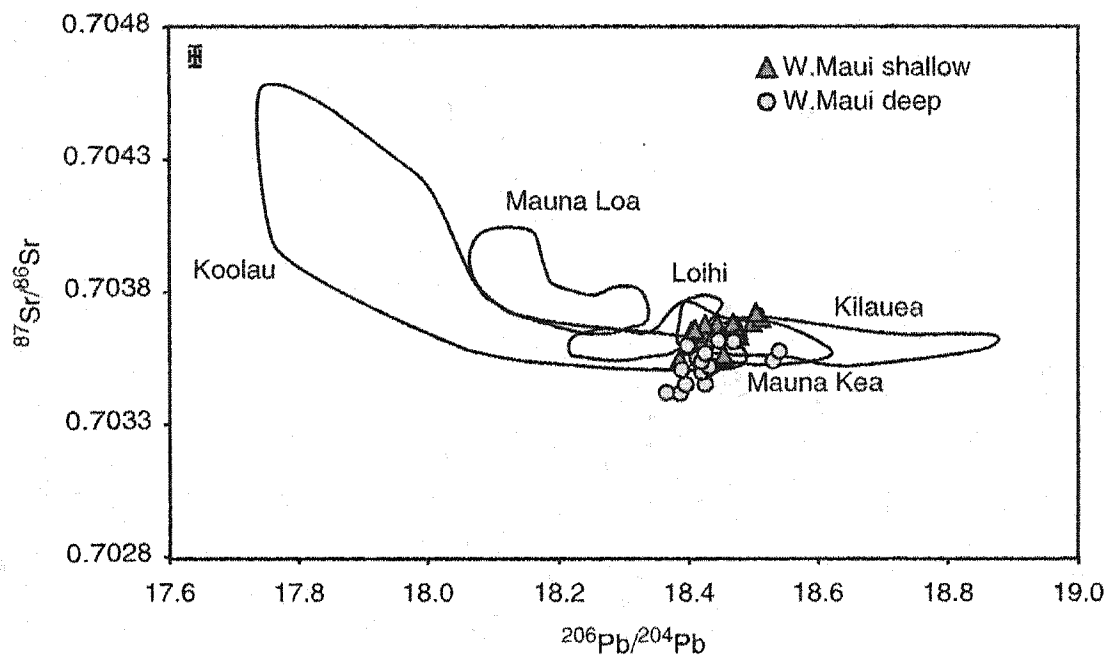


Figure 2.8:  $^{87}\text{Sr}/^{86}\text{Sr}$ - $^{206}\text{Pb}/^{204}\text{Pb}$  compositions of Hawaiian shield-stage lavas. Data sources for other volcanoes: Stille et al. [1983], Stille et al. [1986], West et al. [1987], Garcia et al. [1993], Roden et al. [1994], Garcia et al. [1995], Kurz et al. [1995], Chen et al. [1996], Lassiter et al. [1996], Reiners and Nelson [1998], Blichert-Toft and Albarède [1999], Blichert-Toft et al. [1999], Pietruszka and Garcia [1999], Abouchami et al. [2000], Lassiter et al. [2000], Tanaka et al. [2002], Blichert-Toft et al. [2003].

Table 2.1: Oxygen and osmium isotope compositions of West Maui lavas

Sample	$\delta^{18}\text{O}$	$\pm 1\sigma$	$^{187}\text{Os}/^{188}\text{Os}$	Os (ppm)
<b>Shallow samples</b>				
LP-11	4.995	0.008	0.13371	56
LP-16	4.878	0.071	0.13510	41
UP-37	5.214	0.059	0.13943	119
UP-46	4.930	0.153	0.13434	85
WA-04	4.878	0.019	0.15800	20
WA-19	4.791	0.143	0.13427	49
LT-22	4.954	0.131	0.13330	273
LT-27	4.729	0.076	0.13479	90
OL-29	5.044	0.066		
<b>Deep samples</b>				
WA-22	4.884	0.183	0.13186	221
OL-30	4.815	0.029	0.13157	399
MA-410	4.840	0.081	0.13189	237
MA-650	4.768	0.083	0.13255	61
MA-800			0.13300	88
MA-910	4.526	0.200	0.13277	75

$\delta^{18}\text{O}$  indicates deviation from SMOW (standard mean ocean water), defined as:  $\left(\frac{(^{18}\text{O}/^{16}\text{O})_{\text{sample}}}{(^{18}\text{O}/^{16}\text{O})_{\text{SMOW}}}-1\right)\times 1000$ ;  $\pm 1\sigma$  (standard deviation) of  $\delta^{18}\text{O}$  determined from multiple (2-3) analyses.

## Chapter 3

**MELTING IN THE HAWAIIAN PLUME AT 1-2 MA AS RECORDED  
AT MAUI NUI: THE ROLE OF ECLOGITE, PERIDOTITE AND  
SOURCE MELTING****3.1 Introduction**

The extent of chemical variability in Hawaiian shield-stage lavas is typically described as mixing between at least two, sometimes up to five or six, distinct compositional components or endmembers that originate in the Hawaiian plume, Pacific lithosphere, or local asthenosphere [e.g., Chen and Frey, 1985; Hauri, 1996a; Eisele et al., 2003]. These endmembers are commonly described on the basis of their radiogenic isotope composition, but in some studies are ascribed distinctive major or trace element or stable isotope characteristics as well [e.g., Frey et al., 1994; Eiler et al., 1996; Hauri, 1996a]. These compositional endmembers, their sources and their relative contributions to shield-stage magmas have been defined to best describe the range of Hawaiian lavas erupted over the past 5 My- the time frame sampled by the best-studied and youngest Hawaiian islands and seamounts: Kauai at the oldest end and Loihi at the youngest.

Hypotheses that describe the compositional range of Hawaiian lavas as originating from ancient oceanic lithosphere in the Hawaiian plume implicitly or explicitly infer lithologic heterogeneity in the plume [e.g., Hauri, 1996a; Lassiter and Hauri, 1998]. Eclogite derived from ancient oceanic lithosphere may contribute unique chemical signals to plume-derived melts that stem from the oceanic crustal-derived eclogite as well as the dominantly clinopyroxene-garnet composition of eclogite, and mineral composition-sensitive partition coefficients.

The distribution of lava compositions in space and time provides a window on the temporal structure of the Hawaiian plume. These data have been used to describe the general sense of compositional variability among the Hawaiian volcanoes over the past 5 My, the

detailed variability exhibited by individual volcanoes, and the structure of the Hawaiian plume within the past 1 My (through the volcanoes on the Big Island). However, there does not yet exist a comprehensive study of the plume prior to  $\sim 1$  Ma. The volcanoes of Maui Nui (West and East Molokai, Lanai, West Maui, Kahoolawe and Haleakala; also known as the Maui Volcano Complex) provide an opportunity to explore the detailed structure of the Hawaiian plume at  $\sim 1$ -2 Ma. The compositions of the shield-stage lavas of Maui Nui volcanoes span nearly the range of compositions erupted across the whole Hawaiian chain and there now exists a data set that is comprehensive enough to warrant a more detailed analysis of the Hawaiian plume as it is sampled by the Maui Nui volcanoes.

This study complements the current detailed understanding of Hawaiian plume activity and structure over the past 1 My, as expressed on the Big Island of Hawaii [DePaolo et al., 2001]. Maui Nui contains the youngest Hawaiian volcano to erupt extremely enriched isotope compositions (Lanai), and contains the oldest volcano (East Molokai) to erupt extremely depleted isotope compositions. This suggests that plume structure, composition and perhaps magma generation processes during Maui Nui time also may have important contrasts with the Big Island.

Only a few dates exist for shield-stage lavas from the Maui Nui volcanoes. In general, shield-stage lavas erupted from 2 to 0.7 Ma [McDougall, 1964; Naughton et al., 1980]. Published ages for each volcano are listed in Fig. 3.1. Several of these volcanoes overlap in age, and it is likely that each volcano erupted contemporaneously with its neighbor(s) for at least part of its growth. By analogy to the Big Island, where Mauna Loa, Kilauea and Hualalai all have had historic eruptions, contemporary shield-building activity of two or more volcanoes should be a common process. The volcanoes of Maui Nui span a greater compositional diversity than observed in the Big Island volcanoes, and may have sampled sources that are not reflected in these younger volcanoes. However, only the youngest shield-stage lavas of any volcano are exposed at the surface, and with few exceptions (e.g., Hawaii Scientific Drilling Project (HSDP), submarine landslide blocks), it is possible to obtain samples only of the latest-shield stage lavas of each volcano. Thus, one generally can compare the same episode of relative shield growth for each volcano: the waning shield-stage magmatism as the volcano passes to the periphery of the plume.



With this paper, we, 1) describe the compositional range of lavas erupted from the Maui Nui volcanoes, 2) identify mixing relationships among compositional endmembers that are consistent with observed variability in Maui Nui, 3) incorporate recent experimental data to model petrologic and compositional variability in the mantle source and the related controls on partial melting processes, and 4) discuss heterogeneity in the Hawaiian plume evident on intra- and inter-volcano time and length scales.

### ***3.2 The Hawaiian endmembers, their compositions and sources - a review***

Most studies of isotopic variability in shield-stage lavas of Hawaiian volcanoes conclude that three primary compositional endmembers are necessary to account for the compositional range of shield-building stage lavas across the Hawaiian chain [e.g., Stille et al., 1986; West and Leeman, 1987; Hauri, 1996a; Eiler et al., 1996; Hauri, 1997; Mukhopadhyay et al., 2003]. These are commonly labeled the Kea (sampled dominantly at Mauna Kea, Kilauea, West Maui and East Molokai volcanoes), Koolau (sampled dominantly at Koolau, Lanai and Kahoolawe volcanoes) and Loihi (sampled dominantly at Loihi) components [Hauri, 1996a; Eiler et al., 1996, 1998]. The Kea component is defined by relatively depleted  $^{87}\text{Sr}/^{86}\text{Sr}$ ,  $^{143}\text{Nd}/^{144}\text{Nd}$  and  $^{176}\text{Hf}/^{177}\text{Hf}$  and higher  $^{206}\text{Pb}/^{204}\text{Pb}$ , whereas the Koolau component is defined by relatively enriched  $^{87}\text{Sr}/^{86}\text{Sr}$ ,  $^{143}\text{Nd}/^{144}\text{Nd}$  and  $^{176}\text{Hf}/^{177}\text{Hf}$  and lower  $^{206}\text{Pb}/^{204}\text{Pb}$  [Lassiter et al., 1996; Eiler et al., 1996; Blichert-Toft et al., 1999]. The Loihi component is intermediate to Kea and Koolau in all isotopic compositions except  $^3\text{He}/^4\text{He}$  and  $^{208}\text{Pb}/^{204}\text{Pb}$ , for which it is higher than predicted by Kea-Koolau mixing. Principal component analysis has shown that the Kea and Koolau endmembers can account for 89% of the compositional variability in shield-stage lavas [Eiler et al., 1996]. The Loihi component accounts for an additional 4% of variability [Eiler et al., 1996], and only makes a significant contribution at Loihi, Manua Loa, Haleakala and Kauai volcanoes.

Because of its relatively enriched isotope composition, the source of the Koolau component has been interpreted as ancient recycled oceanic crustal material (basalt + pelagic sediment) in the Hawaiian plume [Lassiter and Hauri, 1998; Blichert-Toft et al., 1999]. The relatively  $\text{SiO}_2$ -rich primary magmas for Koolau are consistent with this interpretation

[Hauri, 1996a; Norman et al., 2002]. The origin of the Kea component is more ambiguous. It has been interpreted as MORB-source mantle, entrained asthenospheric mantle, Pacific oceanic lithosphere, or recycled lower oceanic crust (gabbro + harzburgite/lherzolite) in the plume [Chen and Frey, 1985; Hauri, 1996a; Eiler et al., 1996; Lassiter and Hauri, 1998]. Because of its primitive  $^3\text{He}/^4\text{He}$ , the Loihi component is commonly interpreted as a Hawaiian plume component associated with primitive mantle [Eiler et al., 1998].

It is commonly inferred that the Hawaiian plume is approximately concentrically-zoned, and that the Loa-trend volcanoes tap sources in the core of the plume and the Kea-trend volcanoes tap sources on the edge of the plume [Lassiter et al., 1996; Hauri, 1996a; DePaolo et al., 2001]. One primary support for this axisymmetric plume model is the observation that all volcanoes erupting extreme Koolau-type compositions lie on the Loa-trend, and volcanoes erupting extreme Kea-type lavas lie on the Kea-trend (Fig. 3.1). Both Loa- and Kea-trends contain volcanoes of intermediate composition. DePaolo et al. [2001] mapped the isotopic composition of the Hawaiian plume based upon estimated magma capture areas, plume upwelling rates and Pacific plate motion, and also concluded that the plume is approximately concentrically zoned. A contrasting model postulates that the plume is not concentrically zoned, but on the My time-scale melting samples long, narrow heterogeneities that are strung out vertically in the plume [Farnetani et al., 2002; Hofmann et al., 2002]. Although this plume structure could episodically produce lavas that appear to result from a concentric zonation in the plume, this would not be a fundamental reflection of plume structure. In this model, the heterogeneities in the plume are inherited from the plume source region in the mantle, whereas in the concentric-zoning model, heterogeneities can be entrained along the periphery of the upwelling plume [Hauri et al., 1994].

### ***3.3 Data selection, normalization, filtering and assumptions***

For the following discussion, we have compiled the available data for Maui Nui volcanoes (East Molokai, West Maui, Lanai, Kahoolawe and Haleakala) from literature sources as well as some unpublished data sets (all sources cited in Appendix B). We do not include or discuss any West Molokai data because very few data exist, and most rock exposures

are severely weathered, so collection and analysis of additional samples is not feasible. We use all isotopic data as they were reported in the original publications. Most of the Pb isotope data has been normalized to NBS 981 values of Todt et al. [1996], and some of the  $^{87}\text{Sr}/^{86}\text{Sr}$  has been normalized to the Eimer and Amend  $\text{SrCO}_3$  standard ( $^{87}\text{Sr}/^{86}\text{Sr} = 0.70800$ ). Normalization procedures and values of standards obtained are not given consistently in the literature from which these data come, thus we are not able to make a standard normalization for all the data that we compare in this paper. All of the West Maui and East Molokai, and most of the Lanai samples were leached in 6N HCl prior to Pb and Sr isotope analysis. It is unknown whether samples for the other volcanoes were leached prior to Pb and Sr isotope analysis.

We have normalized all major element compositions to 100% totals for the oxides, with all Fe reported as FeO. We corrected major element compositions for variable olivine fractionation by adding back 1% increments of equilibrium olivine until the bulk rock composition was in equilibrium with Fo<sub>90</sub> olivine. We also tested this correction using 0.1% increments of olivine, and found no significant difference in the results. For this correction, we assumed that  $\text{Fe}^{2+} = 0.9 \cdot \text{FeO}$ , and that  $K_{ol-liq}^{Fe-Mg} = 0.3$  (Roeder and Emslie, 1970). This correction is dependent on  $\text{Mg}/(\text{Fe}^{2+} + \text{Mg})$  rather than only MgO composition of the melt, and thus preserves MgO variability inherent in the primary magmas. For the olivine-accumulation correction, we excluded lavas with  $\text{MgO} < 7$  wt. %. This filters out whole rock compositions that may have been affected by fractionation of clinopyroxene in addition to olivine [Helz and Wright, 1992; Montierth et al., 1995]. To calculate average compositions, we include all samples in the average, regardless of whether the sample has complete or partial elemental and isotopic data. This does not yield significantly different results than if we included only completely characterized samples.

Subaerial, low-temperature alteration and weathering may affect major and trace element and isotopic compositions of Hawaiian lavas.  $\text{K}_2\text{O}/\text{P}_2\text{O}_5$  is commonly used as an index of alteration, as this ratio decreases during alteration. Samples with  $\text{K}_2\text{O}/\text{P}_2\text{O}_5 > 1-1.25$  are generally considered unaltered, whereas samples with lower  $\text{K}_2\text{O}/\text{P}_2\text{O}_5$  may have undergone some degree of subaerial weathering [Frey et al., 1994]. In the Maui Nui samples, none of the volcanoes shows a significant correlation between  $\text{K}_2\text{O}/\text{P}_2\text{O}_5$  and  $^{87}\text{Sr}/^{86}\text{Sr}$ ,  $^{206}\text{Pb}/^{204}\text{Pb}$  or

$^{208}\text{Pb}/^{204}\text{Pb}$ , suggesting that these isotopic compositions have not been significantly modified by alteration. Decrease in  $\text{SiO}_2$  is also an effect of low-temperature alteration. Of all the volcanoes, only Lanai has samples (two samples) that show anomalously low  $\text{SiO}_2$  at low  $\text{K}_2\text{O}/\text{P}_2\text{O}_5$ . For the following discussion, we do not include these two Lanai samples. It is difficult to evaluate effects of alteration on isotopic composition in samples for which no major element data are available. However, for all volcanoes except Lanai, the range and pattern of variability in isotopic composition of the samples without major element data is approximately the same as the samples with major element data, so we include all isotopic data for these volcanoes in the following analysis and discussion. The isotopic range of Lanai samples for which no major element data exist is greater than the isotopic range of samples for which we can evaluate alteration. However, the Lanai range extends in the opposite direction of what we would expect from subaerial weathering (i.e., to more radiogenic  $^{87}\text{Sr}/^{86}\text{Sr}$ ), so we believe that this extended range is not caused by alteration. With the exception of the two Lanai samples, we include all data from the sources cited in Appendix B in our analysis and discussion.

Our olivine-fractionation correction implies that magmas formed in equilibrium with  $\text{Fo}_{90}$  olivine, typical of fertile mantle peridotite, corresponding to some of the most Mg-rich olivine phenocrysts observed in Hawaiian shield-stage lavas. If any of the magmas have a different source (e.g., eclogite, depleted peridotite), then this assumption may require reconsideration. An MgO content of 14-18 wt. % is commonly assumed for primary Hawaiian tholeiites [Chen, 1993; Clague et al., 1995; Norman et al., 2002]. These estimates are based upon both glass compositions and Fo content of olivine phenocrysts. For the first part of the following discussion, we assume that the parental magmas for each volcano formed in equilibrium with  $\text{Fo}_{90}$  olivine, and then revisit the issue of the magma source lithology at the end of the discussion.

### **3.4 Observations**

The Kea, Koolau and Loihi endmembers are apparent in the isotopic composition of Maui Nui volcanoes. The Kea component dominates both West Maui and East Molokai compo-

sitions. Lanai is dominated by the Koolau component, and Kahoolawe shows contributions from the Koolau component, but to a lesser degree than Lanai. Haleakala has the elevated  $^{208}\text{Pb}/^{204}\text{Pb}$  and  $^3\text{He}/^4\text{He}$  unique to the Loihi component, but it is not as extreme in its composition as Loihi lavas. Because the focus of this study is the composition and structure of the Hawaiian plume at 1-2 Ma, as sampled by the volcanoes of Maui Nui, we will define and discuss endmembers for 'Lanai', 'Haleakala' and 'West Maui/East Molokai'. These endmembers are analogous to, but not always the same as, the Koolau, Loihi and Kea components, respectively, as defined to describe the all-Hawaii variation. In the Discussion, we address the distinctions and similarities of the Maui Nui vs. all-Hawaii endmembers.

West Maui and East Molokai have  $^{87}\text{Sr}/^{86}\text{Sr}$ ,  $^{143}\text{Nd}/^{144}\text{Nd}$  and  $^{176}\text{Hf}/^{177}\text{Hf}$  at the depleted end of the Maui Nui array (Figs. 3.2, 3.3 and 3.4). The  $^{87}\text{Sr}/^{86}\text{Sr}$ ,  $^{143}\text{Nd}/^{144}\text{Nd}$  and  $^{176}\text{Hf}/^{177}\text{Hf}$  of these volcanoes show very little variability (% variation in  $^{87}\text{Sr}/^{86}\text{Sr}$  = 0.011% and 0.010%,  $^{143}\text{Nd}/^{144}\text{Nd}$  = 0.0035% and 0.0009%, and  $^{176}\text{Hf}/^{177}\text{Hf}$  = 0.0047% and 0.0047% for West Maui and East Molokai, respectively; % variability defined as  $100 \times \text{standard deviation/average}$ ).  $^{87}\text{Sr}/^{86}\text{Sr}$ - $^{143}\text{Nd}/^{144}\text{Nd}$  in both West Maui and East Molokai, and  $^{176}\text{Hf}/^{177}\text{Hf}$ - $^{143}\text{Nd}/^{144}\text{Nd}$  in East Molokai are not correlated at the 99% confidence interval, and the  $^{143}\text{Nd}/^{144}\text{Nd}$ - $^{176}\text{Hf}/^{177}\text{Hf}$  correlation in West Maui, though significant, is poor. Table 3.1 lists correlation coefficients and indicates statistical significance of correlations in isotope compositions for the five volcanoes [Sachs, 1984]. In contrast, Lanai and Kahoolawe, which lie at the more enriched end of the Maui Nui array, are well-correlated and show a larger degree of variability in  $^{87}\text{Sr}/^{86}\text{Sr}$ ,  $^{143}\text{Nd}/^{144}\text{Nd}$  and  $^{176}\text{Hf}/^{177}\text{Hf}$  (variation in  $^{87}\text{Sr}/^{86}\text{Sr}$  = 0.030% and 0.01%,  $^{143}\text{Nd}/^{144}\text{Nd}$  = 0.013% and 0.014%, and  $^{176}\text{Hf}/^{177}\text{Hf}$  = 0.018% and 0.014%, respectively). Haleakala shows approximately the same absolute range of variation in  $^{87}\text{Sr}/^{86}\text{Sr}$  and  $^{143}\text{Nd}/^{144}\text{Nd}$  as do West Maui and East Molokai (variation in  $^{87}\text{Sr}/^{86}\text{Sr}$  = 0.010%, and  $^{143}\text{Nd}/^{144}\text{Nd}$  = 0.045%) and does not show significant correlation. Only three  $^{176}\text{Hf}/^{177}\text{Hf}$  analyses for Haleakala are available, and they show less variability (0.0034%) than for West Maui or East Molokai; this likely is an artifact of the small sample set. The  $^{87}\text{Sr}/^{86}\text{Sr}$ ,  $^{143}\text{Nd}/^{144}\text{Nd}$  and  $^{176}\text{Hf}/^{177}\text{Hf}$  of Haleakala fall close to the center of the Maui Nui array, displaced slightly towards the depleted end of the array.

Although the  $^{87}\text{Sr}/^{86}\text{Sr}$ ,  $^{143}\text{Nd}/^{144}\text{Nd}$  and  $^{176}\text{Hf}/^{177}\text{Hf}$  correlations among Maui Nui vol-

canoes can be described by mixing between two endmembers, the Pb isotope compositions require a third component.  $^{206}\text{Pb}/^{204}\text{Pb}$ - $^{208}\text{Pb}/^{204}\text{Pb}$  in lavas from West Maui, East Molokai and Kahoolawe are significantly correlated, but not in Lanai or Haleakala lavas (Fig. 3.4, Table 3.1). Intra-volcano variation in  $^{206}\text{Pb}/^{204}\text{Pb}$  is  $\sim 0.22\%$  for West Maui, East Molokai and Haleakala,  $0.4\%$  for Lanai and  $0.8\%$  for Kahoolawe, whereas  $^{208}\text{Pb}/^{204}\text{Pb}$  variability is  $\sim 0.1\%$  for all volcanoes except Kahoolawe ( $0.24\%$ ). Lead isotope variation within each volcano is not an artifact of measuring these samples in various laboratories, with unrecognized interlaboratory biases and external reproducibility of analyses. Lead extractions for samples from East Molokai, West Maui and Lanai were processed by identical chemistry at the University of Washington. All East Molokai samples were measured on the same TIMS (University of Washington) and all West Maui and Lanai samples were measured in a single MC-ICP-MS (ENS, Lyon).

In contrast to  $^{87}\text{Sr}/^{86}\text{Sr}$ ,  $^{143}\text{Nd}/^{144}\text{Nd}$  and  $^{176}\text{Hf}/^{177}\text{Hf}$ , in Pb isotope space, the composition of Haleakala is not intermediate to the other volcanoes. Its  $^{208}\text{Pb}/^{204}\text{Pb}$  is elevated relative to  $^{206}\text{Pb}/^{204}\text{Pb}$ . Consistent with this,  $^{206}\text{Pb}/^{204}\text{Pb}$ - $^{87}\text{Sr}/^{86}\text{Sr}$  (not shown) and  $^{206}\text{Pb}/^{204}\text{Pb}$ - $^{176}\text{Hf}/^{177}\text{Hf}$  (Fig. 3.5) variation in the Maui Nui lavas tend to define curved, rather than linear arrays. In  $^{206}\text{Pb}/^{204}\text{Pb}$ - $^{207}\text{Pb}/^{204}\text{Pb}$  (Fig. 3.4) and  $^{206}\text{Pb}/^{204}\text{Pb}$ - $^{176}\text{Hf}/^{177}\text{Hf}$  (Fig. 3.5) compositional space, Haleakala lies along the trend defined by other volcanoes, suggesting that it is  $^{208}\text{Pb}/^{204}\text{Pb}$  rather than  $^{206}\text{Pb}/^{204}\text{Pb}$  which is distinct at Haleakala.

Major element trends in Maui Nui volcanoes, for example as reflected in MgO vs. SiO<sub>2</sub> and MgO vs. TiO<sub>2</sub> (Fig. 3.6), also show intervolcano correlation with isotopic and trace element compositions when corrected for effects of olivine crystallization (Figs. 3.7, 3.8). Lanai, the lavas of which make up one compositional end of the Maui Nui isotopic array, has the highest average SiO<sub>2c</sub>, and lowest average MgO<sub>c</sub>, FeO<sub>c</sub> and TiO<sub>2c</sub> (all fractionation corrected; Fig. 3.7). Haleakala, which is not extreme in any of its isotopic compositions (except perhaps for  $^{208}\text{Pb}/^{204}\text{Pb}$ ), has the lowest average SiO<sub>2c</sub> and highest average MgO<sub>c</sub>, FeO<sub>c</sub> and TiO<sub>2c</sub> (Fig. 3.7). West Maui and East Molokai, which lie at an extreme end of the isotopic array, and Kahoolawe, which does not, all have intermediate values of these major element compositions. West Maui and East Molokai have the lowest average Al<sub>2</sub>O<sub>3c</sub> (not

shown), whereas Lanai, Kahoolawe and Haleakala all have similar  $\text{Al}_2\text{O}_{3c}$ . The Maui Nui volcanoes show no distinction in average  $\text{CaO}_c$  or  $\text{K}_2\text{O}_c + \text{Na}_2\text{O}_c$  compositions (not shown). Although the major element differences among these volcanoes could result from distinct source melting histories (melt fraction (F) or mean pressure of magma segregation), the isotopic compositions require that three distinct source components contribute to these lavas. Correlation of  $\text{SiO}_{2c}$  and  $\text{TiO}_{2c}$  with  $^{206}\text{Pb}/^{204}\text{Pb}$  among Lanai, Kahoolawe and Haleakala show that mixing between at least two of these source components, or magmas derived from two source components, contributes to both major element and isotopic variability (Fig. 3.8).

There is modest variation in REE slopes, as quantified by both La/Yb and Sm/Yb, among the volcanoes (Fig. 3.9). West Maui and Haleakala have the steepest slopes (La/Yb  $\sim 8$ , Sm/Yb  $\sim 3.3$ ) and Lanai, Kahoolawe and East Molokai have the shallowest slopes (La/Yb  $\sim 4$ , Sm/Yb  $\sim 2$ ). However, the range of REE slopes for each volcano spans nearly the entire range for all Maui Nui volcanoes. Among the Maui Nui volcanoes as a whole, there is a positive correlation between  $\text{TiO}_{2c}$  and both La/Yb and Sm/Yb. Such correlations are expected to result from variable extents of melting.

Based upon small intra-volcano variability in  $^{87}\text{Sr}/^{86}\text{Sr}$ ,  $^{143}\text{Nd}/^{144}\text{Nd}$  and  $^{176}\text{Hf}/^{177}\text{Hf}$ , West Maui, East Molokai and Haleakala appear either to have sampled distinct, individual sources, or consistently and reproducibly sampled a mixture of sources in constant proportions. In contrast, the more linear arrays of Lanai, and to a lesser extent Kahoolawe, are consistent with the lavas from these volcanoes resulting from variable extents of mixing between two components. Further consideration of Pb isotope data indicates that the West Maui/East Molokai endmember is composed of sub-components that are variable in their Pb isotope composition, and thus produce sub-parallel linear  $^{206}\text{Pb}/^{204}\text{Pb}$ - $^{208}\text{Pb}/^{204}\text{Pb}$  arrays. In Pb isotope space, as well as in several major element compositions, Haleakala is not intermediate between the Lanai and West Maui/East Molokai endmembers, and thus requires a third, distinct mantle source. Based upon the Maui Nui  $^{206}\text{Pb}/^{204}\text{Pb}$ - $^{208}\text{Pb}/^{204}\text{Pb}$  variation, as well as Pb isotope-major element variation (e.g.,  $^{206}\text{Pb}/^{204}\text{Pb}$ - $\text{SiO}_2$ ,  $^{206}\text{Pb}/^{204}\text{Pb}$ - $\text{TiO}_2$ ) it appears that the Lanai and Kahoolawe lava compositions are the result of mixing between the Haleakala primary magmas or source and some enriched component.

Using this construction of endmembers, in the simplest-case scenario West Maui/East Molokai and Haleakala each sample primarily a single endmember (which, in the case of West Maui/East Molokai, comprises two sub-components defined by Pb isotope composition but not resolvable in  $^{87}\text{Sr}/^{86}\text{Sr}$ ,  $^{143}\text{Nd}/^{144}\text{Nd}$  or  $^{176}\text{Hf}/^{177}\text{Hf}$ ), whereas Lanai and Kahoolawe sample the enriched endmember only in combination or mixture with the Haleakala endmember. Although West Maui/East Molokai and Haleakala lavas could result from mixing multiple mantle sources in constant proportions, this would require a consistently-reproducible process that operates on time scales that are significant relative to the life span of the volcano. Thus we favor the homogeneous endmember interpretation and we treat West Maui/East Molokai and Haleakala sources as two individual plume components.

The strong intravolcano correlations in West Maui and East Molokai  $^{206}\text{Pb}/^{204}\text{Pb}$ - $^{208}\text{Pb}/^{204}\text{Pb}$  (Table 3.1) indicate that these magmas result from mixing between two compositional endmembers for each volcano. Although these two volcanoes have similar slopes in the  $^{206}\text{Pb}/^{204}\text{Pb}$ - $^{208}\text{Pb}/^{204}\text{Pb}$  arrays, the arrays are slightly offset, with East Molokai to slightly higher  $^{206}\text{Pb}/^{204}\text{Pb}$  relative to West Maui. The non-correlation in Pb isotope variation in Lanai and Kahoolawe indicates that these magmas sample an endmember that is heterogeneous in Pb isotope composition, or are mixtures of two endmembers that are each heterogeneous in Pb isotope composition, rather than form through mixing between two endmembers that are relatively homogeneous in their Pb isotope composition.

### **3.5 *Geochemical evaluation of oceanic lithosphere in Maui Nui lavas***

Many aspects of major and trace element and isotope compositions of Hawaiian shield-stage lavas are consistent with ancient, recycled oceanic crust in the plume sources of Kea- and Koolau-type magmas. The negative  $\delta^{18}\text{O}$ - $^{187}\text{Os}/^{188}\text{Os}$  correlation among Hawaiian shield-stage lavas, with  $\delta^{18}\text{O} < 5.0$  ‰ and unradiogenic  $^{187}\text{Os}/^{188}\text{Os}$  in the Kea-type lavas, and  $\delta^{18}\text{O} > 5.5$  ‰ and radiogenic  $^{187}\text{Os}/^{188}\text{Os}$  in the Koolau-type, lavas is compelling evidence for the incorporation of hydrothermally-altered oceanic lithosphere in sources of both Kea- and Koolau-type magmas [Lassiter and Hauri, 1998]. Conversely, the normal-mantle-like  $^{187}\text{Os}/^{188}\text{Os}$  and  $\delta^{18}\text{O}$  and elevated  $^3\text{He}/^4\text{He}$  of Haleakala lavas [Kurz et al., 1987; Martin



et al., 1994; Eiler et al., 1996; Lassiter and Hauri, 1998] does not seem to implicate recycled crustal material in the Haleakala magma source. The hyperbolic correlation of  $^{206}\text{Pb}/^{204}\text{Pb}$  and  $^{176}\text{Hf}/^{177}\text{Hf}$  (Fig. 3.5) is consistent with the presence of pelagic sediment in the Koolau plume source [Blichert-Toft et al., 1999]. These models that use isotopic and trace element relations to infer oceanic lithosphere in the plume source generally have not investigated the phase petrology of melting of this type of source and the implications that has for both major and trace element evolution of the magmas. Specifically, recycled oceanic crust in the mantle would be present as eclogite/pyroxenite embedded in peridotite. In addition to isotopic and trace element contrasts with mantle peridotite, an eclogitic mantle source would have strongly contrasting thermodynamic properties and melting behavior that must be incorporated into chemical models of Hawaiian sources.

The physical mechanisms for incorporation of ancient oceanic lithosphere into the plume, its interaction with other plume materials, and the process of melting and transport of eclogite/pyroxenite partial melts to the surface would have effects on lava compositions that may be both predictable and distinctive. We incorporate available experimental observations and thermodynamic modeling of melting interactions between eclogite and peridotite, and connect this to geochemical (major and trace element and isotopes) predictions. This model complements previous studies that argue for the existence of recycled oceanic lithosphere in OIB sources based upon geochemical arguments, but that do not discuss a physical and phase petrological framework [Lassiter and Hauri, 1998; Chauvel and Hémond, 2000], and for petrologic studies that address the physical and chemical aspects of eclogite and peridotite interactions in OIB genesis, but do not discuss the isotope and trace element implications [Yaxley and Green, 1998; Takahashi and Nakajima, 2002; Pertermann and Hirschmann, 2003a].

The petrology and thermodynamics of eclogite and peridotite melting interactions provide the physical basis for the models that we consider. Recycled oceanic crust will exist in the mantle as eclogite, unless it is very efficiently and effectively mixed back in to ambient mantle or plume. However, numerical modeling and the existence of geochemical heterogeneity in erupted lavas suggests that eclogite heterogeneities in the mantle are preserved on long (>1 Gyr) time scales [van Keken and Zhong, 1999; du Vignaux and Fleitout, 2001;

Kogiso et al., 2004]. Eclogite has a higher temperature solidus than peridotite, and a higher melt productivity during adiabatic decompression [Green and Ringwood, 1967; Thompson, 1974, 1975; Takahashi, 1986; Yaxley and Green, 1998; Takahashi and Nakajima, 2002], thus the interaction of pyroxenite melts with solid peridotite will contribute to the geochemical characteristics of magmas derived from a mixed lithology source. A number of high-pressure experiments specifically address melting of pyroxenite heterogeneities in a peridotite matrix in the context of eclogite contributions to OIB petrogenesis [Kogiso et al., 1998; Yaxley and Green, 1998; Takahashi and Nakajima, 2002; Kogiso et al., 2003; Pertermann and Hirschmann, 2003a,b]. These experiments illustrate two endmember cases for interaction of eclogite melts with solid peridotite.

In one case, eclogite melts are insulated from surrounding peridotite, and thus maintain geochemical signatures that reflect their equilibration with an eclogite, not peridotite, residue. A fertilized peridotite reaction zone between eclogite melt and non-fertilized peridotite can effectively armor either a solid eclogite pod or a conduit through which eclogite melts can travel without equilibrating with surrounding peridotite [Takahashi and Nakajima, 2002]. Alternatively, a sub-solidus orthopyroxene-rich reaction zone may develop at the interface of eclogite and peridotite [Pertermann and Hirschmann, 2003b].

As a second endmember case, eclogite melt infiltrates and reacts with surrounding solid peridotite to form a solid fertilized peridotite. This has been observed in eclogite-peridotite 'sandwich' experiments [Yaxley and Green, 1998; Takahashi and Nakajima, 2002], and is simulated in pMELTS calculations [Ghiorso et al., 2002]. Eclogite melt reacts incongruently with olivine in peridotite to form orthopyroxene, and upon subsequent melting of this fertilized peridotite, the major element composition of the melt will reflect a peridotite source [Hirschmann et al., 2003]. Although these melts may have enriched isotope and trace element compositions reflecting the eclogite contributions, they will produce lower  $\text{SiO}_2$ , higher MgO melts indicative of a peridotite, not eclogite source [Yaxley and Green, 1998; Hirschmann et al., 2003].

Case one is the basis for our model of the Lanai plume source. We model the Lanai source as eclogite derived from a mixture of hydrothermally-altered oceanic crust and pelagic sediment. These eclogite melts form and separate from their source, and mix in variable

proportions with melts derived from the Haleakala source prior to eruption. Case two is the basis for our model of the West Maui/East Molokai source. We postulate that lower oceanic crust gabbro-derived eclogite melts, and that this melt infiltrates, reacts with and freezes in to the associated depleted recycled lithosphere, thereby creating a hybrid re-fertilized depleted peridotite source. This source subsequently melts to produce the West Maui/East Molokai lavas. In these models, we do not specify a physical interpretation for the Haleakala source. We present details on the chemical and isotopic implications of these models below.

### **3.6 Lanai source model**

We model the Lanai and Kahoolawe magma compositions as the product of mixing between partial melts of upper oceanic crust + pelagic sediment-derived eclogite and partial melts of the Haleakala plume component. Similar models for the origin of the Koolau component in dacitic partial melts of eclogite have been proposed by Hauri [1996a] and Takahashi and Nakajima [2002]. In this model, we incorporate the known effects of subduction-zone dehydration on the trace element composition of pelagic sediment and hydrothermally-altered upper oceanic crust, variable proportions of pelagic sediment:upper oceanic crust, as well as variable amounts of melting of this eclogite component in the plume. For this model, we assume that after dehydration of the sediment and crust, the pelagic sediment is incorporated completely, as a solid, into the upper oceanic crust, and that this mixture undergoes all subsequent melting or mixing as a single compositional unit. For the trace element composition of the dehydrated pelagic sediment, we use analyses of residues from dehydration experiments on pelagic clay done by Johnson and Plank [1999]. For the trace element composition of dehydrated hydrothermally-altered upper oceanic crust, we use the experimental products of oceanic crust amphibolite high-pressure dehydration experiments done by Kogiso et al. [1997] and low-MgO eclogite xenoliths inferred to be fragments of Archean dehydrated oceanic lithosphere from west Africa [Barth et al., 2001] (Table 3.2). We assume that the  $^{87}\text{Sr}/^{86}\text{Sr}$  of this dehydrated composite upper crust is 0.7048, consistent with literature estimates of the composition of the Koolau component [e.g., Eiler et al., 1998], and corresponding to the  $^{206}\text{Pb}/^{204}\text{Pb}$  of the Koolau component (17.85) inferred by Blichert-

Toft et al. [1999]. For calculating the composition of melts derived from this eclogite source, we assume batch melting and use the partition coefficients of Klemme et al. [2002], which were determined specifically for high pressure (3 GPa) systems and garnet and clinopyroxene compositions that are consistent with an eclogite derived from mid-ocean ridge basalt.

Most previous work in Koolau, which is geochemically similar to Lanai, has identified La/Nb higher than other Hawaiian shield-stage lavas [Frey et al., 1994; Roden et al., 1994; Huang and Frey, 2003]. Jackson et al. [1999] discuss the possible association of this anomalously high ratio with a crustal source in the plume. Pelagic sediments are characterized by very high REE concentrations relative to high field strength elements (HFSE), so (light, middle REE)/HFSE is a sensitive indicator for presence and proportion of pelagic sediment in an oceanic crust-derived magma source. In Fig. 3.10, we show calculated compositions for melts of upper oceanic crust-derived eclogite containing 4-7% pelagic sediment. The calculated La/Nb for this melt is not sensitive to clinopyroxene/garnet (cpx/gt) in the residue, nor to  $F$  (for  $F > \sim 0.3$ ). For  $F > 0.3$ , the observed La/Nb is consistent with 5-7% sediment in the Lanai source. Mixing of 60-75% of this eclogite-melt with the average Haleakala magma composition generates the range of compositions that we see in the lavas erupted at Lanai (Fig. 3.10).

La/Nb, Sm/Hf and Sm/Nb are higher in pelagic sediment than in Maui Nui lavas, and are lower in dehydrated upper oceanic crust than in Maui Nui lavas. Thus, these ratios are useful for modeling the proportion of pelagic sediment in the Lanai magma source. As with La/Nb, Sm/Hf and Sm/Nb are more sensitive to a difference of 1% in the amount of pelagic sediment in the Lanai source than they are to reasonable variation of  $F$  (0.5-0.9) or cpx/gt (1-9) in the residue. The Sm/Nb of the Lanai lavas is consistent with 5-10% sediment in the Lanai source. Sm/Hf is best-modeled with addition of 1% sediment to the upper oceanic crust. However, Sm/Hf of the dataset that we use for the eclogite starting composition of this model [Barth et al., 2001] has a standard deviation of about 20%, which encompasses the range of Sm/Hf predicted for 1-3% sediment addition. The small amount (<10%) of sediment in the Lanai source predicted by these calculations is consistent with previous work that uses isotope compositions of Koolau lavas to conclude that the sediment proportion in the Koolau source is 3-20% [Eiler et al., 1996; Lassiter and Hauri, 1998].

Sm/Yb is far more sensitive to residual cpx/gt and F than to sediment proportion, and therefore is useful for constraining the amount of melting of the Lanai source to produce compositions that are consistent with observation. To identify the dependencies of cpx/gt and F on the mantle thermal and melting regime, we performed a series of experiments with the pMELTS algorithm [Ghiorso et al., 2002]. Using a MORB major element starting composition [Allan et al., 1988] and dehydrated eclogite + 5% dehydrated sediment as the trace element starting composition [Kogiso et al., 1997; Johnson and Plank, 1999]. With pMELTS, we calculated the amount of melting (F) and cpx/gt proportion for isentropic (adiabatic) melting, from 3 to 2 GPa, for starting temperatures ranging from 1500° to 1550° C. We also ran pMELTS simulations for isobaric melting at 2 and 3 GPa, for comparison to isobaric melting experiments. With the F and mineralogical parameters from pMELTS, we calculated melt Sm/Yb as a function of F (Fig. 3.11). Because Sm/Yb is very sensitive to the extent of eclogite partial melting, for any particular melting curve even at rather high F (>0.6) there is only a very narrow range in F (2% to 3%) over which the observed Lanai Sm/Yb (~2.3) is obtained. For adiabatic melting, the absolute F ranges from about 0.6 to 0.85, depending upon which adiabat the eclogite parcel follows. Regardless of which adiabat the eclogite is on, as long as there is garnet in the residue, there is a very small range in F which will produce Sm/Yb typical of Lanai (2.3-2.5). These magmas are the result of a specific, reproducible, large degree of melting, which may be controlled by the lithosphere thickness and thus the pressure at which Lanai melts segregate from the source. However, it is difficult to constrain F to a range narrower than 0.6 to 0.85.

Using the 1540° C adiabat as a reference, we calculate mixing curves between average Haleakala magmas and predicted Lanai melts for F ranging from F=0.70 to F=0.76 of the eclogite source (Fig. 3.12). This produces a wide enough range in Sm/Yb to account for the observed range in Lanai lavas obtained by 60-70% mixing of eclogite melt with 30-40% Haleakala melt.

The low TiO<sub>2</sub> content of Lanai lavas relative to other Maui Nui lavas is one of their most distinctive major element characteristics, and we use this to estimate relative mixing proportions of Lanai component melts with Haleakala component melts. Takahashi and Nakajima [2002] determined experimentally the compositions of pyroxenite partial melts of

an Archean MORB. At 2.7 GPa, and 85% melting, the melt had 1.16 wt. %  $\text{TiO}_2$  and 7.62 wt. % MgO [Takahashi and Nakajima, 2002]. In a similar experiment at 3.5 GPa, Yaxley and Green [1998] reported 85% partial melts of average oceanic basalt with 1.5 wt. %  $\text{TiO}_2$  and 6.9 wt. % MgO. Pyroxenite melting experiments show a general trend of decreasing  $\text{TiO}_2$  with increasing MgO and melt fraction [Yaxley and Green, 1998; Takahashi and Nakajima, 2002; Pertermann and Hirschmann, 2003a], which implies that the low  $\text{TiO}_2$  component in the Lanai lavas derives from high-degree, basaltic andesitic melts of eclogite, rather than smaller degree, dacitic melts as proposed by Hauri [1996a]. Higher degree eclogite melts are also more consistent with the higher-temperature solidus for eclogite compared to peridotite.

These experiments imply that low-MgO partial melts are produced from eclogite in the Hawaiian plume. However, our trace element calculations and observed MgO compositions indicate that these melts do not make it to the surface without mixing with Mg-rich Haleakala melts. At a given MgO, Lanai and Kahoolawe lavas generally have slightly higher Ni than other Maui Nui lavas (data sources from Appendix B), which may indicate that the Lanai and Kahoolawe lavas have not fractionated as much olivine as the other Maui Nui lavas. This in turn implies that the Lanai and Kahoolawe lavas contain a component of low-MgO primary magma, as predicted for an eclogite melt. Taking the Takahashi and Nakajima [2002] and Yaxley and Green [1998] experimental results as the composition of the eclogite-derived melt for the Lanai source, mixing of this melt with 30-70% of the Haleakala primary melt will produce the range of magmas parental to Lanai lavas, and mixing of this Lanai primary melt with 70-80% Haleakala melt will result in the Kahoolawe parental magmas. Imposing olivine fractionation trajectories on these parental magmas can produce the observed lava compositions (Fig. 3.13). Although these major element trends allow for a broader range in eclogite melt-Haleakala melt mixing proportions than predicted from the trace element compositions, the mixing proportions are consistent for the major and trace element calculations and isotope observations.

### 3.7 West Maui/East Molokai source model

For the West Maui and East Molokai magmas, we model the plume source as the gabbro+depleted lithosphere package of ancient oceanic lithosphere [Lassiter and Hauri, 1998]. Gabbro-derived eclogite has a higher pressure solidus than the associated depleted lithosphere, and so begins to melt first during ascent in the plume. Its melt percolates into and fertilizes the adjacent segment of depleted lithosphere. Various metasomatic processes have been proposed for the source of Hawaiian lavas xenoliths [Wright, 1984; Chen and Frey, 1985; Sen, 1987; Salters and Zindler, 1995; Norman and Garcia, 1999; Sobolev et al., 2000; Sen et al., 2003], but in most models the metasomatic agent is very small degree melts ( $F=0.001-0.03$ ) of a mantle or recycled crustal source. Here, we specifically propose larger ( $F=0.2-0.4$ ) degree melts of oceanic crust gabbro-derived eclogite as the metasomatic agent. We calculated the compositions of four different degrees of melt of the gabbro-derived eclogite ( $F=0.2, 0.4, 0.6, 0.8$ ), using the major and trace element compositions of the ODP 735 drill core gabbros and Gabal Gerf ophiolite gabbros [Zimmer et al., 1995; Hart et al., 1999], partition coefficients determined for clinopyroxene and garnet from mid-ocean ridge basalt-derived eclogite [Klemme et al., 2002], and residual clinopyroxene and garnet proportions determined from pMELTS calculations of the desired  $F$  at 3 GPa. Clinopyroxene/garnet in the eclogite melting residue range from 2.6 at  $F=0.2$  to 0.9 at  $F=0.8$ . We determined the trace element composition of the depleted lithosphere as the residue from MORB-melting, using phase proportions calculated with MELTS [Ghiorso and Sack, 1995] for 18% melting of the MM3 experimental composition [Baker and Stolper, 1994], at 0.5 GPa, and with MORB trace element compositions from Sun and McDonough [1989]. For partition coefficients of peridotite melting, we chose clinopyroxene and garnet partition coefficients determined experimentally for high pressure (2.8-3 GPa) melting of a moderately depleted lherzolite [Hart and Dunn, 1993; Salters and Longhi, 1999; van Westrenen et al., 1999] (see Tables 3.3 and 3.4 for partition coefficients and references).

We modeled mixing of the eclogite melts with the depleted lithosphere in 10:90 proportions, and then calculated trace element compositions of melts of these re-fertilized peridotite sources. Trace element melting trajectories for depleted peridotites fertilized by 10%

of  $F=0.2, 0.4, 0.6$  and  $0.8$  melts are shown in Figs. 3.14 and 3.15. These melt compositions and trajectories are illustrated for residual phase proportions of ol:opx:cpx:gt of 43:38:14:4. These proportions, based on pMELTS calculations, are generally consistent with proportions calculated or inferred as residual to melting in the Hawaiian plume [Hofmann et al., 1984; Wagner and Grove, 1998]. Garnet and clinopyroxene mode and cpx/gt are the main controls on REE and HFSE melt compositions. Larger proportions of garnet or clinopyroxene or lower cpx/gt will generate higher Sm/Yb and lower Hf/Zr at smaller degrees of melting. Experiments and theoretical calculations have shown that partition coefficients are dependent on clinopyroxene and garnet composition [Beattie, 1994; Wood and Blundy, 1997; van Westrenen et al., 1999], so in our calculations, we use partition coefficients experimentally determined for melting of moderately depleted peridotite at  $\sim 3$  GPa (Table 3.3). This introduces a sensitivity to the model that allows us to distinguish between melting of eclogite vs. peridotite sources.

Hf/Zr is much more sensitive to peridotite melting than eclogite melting, as result of partition coefficient dependency on clinopyroxene and garnet compositions [van Westrenen et al., 2001]. We model Hf/Zr (Fig. 3.15) because it is particularly diagnostic of the fertilization and melting processes we propose. In the eclogite melting system, the relative proportions and partition coefficients for garnet and clinopyroxene maintain a relatively constant Hf/Zr (0.029-0.032) during progressive eclogite melting ( $F=0.2-0.8$ ). However, partition coefficients appropriate for a peridotite residue lead to a fractionation of Hf/Zr during progressive melting, thus Hf/Zr is useful for constraining the degree of melt of the fertilized peridotite source. The predicted compositions are consistent with derivation of the West Maui lavas from 5-15% melting of a hybrid source derived from 10% eclogite melt ( $F=0.2-0.4$ ) and 90% depleted lithosphere. pMELTS simulations also result in 9-15% melt for this lithology, on the same adiabat as discussed for the Lanai model ( $1540^\circ$ ), at the point where the melting parcel reaches the base of the lithosphere.

Melting of eclogite generates sizable fractionations in Hf/Nb at larger degrees of melt (Hf/Nb = 0.36-0.49 at  $F = 0.2-0.4$ ), whereas comparable Hf/Nb fractionation in peridotite melting occurs at lower degrees of melt (Hf/Nb = 0.22-0.4 at  $F = 0.05-0.2$ ). At larger degrees of peridotite melt, Hf/Nb fractionation is insignificant. Sm/Yb is sensitive to residual garnet



and residual cpx/gt in both systems, although the Sm/Yb fractionation is slightly less at the same F for a peridotite source relative to an eclogite source. The melting trajectories that we illustrate in Figs. 3.14 and 3.15 are for 14% cpx and 4% garnet in the residue (cpx/gt = 3.5). With larger amounts of residual garnet, the Hf/Zr (to lower values) and Sm/Yb (to higher values) fractionations in the melt are much larger at a given F. Eclogite melt-depleted lithosphere proportions of 10:90 provide the best simultaneous fit for the three element ratios we consider. Holding all other parameters constant, larger proportions of eclogite melt results in Sm/Yb too high to fit the Maui Nui data.

### **3.8 Discussion of the source models**

Our models of the Lanai and West Maui/East Molokai sources address physical processes for mixing of source components (liquid-liquid vs. liquid-solid) and also account for the existence of eclogite heterogeneities derived from ancient oceanic crust and their melting behavior in the plume. We also incorporate the effects of subduction zone dehydration and variability in the amount of sediment in the Lanai source, and address the sensitivities of the model to residual garnet and cpx/gt, as well as the dependence of partition coefficients on residual phase compositions. We chose partition coefficients that had been determined experimentally at pressures ( $\sim 3$  GPa) and for clinopyroxene and garnet compositions appropriate to the processes we model, and that had been determined during the same experiment or sets of experiments. This criterion significantly limited the available range of partition coefficients. We found that within this range, the choice of clinopyroxene partition coefficients did not significantly influence our results. However, mixing partition coefficients from multiple studies does yield significantly different results, so we avoided doing this for all minerals except olivine.

Our model naturally explains the relative geochemical heterogeneity of Lanai magmas compared to West Maui/East Molokai magmas. The data are most consistent with the origin of Lanai lavas in melt-melt mixing between magmas derived independently from the Lanai and Haleakala plume sources. Solid-solid mixing of the Lanai (eclogite) and Haleakala (peridotite) plume sources prior to melting, in proportions appropriate to the observed Lanai

lava trace element and isotope compositions, would increase the modal amount of garnet in this mixed source. For extents of melting commonly inferred for peridotite in the Hawaiian plume [ $\sim 6$ -20%, Hofmann et al., 1984; Eggins, 1992; Sims et al., 1995, 1999], the increased abundance of garnet in the source would generate much higher Sm/Yb than is observed in Lanai lavas. However, high degrees of melting ( $F > 0.7$ ) of the Lanai source prior to mixing with Haleakala source melts is consistent with the observed Sm/Yb. A melt-melt mixing scenario implies that unmixed melts exist to relatively shallow depths within the plume, and possibly even within the lithosphere and crustal magma chambers. Observations of melt inclusions in individual olivine crystals indicate that melt heterogeneities exist on scales that can readily be trapped over the course of crystallization of individual phenocrysts in the shallow magma chamber [Sobolev et al., 2000; Norman et al., 2002]. These independent observations support the plausibility of high-level mixing of heterogeneous melts that we propose.

The fertilization model for the West Maui/East Molokai source is a process that can generate the characteristic isotopic homogeneity of Kea-type lavas. The infiltration/fertilization of the depleted lithosphere by the gabbro melts is a stage of pre-mixing of these two lithologic segments prior to the melting event that generates the erupted lavas. The infiltration of gabbro-eclogite melt is a self-buffering process, as gabbro melt can only 'freeze-in' to the peridotite up to proportions of about 40:60 eclogite melt:peridotite, based upon pMELTS calculations and experiments designed to address this process in the mantle wedge above subduction zones [Rapp et al., 1999]. Because this model of melt-solid (metasomatic) interaction provides a mechanism for pre-mixing or homogenization in the Kea source, we favor this model over solid-solid or melt-melt mixing scenarios. Although either of these mechanisms could potentially generate homogeneous magmas, the processes and proportions of mixing would need to be consistently reproducible over millions of years. In contrast, the fertilization or metasomatic model of gabbro-eclogite melt infiltration in peridotite is inherently buffered at a constant proportion and naturally gives rise to homogeneous magmas.

The Lanai and West Maui/East Molokai models present contrasting mechanisms for interaction of eclogite-derived melt with surrounding peridotite. These contrasts may be understood through consideration of the relative eclogite melt:peridotite proportions.

At high ratios (>40:60), peridotite is effectively soluble in eclogite melt. Through reaction/infiltration processes [c.f., as modeled by Spiegelman et al., 2001], the eclogite melt would infiltrate and dissolve peridotite along initial higher permeability zones, and self-organize into steady-state channels that localize and isolate much of the eclogite melt flux. This process can account for the separation of eclogite melt from the residue and its transport through peridotite without much apparent chemical modification. Numerical modeling of flow in porous media involving precipitation instead of dissolution, such as expected for lower eclogite melt:peridotite, shows that incipient melt channels will crystallize and choke, forcing the melt to divert to other regions [Aharonov et al., 1997]. In this case, the flow of eclogite melt into the peridotite is diffuse, and may generate a homogeneous, fertilized peridotite.

The mixing mechanisms and proportions in the fertilization model are consistent with observed and inferred  $\delta^{18}\text{O}$  and  $^{187}\text{Os}/^{188}\text{Os}$  for ancient oceanic lithosphere. Both of these isotope systems should have contrasting signatures for oceanic crust vs. the associated complementary residual oceanic lithosphere and thus trace lithospheric contribution to the Maui Nui source. Oxygen in the gabbroic section of oceanic crust is modified by mid-ocean ridge hydrothermal alteration, while the residual lithosphere apparently generally escapes this process. Observations indicate oceanic gabbro has  $\delta^{18}\text{O} \sim 0\text{-}3\text{‰}$  [Gregory and Taylor Jr., 1981; Stakes, 1991; Hart et al., 1999; Miller et al., 2001] while the serpentinized residual oceanic lithosphere has  $\delta^{18}\text{O}$  in olivine of  $3\text{-}5\text{‰}$  [Cocker et al., 1982; Hoffman et al., 1986] and mixing of these components in 10:90 proportions will result in  $\delta^{18}\text{O}=4.5\text{-}5\text{‰}$ , as observed in West Maui lavas (Chapter 2). Because of the strong relative compatibility of Os with respect to Re during mantle melting, ancient depleted oceanic lithosphere should be Os-rich and have low  $^{187}\text{Os}/^{188}\text{Os}$ , whereas ancient oceanic gabbro should have low Os concentrations and high  $^{187}\text{Os}/^{188}\text{Os}$ . However, because residual sulfides in the gabbro-eclogite may retain most of the Os during its partial melting [Fleet et al., 1996; Hart and Ravizza, 1996; Burton et al., 1999], the radiogenic  $^{187}\text{Os}/^{188}\text{Os}$  signature of the recycled oceanic gabbro may not be transferred to the fertilized peridotite. Outside of West Maui, few  $^{187}\text{Os}/^{188}\text{Os}$  analyses of Maui Nui lavas are available, but at least in West Maui they are consistent with our model for the West Maui/East Molokai source [Gaffney et al., 2003].

Stracke et al. [2003] and Kogiso et al. [1997] present quantitative models that specifically address the role of subduction zone dehydration on the isotopic evolution of recycled oceanic crust, and show that Rb/Sr and  $^{87}\text{Sr}/^{86}\text{Sr}$  are particularly sensitive to alteration and dehydration processes ( $^{87}\text{Sr}/^{86}\text{Sr}$  of 2 Ga crust: 0.7015-0.7045, Kogiso et al. [1997];  $>0.708$ , Stracke et al. [2003]). Eiler et al. [1996], Hauri [1996a], Lassiter and Hauri [1998], Blichert-Toft et al. [1999] and Gaffney et al. [2004] have modeled or inferred radiogenic isotope compositions as well as  $\delta^{18}\text{O}$  for postulated recycled oceanic lithosphere components specific to the Hawaiian plume. These Hawaii studies make variable assumptions about perturbation of parent-daughter ratios during hydrothermal alteration at the mid-ocean ridge, and during dehydration of the slab in the subduction zone. Although the predicted radiogenic isotope compositions of recycled oceanic crust can vary greatly, the models we propose for the Lanai (larger degree melts of eclogite derived from basalt+sediment) and West Maui/East Molokai sources (depleted lithosphere fertilized by smaller degree melts of gabbro-eclogite) are broadly consistent with this previous work. Furthermore, the  $^{87}\text{Sr}/^{86}\text{Sr}$  composition for Lanai that we use in our modeling was determined empirically, and so is not dependent upon assumptions of the  $^{87}\text{Sr}/^{86}\text{Sr}$  of ancient crust.

Several arguments have been made against eclogite in the source of Hawaiian magmas. Herzberg and O'Hara [2002] and Feigenson et al. [2003] argue that the inferred high-MgO primary compositions of Hawaiian magmas are inconsistent with contributions from a mafic source in the plume. High-MgO glasses and lavas are observed for several Hawaiian volcanoes, and this is strong support for high-MgO primary magmas in these volcanoes. However, high-MgO glasses or high Fo olivine have not been reported for either Lanai or Kahoolawe, and very few lavas with  $\text{MgO} > 12$  wt. % are observed for either of these volcanoes. Thus, if these volcanoes did have initial MgO as high as proposed for other volcanoes, then they are consistently fractionating large amounts of olivine prior to eruption, so that those primitive compositions are never sampled at these two volcanoes. Norman et al. [2002] use melt inclusions from Koolau, which is isotopically similar to Lanai, to determine that 14 wt. % MgO is a reasonable primary magma composition for this volcano. This is similar to the primary magma that we infer for Lanai and Kahoolawe, which forms from mixing between eclogite-derived melts and primary Haleakala magmas. Trace element and U-series isotope

systematics have also been used to argue against pyroxenite in the Hawaiian plume [Stracke and Sims, 1999; Feigenson et al., 2003], but these studies have all focused on volcanoes for which we do not propose pyroxenite in the source, and thus can not be used to rule out pyroxenite in the Lanai/Kahoolawe magma source.

### ***3.9 Implications for structure and processes in the plume under Maui Nui***

The relative ages of late shield-stage magmatism for Maui Nui volcanoes are W. Molokai > East Molokai  $\geq$  West Maui  $\geq$  Lanai > Kahoolawe > Haleakala [McDougall, 1964; Naughton et al., 1980; Chen et al., 1991]. Probably two, three, or possibly even four of these volcanoes erupted contemporaneously during their shield-building periods. The relative ages given above represent the likely order of cessation of their shield-building periods, and the probable relative ages of the late-shield stage lavas discussed in this paper. The presumed contemporaneity of lavas that span nearly the entire range of compositions seen in the Hawaii archipelago indicates that multiple compositionally extreme components co-existed in the plume and were sampled without apparent significant communication between the magmas (Lanai and East Molokai/West Maui). These contemporaneous volcanoes of Maui Nui show much greater compositional contrast than contemporaneous volcanoes on the Big Island.

Hawaiian compositional endmembers have typically been defined in such a way as to account for the whole range of mantle variability sampled by Hawaiian volcanoes over a 5 My time span. Although this is an appropriate way to describe the system on a large scale, this treatment does not address compositional subtleties apparent on a smaller temporal or spatial scale. Furthermore, the endmembers have not always been sampled regularly over the past 5 My. For example, of all the volcanoes that show extreme Koolau-type compositions (Koolau, Lanai, Kahoolawe), none are younger than Kahoolawe. Conversely, of all the extreme Kea-type compositions (East Molokai, West Maui, Mauna Kea, Kilauea), none are older than East Molokai. The Loihi component is the only endmember that has apparently been sampled regularly throughout the last 5 My (in Kauai, Haleakala, Mauna Loa and Loihi), which suggests that it is a pervasive component of the Hawaiian plume.

Kahoolawe is the youngest volcano for which Koolau-like magmas are observed, and the isotope compositions of its lavas span the range between Lanai and Haleakala. Kahoolawe is also closer in age to Haleakala, and its lavas may represent the exhaustion of long-lived ( $\sim 1$  My) or volumetrically significant Lanai component heterogeneities in the plume, and a transition to Haleakala-dominated magmas.

As the other end of the Lanai/Koolau array, Haleakala is a relatively primitive plume component. Its elevated  $^3\text{He}/^4\text{He}$  [13.1-16.8  $R_A$ , Kurz et al., 1987], high time-integrated Th/U (high  $^{208}\text{Pb}/^{204}\text{Pb}$ ), and normal-mantle-like  $\delta^{18}\text{O}$  are also consistent with the relatively primitive nature of this component [Eiler et al., 1998]. The high MgO, and low  $\text{SiO}_2/\text{FeO}$  of the Haleakala primary magmas imply high pressures of separation of the magma from its source. The intermediate  $^{87}\text{Sr}/^{86}\text{Sr}$ ,  $^{143}\text{Nd}/^{144}\text{Nd}$ ,  $^{176}\text{Hf}/^{177}\text{Hf}$  and  $^{206}\text{Pb}/^{204}\text{Pb}$  of Haleakala make it difficult to identify this as a separate component, but the elevated  $^{208}\text{Pb}/^{204}\text{Pb}$  requires a distinct source that is not a mixture between Lanai and West Maui/East Molokai.

The East Molokai and West Maui lavas are nearly indistinguishable chemically, and thus are both tapping the same or nearly identical mantle sources. The plume component which they are tapping may be a single, very large domain in the plume, which has been effectively homogenized through infiltration and fertilization processes proposed here. This contrasts with the interpretation that the basalt+sediment - derived eclogite (Lanai component) occupies much smaller domains in the plume. Furthermore, these volumes occupy separate places in the plume, such that they are not both sampled at the same volcano, but rather at neighboring volcanoes, at the same time or in close succession. This may reflect the stretching and mixing mechanisms in the mantle and plume [i.e., Farnetani et al., 2002], or the material properties of the different lithologies, and their response to mechanical homogenization in the mantle. These stretching mechanisms are effective at separating the basalt+sediment and gabbro+peridotite oceanic crust layers in the plume.

This interpretation of the components and the way that they are sampled does not require a concentrically zoned plume model at this age as is commonly inferred for recent plume structure from analysis of Big Island magmatism [DePaolo et al., 2001]. The Haleakala component is sampled at volcanoes that lie on both the Kea and Loa trends. The

location of the Koolau volcanoes on the Loa trend and the Kea volcanoes on the Kea trend may instead represent a lateral zonation, as would be predicted by the Farnetani et al. [2002] model for vertical stretching of heterogeneities in the plume. Furthermore, the Lanai component heterogeneities must be of a small enough size that their melts generally mix with the Haleakala component, whereas the West Maui/East Molokai component is of a large enough extent that its melts typically erupt without apparent mixing with Haleakala. However, Haleakala is close enough in composition to West Maui/East Molokai that smaller degrees of mixing between West Maui/East Molokai and Haleakala might not be resolved.

### ***3.10 Summary and relevance to the past 5 My of Hawaiian shield-stage magmatism***

Our interpretations of the Lanai and West Maui/East Molokai endmembers invokes specific melting and mixing processes for generation of the geochemical signatures. Operation of the processes proposed for the Lanai source over a 5 My time scale may generate temporal heterogeneity evident on the larger time scale. Conversely, the processes proposed for West Maui/East Molokai are likely to produce a more uniform, temporally homogenous geochemical signature.

The enriched Koolau component sampled in Maui Nui by Lanai and Kahoolawe volcanoes is also sampled at the older Koolau volcano. However, the Pb-Pb and Sr-Nd isotope correlations of Koolau, Lanai and Kahoolawe are slightly offset from one another, indicating that this enriched component is temporally heterogeneous. Lanai and Koolau are unique relative to the rest of the Hawaiian shield-stage lavas, as compositions this enriched are not observed at any older or younger volcanoes. Thus, the Koolau/Lanai component may represent an episodic recycling process, or possibly even a unique event related to the preservation in the plume of an unusually large domain of ancient subducted pelagic sediment. Furthermore, heterogeneity in this enriched endmember indicates that compositional heterogeneities in the oceanic crust are preserved or perhaps enhanced through the recycling and storage process. For example, Rb/Sr or U/Pb may be variably modified during hydrothermal alteration or subduction processes, which can lead to non-uniform evolution

of  $^{87}\text{Sr}/^{86}\text{Sr}$  or  $^{206}\text{Pb}/^{204}\text{Pb}$  within a single segment of oceanic crust.

The depleted Kea component has been a dominant component in the Hawaiian plume for the past 2 My. Although we and others argue that this component is also created by recycling oceanic crust and lithosphere, it is characterized by a high degree of homogeneity. This contrasts with the Koolau component, where the recycled component exhibits a relatively high degree of heterogeneity. We attribute the homogeneity of the Kea component to the homogenizing and natural buffering by infiltration on a large scale of the gabbro and peridotitic segments of oceanic lithosphere. Some minor heterogeneity is preserved in the Kea component, however, as evident in the linear and distinct Pb isotope arrays observed in East Molokai and West Maui, as well as in Mauna Kea [Eisele et al., 2003].

Our interpretation that the Haleakala component is the pervasive plume component at Maui Nui is also applicable to volcanoes at the older and younger ends of the chain. Haleakala lavas in Maui Nui are analogous to the Loihi component, which is characterized by even higher  $^3\text{He}/^4\text{He}$  than observed at Haleakala [Kurz et al., 1983]. The Loihi component is sampled on Kauai at the oldest end of the chain, at Loihi at the youngest end of the chain, and by Mauna Loa on the Big Island [Kurz et al., 1983, 1987, 1995; Mukhopadhyay et al., 2003]. The relatively continuous presence of this component in lavas erupted over the past 5 my indicates that this is a long-lived plume component and may constitute the matrix of the plume itself. The deepest lavas of Mauna Kea, sampled through HSDP-2, also trend to the lower  $\text{SiO}_2$ , and higher  $^{208}\text{Pb}/^{204}\text{Pb}$  and  $^3\text{He}/^4\text{He}$  characteristic of the Loihi component [Feigenson et al., 2003; Kurz et al., 2004]. The oldest lavas in the Koolau Scientific Drilling Project also show indications of the Loihi component [Huang and Frey, 2003]. Thus, this component has been a long-lived contributor to Hawaiian shield-stage magmas, and was sampled by magmas during the pre-shield and throughout the shield-building stages of magmatism.

In the Maui Nui volcanoes, we see the exhaustion of Koolau and the initiation of Kea as dominant components in the plume. The Loihi component is present in volcanoes both older and younger than Maui Nui. Although deep stratigraphic sections, accessed either through drilling or submersible, in volcanoes are rare, none yet observed show the transition from Kea to Koolau within the lavas of a single volcano. Individual volcanoes transition



from Loihi at depth to either Kea and Koolau compositions in the younger lavas [Feigenson et al., 2003; Huang and Frey, 2003; Kurz et al., 2004]. From this, we might surmise that the extreme compositions of both Koolau and Kea-type lavas are late-stage phenomena, and it is only during the final stages of shield-building magmatism that their signals are preserved.

Interaction of Kea or Koolau component magmas with Loihi-like plume matrix or the Pacific lithosphere as the magmas travel to the surface could dilute or erase their distinctive geochemical signatures. However, development of a channelized network through which magmas can pass, by reaction of magma with the solid mantle matrix [Kelemen et al., 1995; Spiegelman et al., 2001] could allow magmas to preserve their distinctive geochemical signatures. This may be one of the fundamental mechanisms controlling the time-composition trends in Hawaiian volcanoes. Early-generated Koolau or Kea magmas do not erupt at the surface, but instead are exhausted in forming reaction-armored melt-conduit channels that at a later stage of volcanism allow the passage of these melts to the surface with little modification by ambient mantle or Pacific lithosphere. Such processes have been modeled for adiabatically upwelling mid-ocean ridge systems [Kelemen et al., 1995], and may be applicable to upwelling in the Hawaiian plume as well.

### **3.11 Conclusions**

The late shield-building stage lavas of Maui Nui span nearly the entire range of compositions observed across the entire Hawaiian chain. These lavas record the exhaustion of the enriched Koolau component, and the initiation of the depleted Kea component as dominant compositional endmembers.

Isotope compositions are consistent with a component of ancient, recycled oceanic lithosphere in the plume sources of both Kea and Koolau type magmas. We propose physical models for melting this component in the plume. Kea-type magmas derive from melting of homogeneously hybridized gabbro+depleted lithosphere segments of recycled lower oceanic lithosphere. Hybridization and homogenization occur when 20-40% melts of the gabbro-derived eclogite infiltrate and reactively freeze into the depleted lithosphere peridotite in 10:90 eclogite melt:depleted lithosphere proportions. Koolau-type magmas originate from

high-degree ( $F \sim 0.7$ ) melts of recycled upper basaltic crust and sediment that mix with Haleakala-type melts, in proportions that range from 50-70% eclogite melt.

Physical mechanisms of melt-solid interaction and melt transport are important in the generation of both the homogeneity and heterogeneity that we observe in Maui Nui lavas. Infiltration and freezing of gabbro-derived eclogite melts in the depleted oceanic peridotite leads to homogenization of the lower oceanic lithosphere-derived recycled segment in the plume. Organization of upper crust-derived melt into isolated melt channels preserves the Koolau-type compositions from destruction through interaction with peridotite matrix.

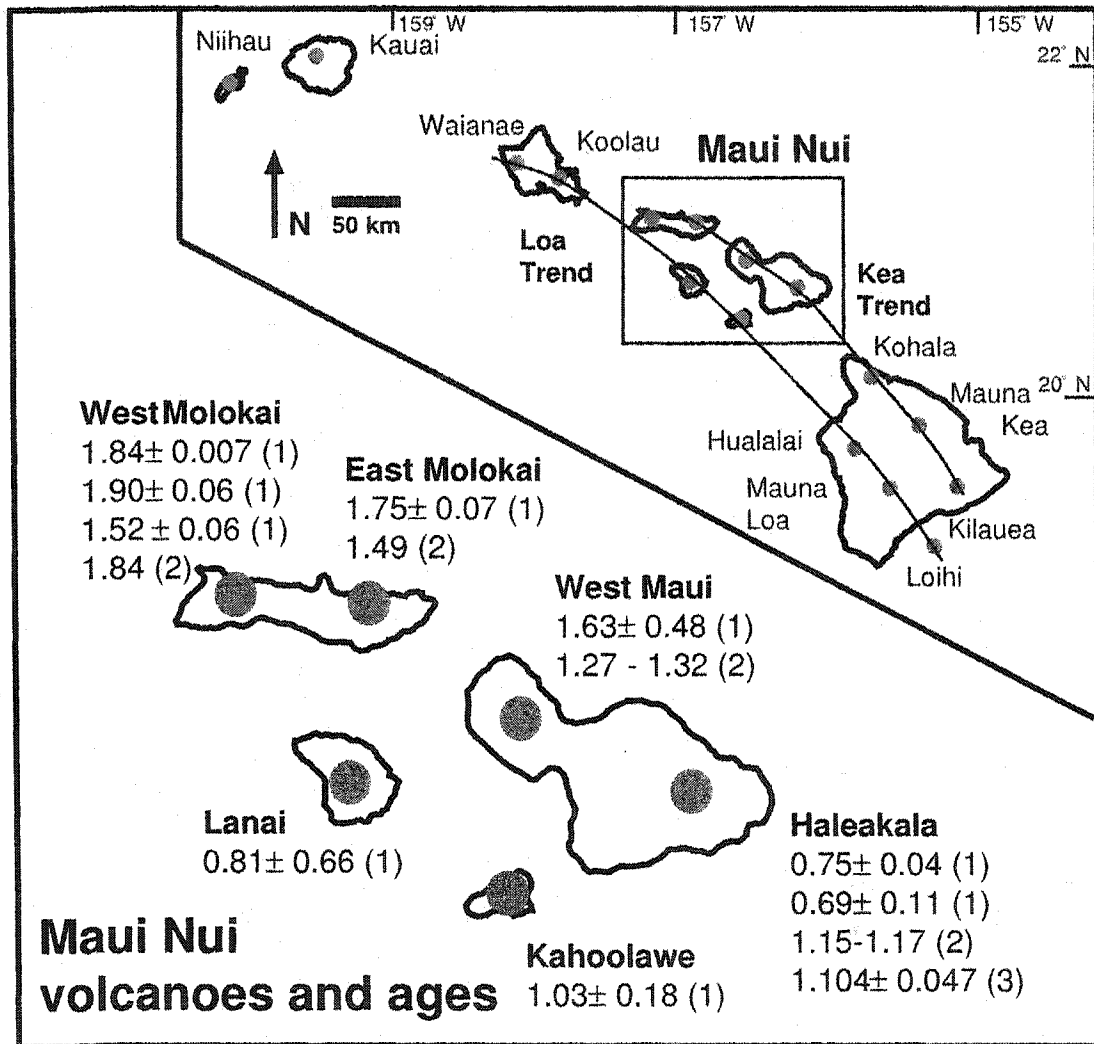


Figure 3.1: Map of the islands and volcanoes of Maui Nui, with an inset of the Hawaiian Islands. Ages are given in Ma, and are from: (1) Naughton et al. [1980], (2) McDougall [1964], and (3) Chen [1993]. Kea and Loa trends from Jackson et al. [1972].

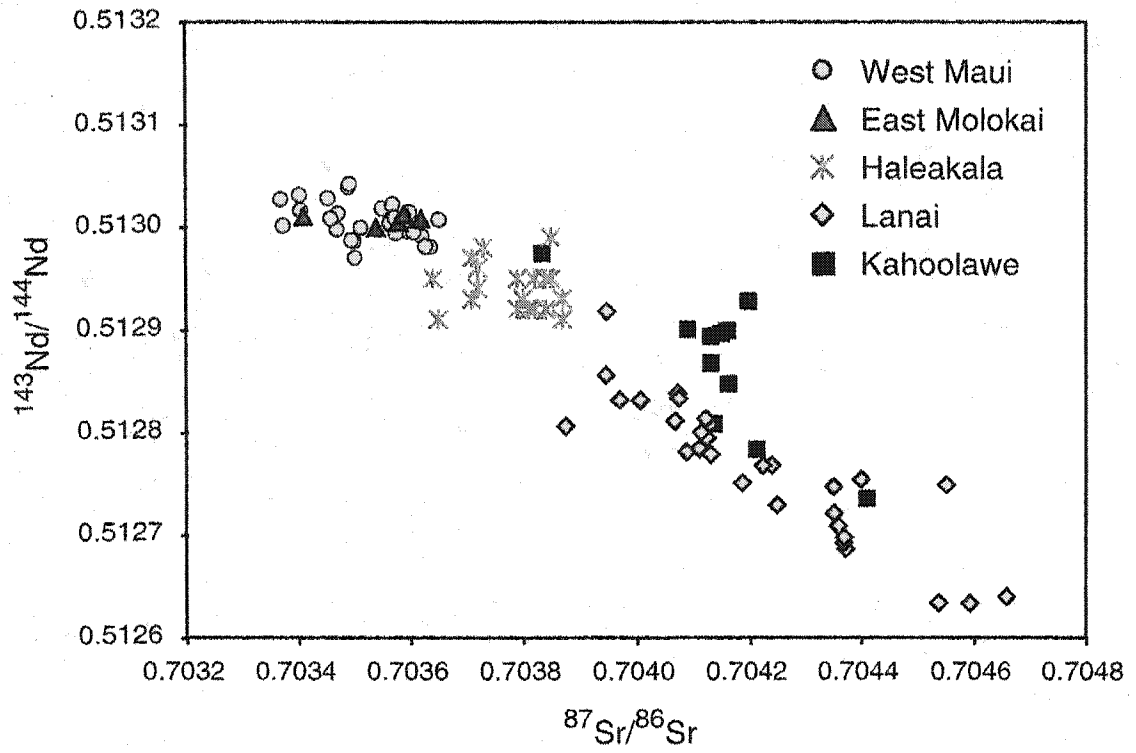


Figure 3.2:  $^{87}\text{Sr}/^{86}\text{Sr}$ - $^{143}\text{Nd}/^{144}\text{Nd}$  variation in Maui Nui shield stage lavas. Data sources given in Appendix B.

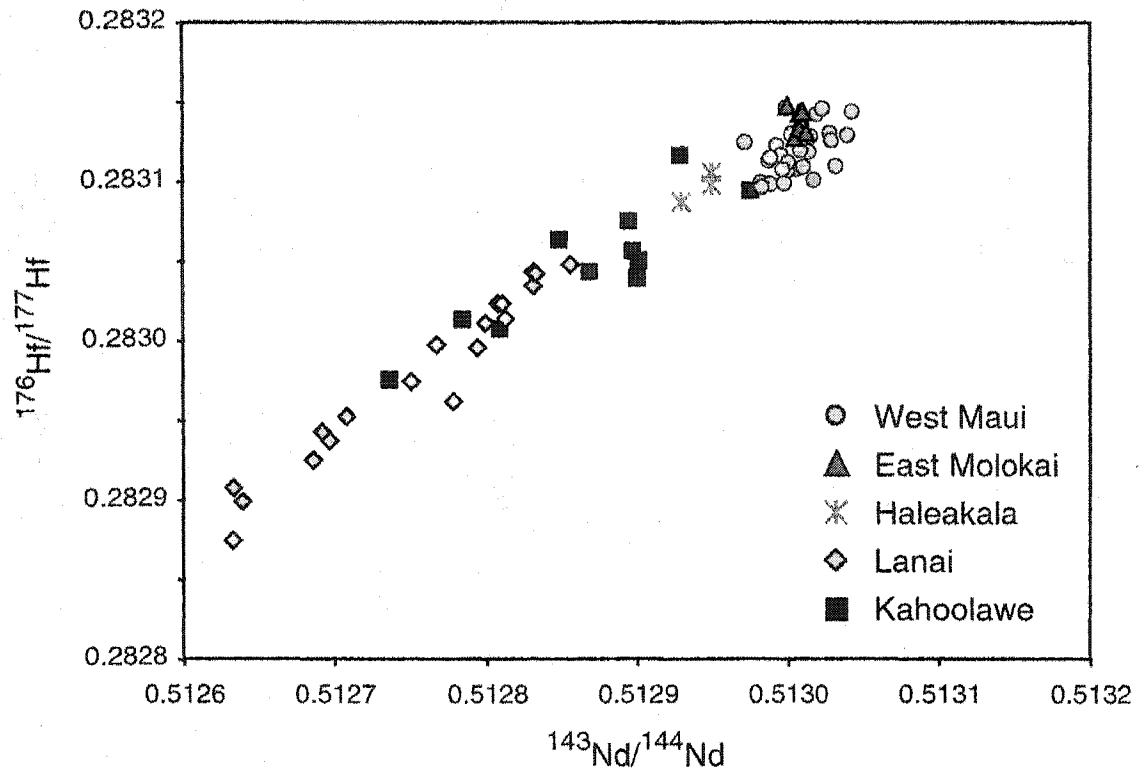


Figure 3.3:  $^{143}\text{Nd}/^{144}\text{Nd}$ - $^{176}\text{Hf}/^{177}\text{Hf}$  variation in Maui Nui shield stage lavas. Data sources given in Appendix B.

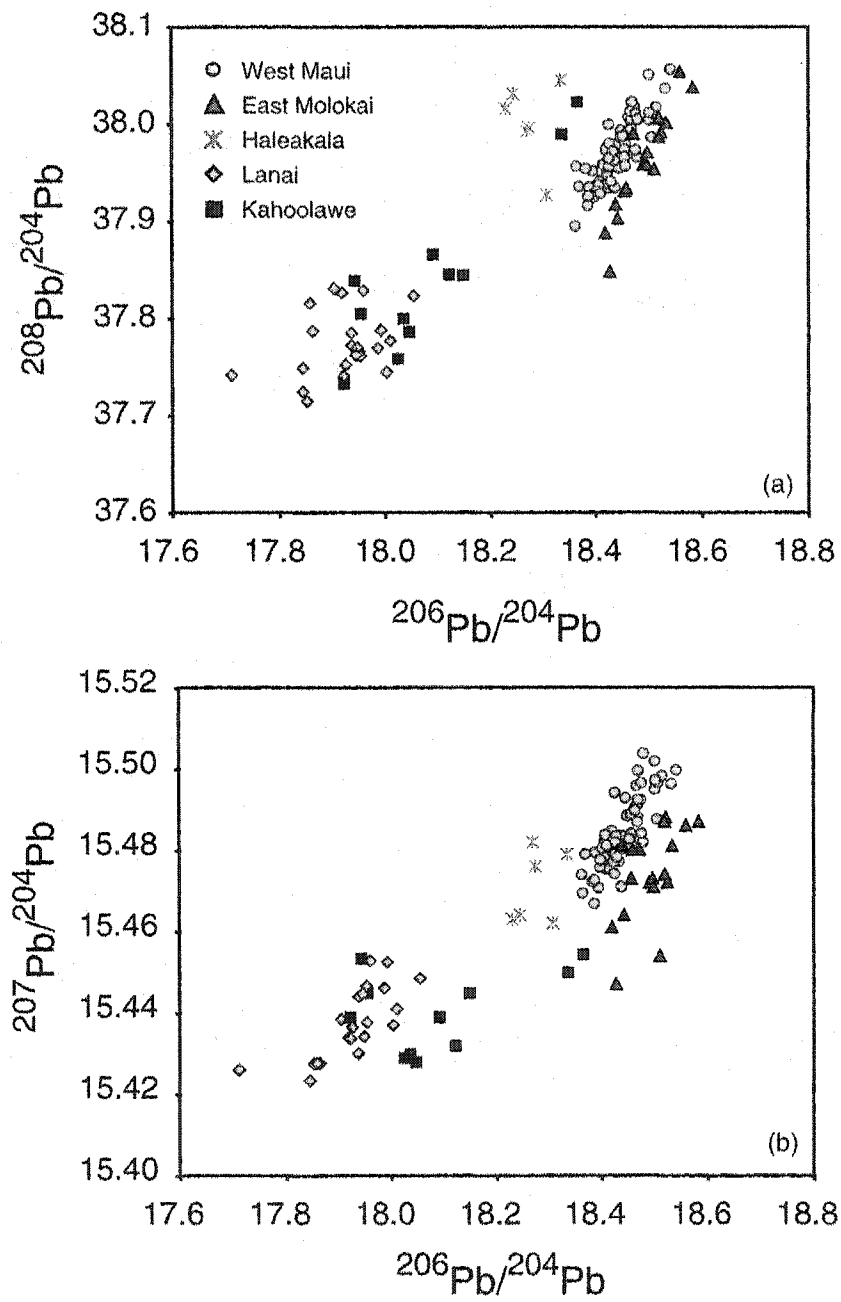


Figure 3.4: (a)  $^{206}\text{Pb}/^{204}\text{Pb}$ - $^{208}\text{Pb}/^{204}\text{Pb}$ , and (b)  $^{206}\text{Pb}/^{204}\text{Pb}$ - $^{207}\text{Pb}/^{204}\text{Pb}$  variation in Maui Nui shield-stage lavas. Data sources given in Appendix B.

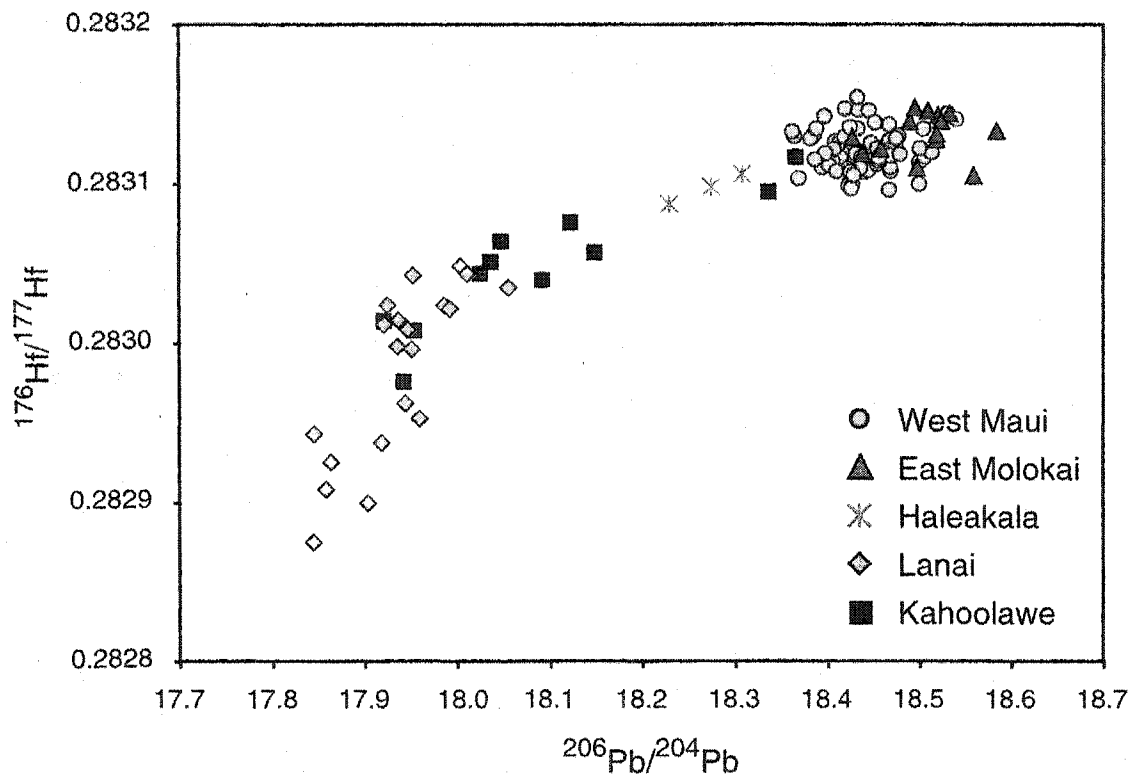


Figure 3.5:  $^{176}\text{Hf}/^{177}\text{Hf}$ - $^{206}\text{Pb}/^{204}\text{Pb}$  variation in Maui Nui shield-stage lavas.

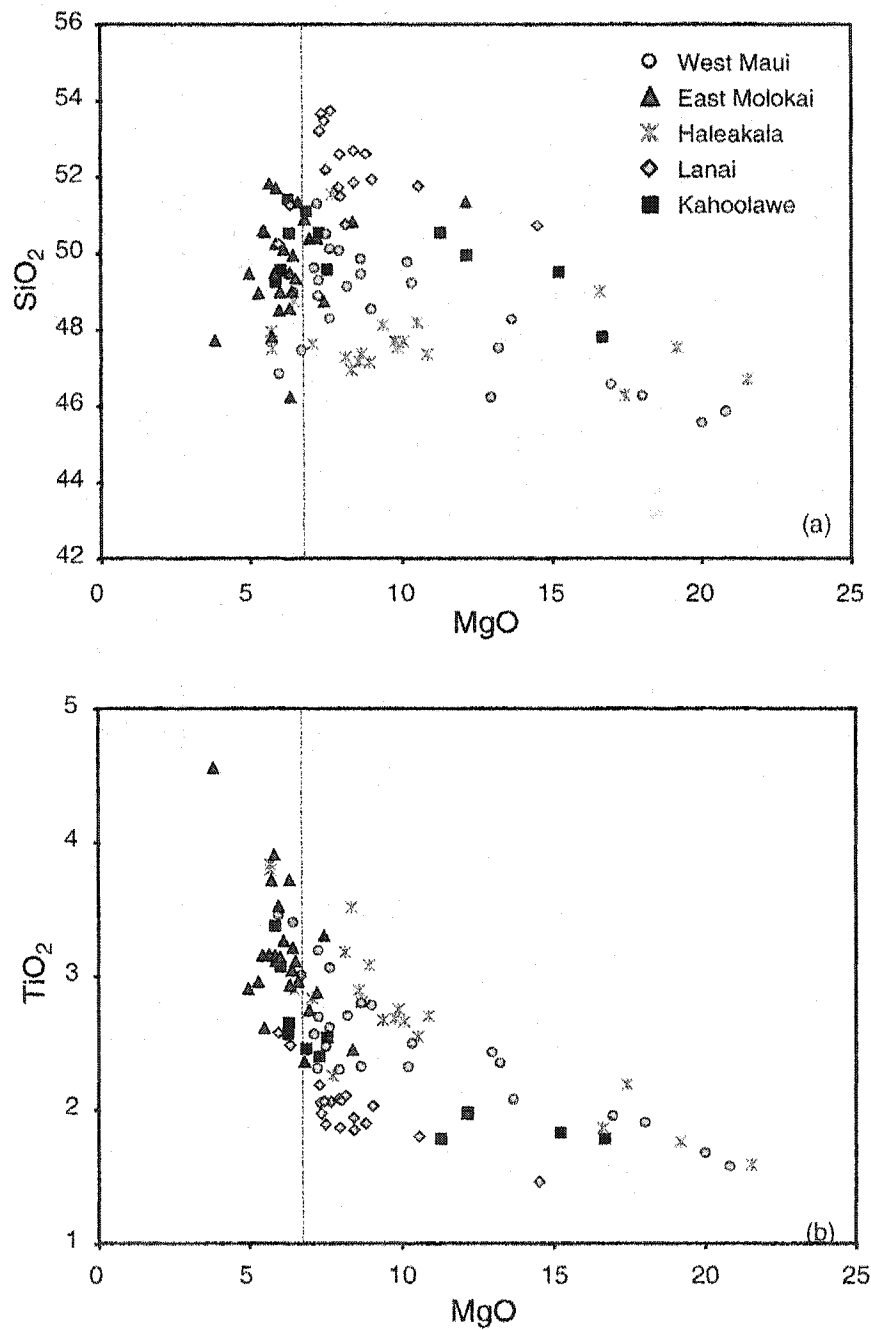


Figure 3.6: (a) SiO<sub>2</sub>-MgO and (b) TiO<sub>2</sub>-MgO variation in Maui Nui shield-stage lavas. Oxides given in wt. %. The vertical line at 7% MgO represents the approximate boundary between olivine-only fractionation (>7%) and clinopyroxene saturation (<7%). Data sources given in Appendix B.



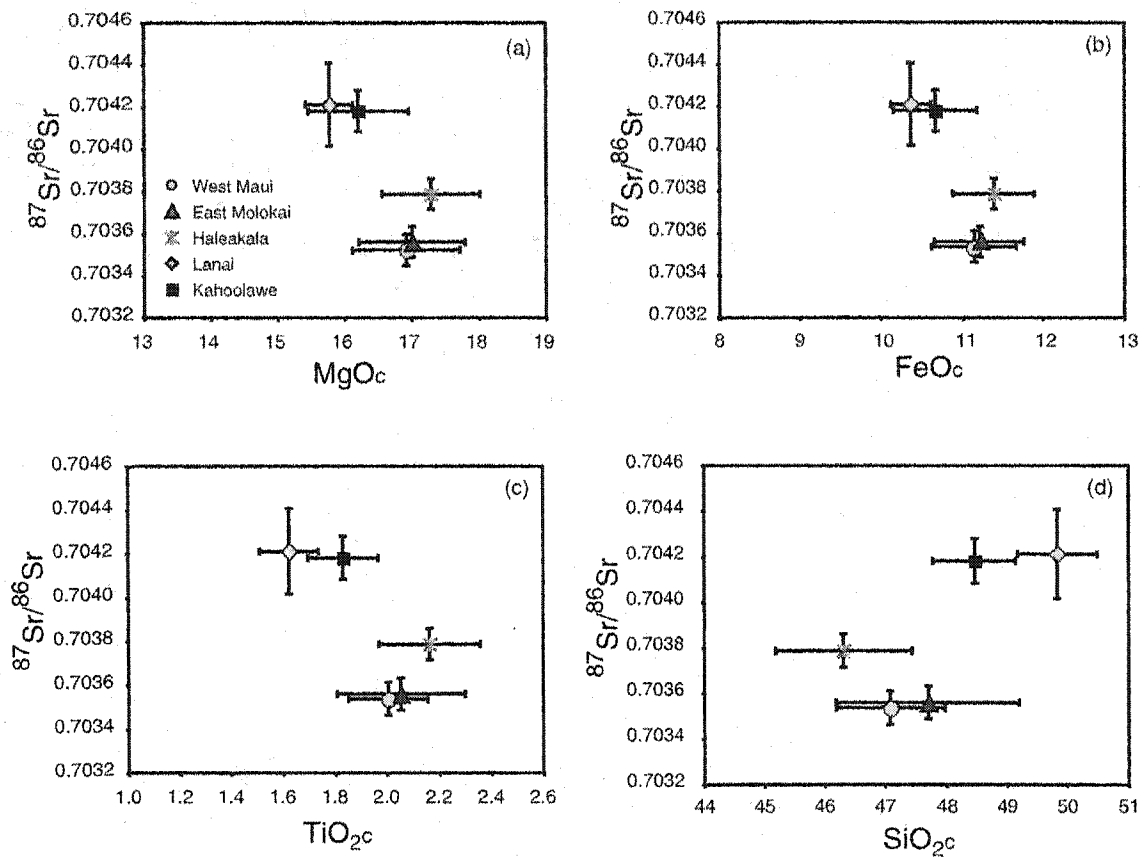


Figure 3.7: Average compositions for Maui Nui volcanoes. Major element compositions are corrected for olivine accumulation, to equilibrium with  $\text{Fo}_{90}$ . Error bars represent one standard deviation. Averages are of all data for a particular volcano, and are not significantly different when averaging only samples for which both major element and isotope data exist.

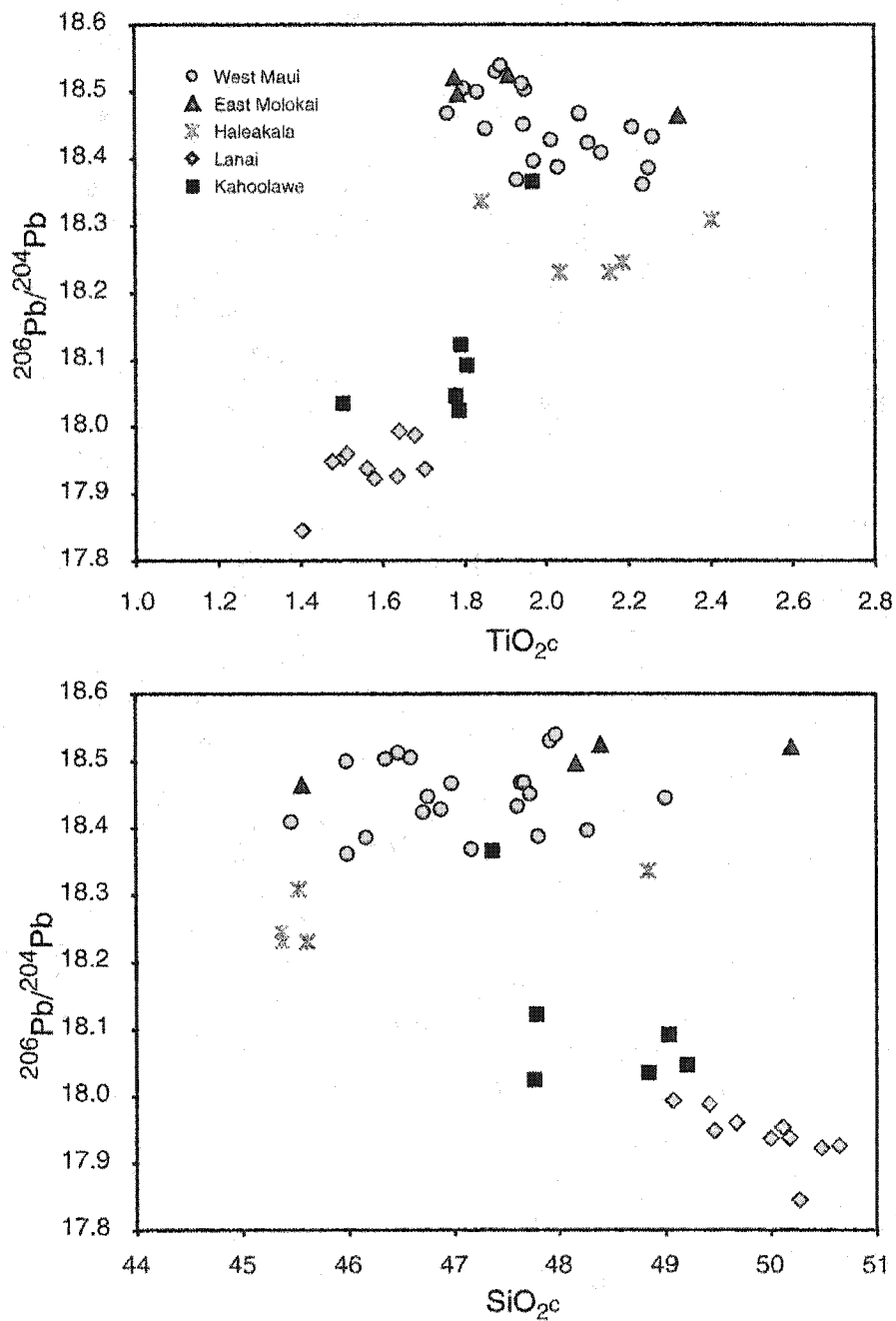


Figure 3.8: (a)  $\text{TiO}_2$ - $^{206}\text{Pb}/^{204}\text{Pb}$  and (b)  $\text{SiO}_2$ - $^{206}\text{Pb}/^{204}\text{Pb}$  variation in Maui Nui shield-stage lavas. Major element compositions have been corrected for olivine accumulation to equilibrium with  $\text{Fo}_{90}$  olivine.

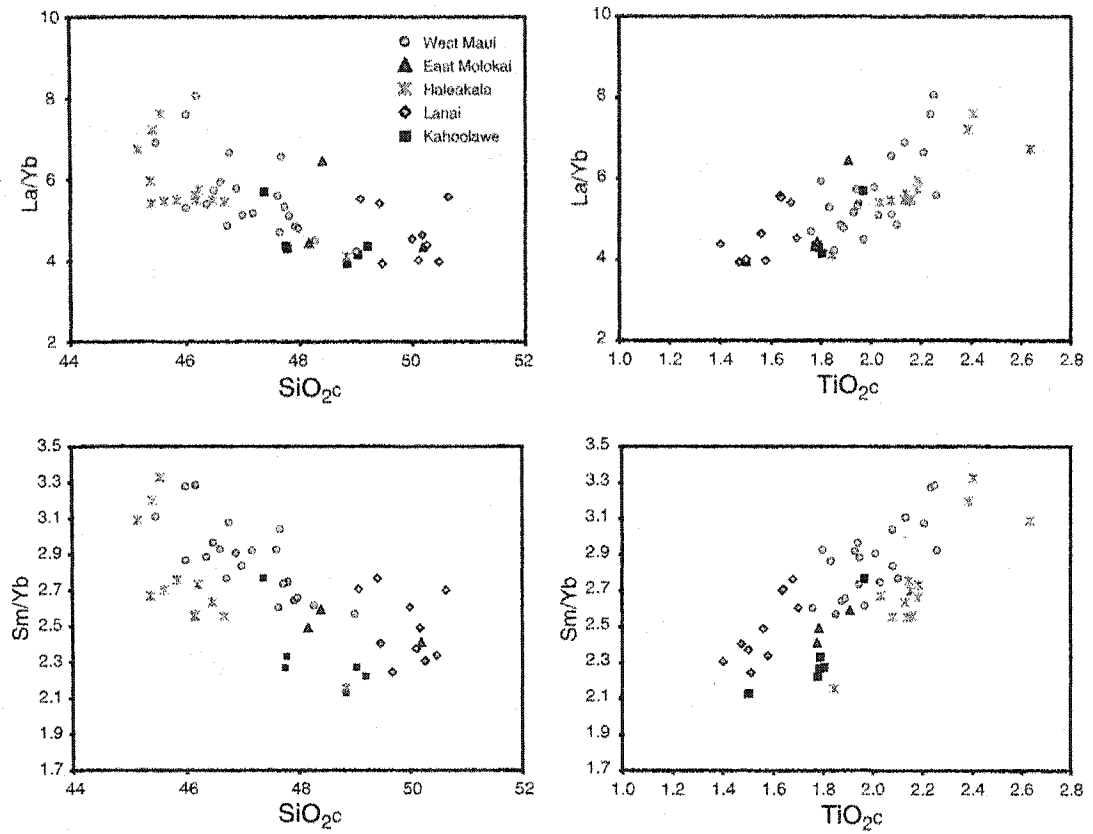


Figure 3.9: REE-major element variation for Maui Nui shield-stage lavas. Major element compositions have been corrected for olivine accumulation to equilibrium with Fo<sub>90</sub> olivine.

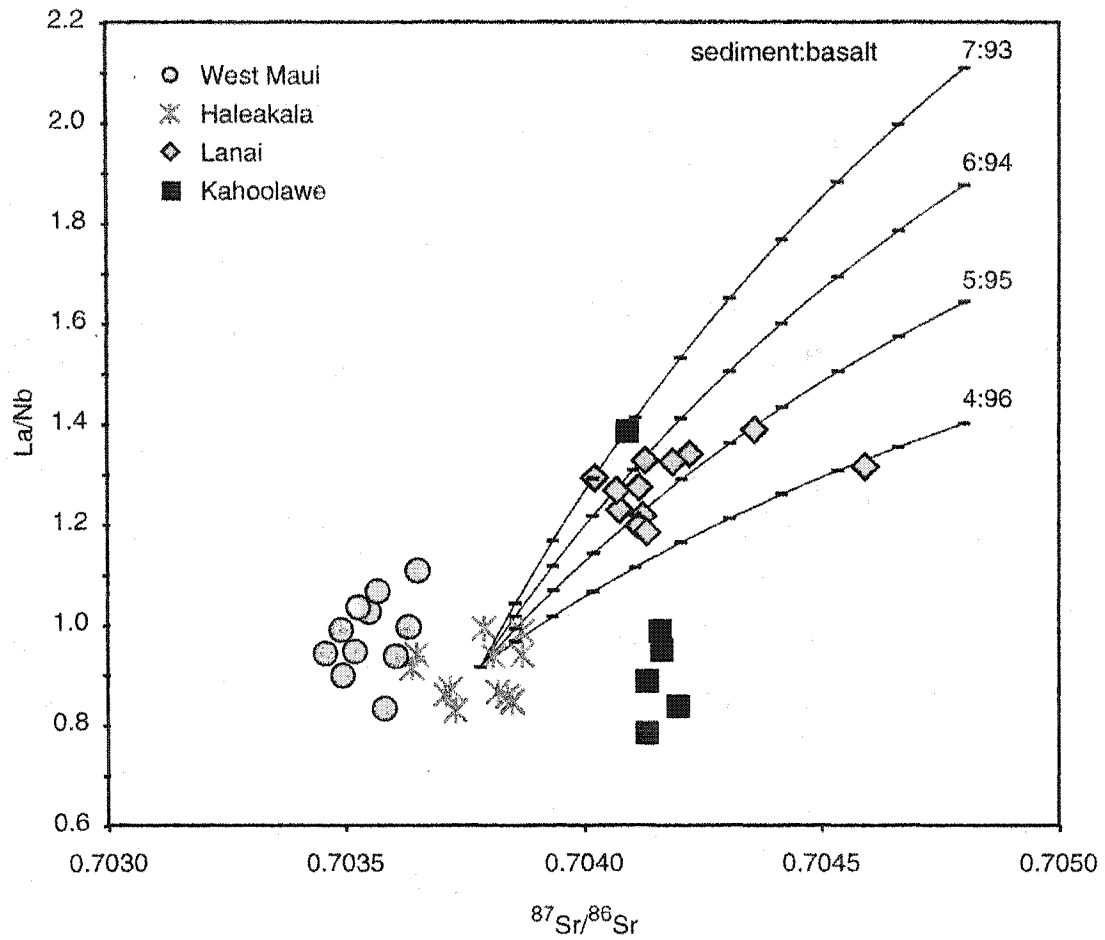


Figure 3.10: La/Nb- $^{87}\text{Sr}/^{86}\text{Sr}$  variation in Maui Nui shield-stage lavas. Lines show mixing between average Haleakala primary melt and melts of ancient upper oceanic crust. Sediment:basalt in upper oceanic crust ranges from 4:96 to 7:93. Mixing lines are marked for 10% increments of mixing. See text and Table 3.2 for detailed discussion of model parameters.

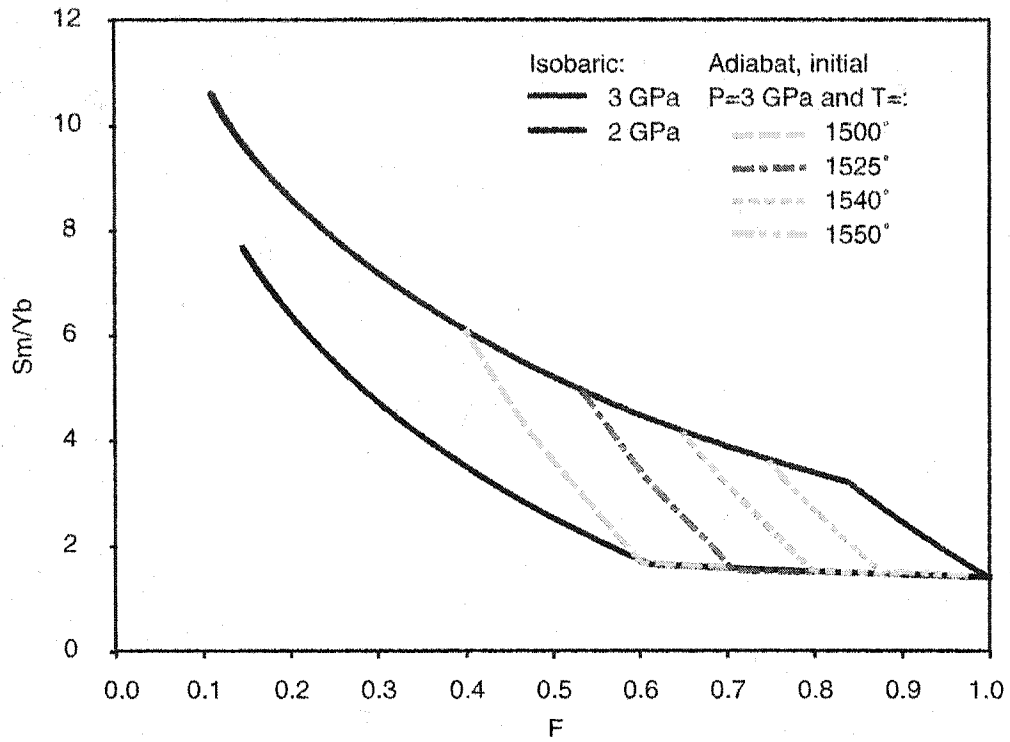


Figure 3.11: Predicted Sm/Yb vs. degree of partial melting (F), for equilibrium batch melts of mid-ocean ridge basalt, calculated with pMELTS [Ghiorso et al., 2002]. Shown are curves for isobaric melting at 2 and 3 GPa, as well as adiabatic decompression from 3 to to 2 GPa, for a range of starting temperatures.

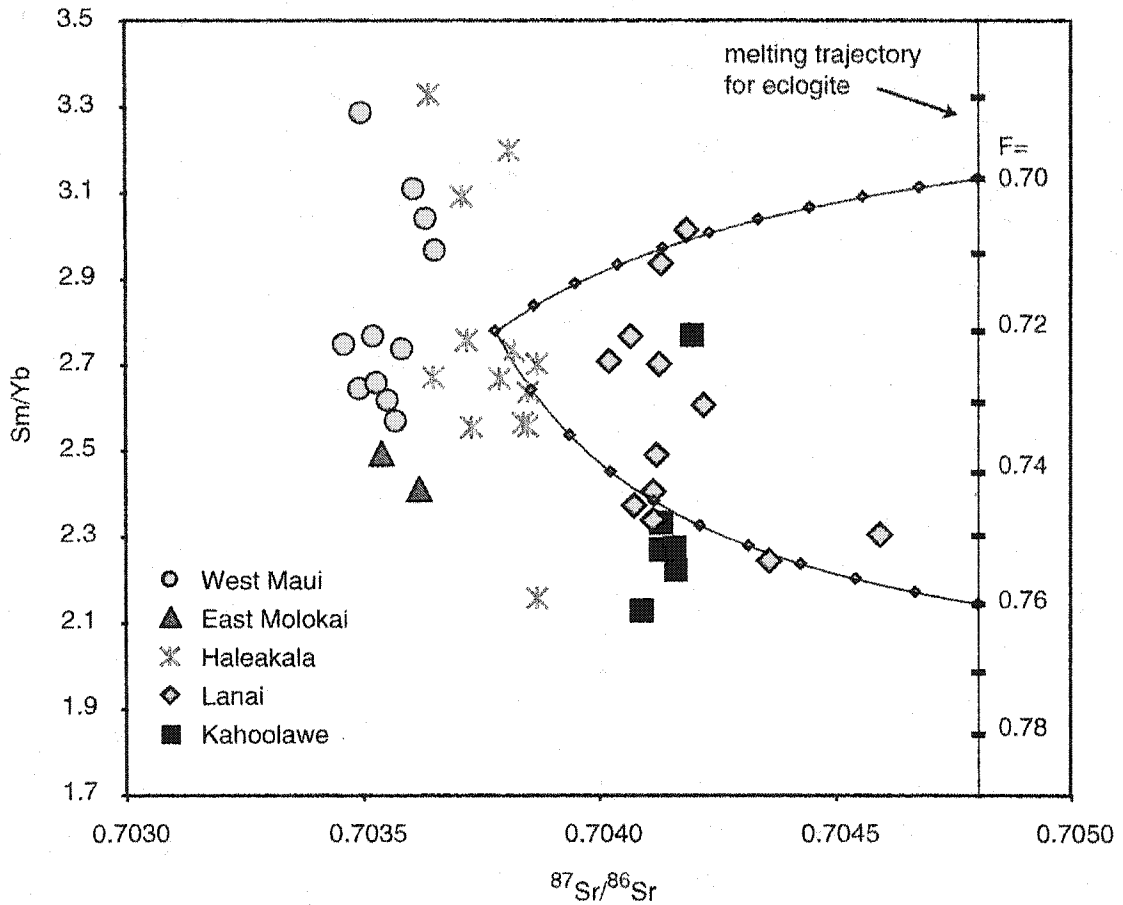


Figure 3.12: Sm/Yb vs.  $^{87}\text{Sr}/^{86}\text{Sr}$  for Maui Nui shield-stage lavas. Eclogite melting trajectory shows Sm/Yb variation with progressive melting, from  $F=0.69$  to  $F=0.78$ . Eclogite is 5:95 mix of sediment:basalt. Mixing lines between eclogite melts and average Haleakala primary melt are marked with 10% mixing increments.

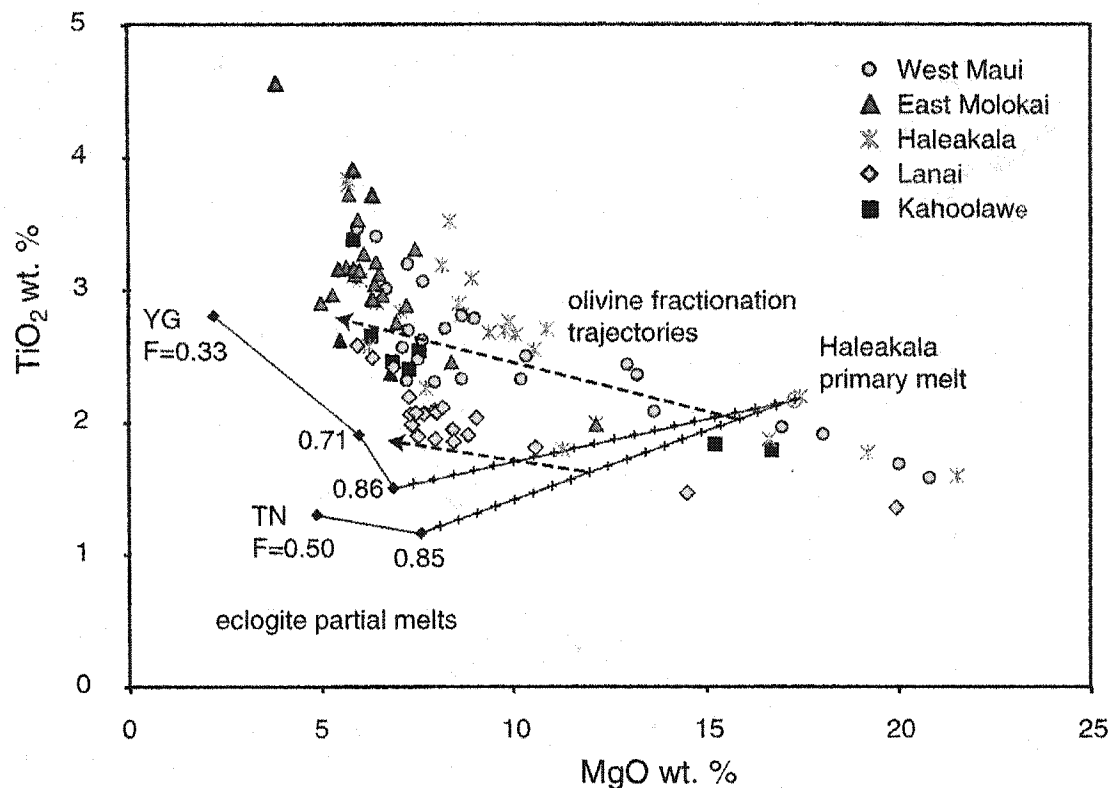


Figure 3.13: MgO-TiO<sub>2</sub> variation in Maui Nui shield-stage lavas. Lines with tick marks show mixing between eclogite partial melts and inferred Haleakala primary melt, calculated to be in equilibrium with Fo<sub>90</sub> olivine. Eclogite melt compositions are from experimental determinations by Yaxley and Green [1998] (YG) and [Takahashi and Nakajima, 2002] (TN). Also shown are smaller-degree melts for YG and TN experiments. Mixing lines are marked in 5% increments. The range of Lanai through Haleakala lavas can be derived through olivine fractionation of magmas formed by 30:70 to 85:15 mixing between eclogite melts and Haleakala primary melts.

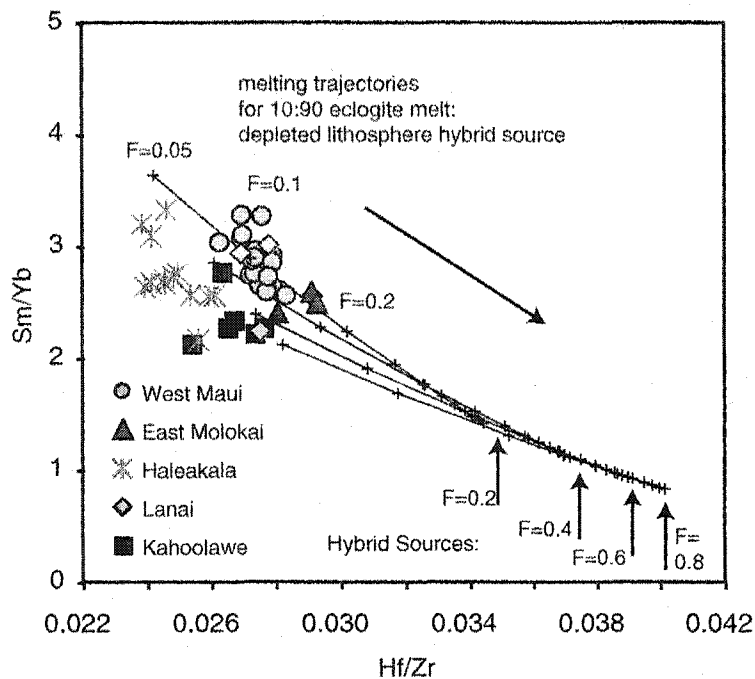


Figure 3.14: Hf/Zr - Sm/Yb variation in Maui Nui shield-stage lavas. Endpoints of melting trajectories (marked with arrows) are for 10:90 mixes of gabbro-derived eclogite melts:depleted oceanic lithosphere. Mixes for 20%, 40%, 60% and 80% gabbro melts are shown. Melting trajectories of hybridized eclogite melt:depleted lithosphere are marked at 5%, 10%, and then in additional 10% melting increments, for  $F > 0.2$ . West Maui and East Molokai lavas are consistent with 5-15% melting of a depleted peridotite source that was fertilized by 10-20% melts of gabbro-derived eclogite.



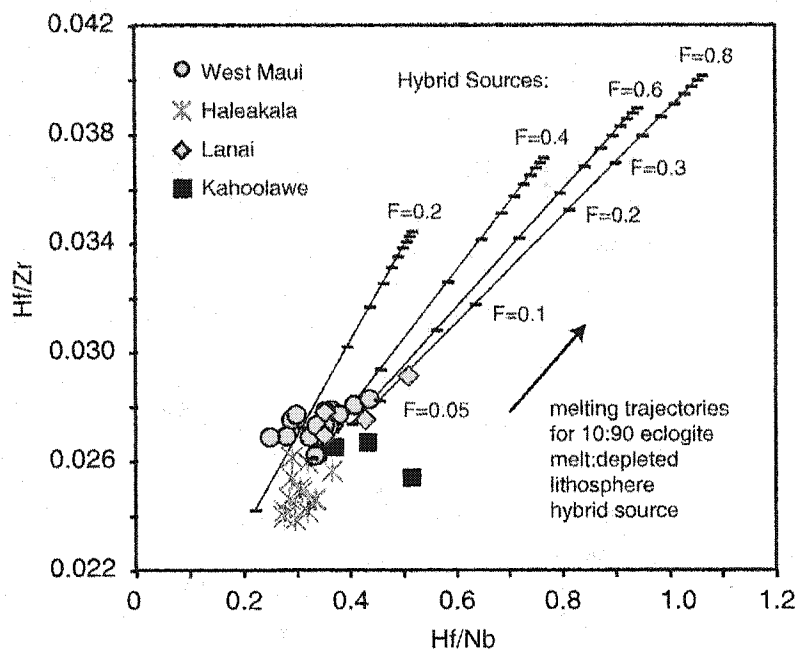


Figure 3.15: Hf/Nb - Hf/Zr variation in Maui Nui shield-stage lavas. Endpoints of melting trajectories (labeled 'Hybrid Sources') are for 10:90 mixes of gabbro-derived eclogite melts:depleted oceanic lithosphere. Mixes for 20%, 40%, 60% and 80% gabbro melts are shown. Melting trajectories of hybridized eclogite melt:depleted lithosphere are marked for 10% melting increments,  $F > 0.2$ . West Maui and East Molokai lavas are consistent with 5-15% melting of a depleted peridotite source that was fertilized by 10-20% melts of gabbro-derived eclogite.

Table 3.1: Pearson's correlation coefficients

	Lanai	Kahoolawe	Haleakala	West Maui	East Molokai
$^{87}\text{Sr}/^{86}\text{Sr}$ - $^{143}\text{Nd}/^{144}\text{Nd}$	<b>-0.894</b>	<b>-0.787</b>	-0.114	-0.403	-0.037
$^{143}\text{Nd}/^{144}\text{Nd}$ - $^{176}\text{Hf}/^{177}\text{Hf}$	<b>0.978</b>	<b>0.888</b>	<b>0.908</b>	<b>0.48</b>	0.384
$^{208}\text{Pb}/^{204}\text{Pb}$ - $^{207}\text{Pb}/^{204}\text{Pb}$	<b>0.757</b>	0.396	0.484	<b>0.815</b>	<b>0.568</b>
$^{208}\text{Pb}/^{204}\text{Pb}$ - $^{206}\text{Pb}/^{204}\text{Pb}$	0.349	<b>0.910</b>	-0.213	<b>0.858</b>	<b>0.923</b>
$^{207}\text{Pb}/^{204}\text{Pb}$ - $^{206}\text{Pb}/^{204}\text{Pb}$	0.436	0.673	0.236	<b>0.860</b>	<b>0.770</b>

Correlations that are statistically significant at the 99% confidence level are **bold**. Limits on the correlation coefficient above which the correlations are accepted as statistically significant at the 99% confidence level depend upon sample size, which ranges from  $n=3$  to  $n=70$  for the data we discuss (Sachs, 1984). If a correlation is determined to be significant at the 99% confidence level, but the calculated Pearson's correlation coefficient differs by less than 0.1 from the acceptance limit, we consider the correlation to be significant but poor. These values are **bold and italicized**.

Table 3.2: Oceanic lithosphere model compositions

<b>Model parameters</b>				
	dehydrated sediment <sup>1</sup>	dehydrated UOC-eclogite <sup>2</sup>	gabbro- eclogite <sup>3</sup>	depleted lithosphere <sup>4</sup>
La/Nb	15.17	0.41		
Sm/Yb	2.31	1.06	1.88	0.39
Sm/Hf	14.69	1.85		
Sm/Nb	4.02	0.48		
Hf/Zr			0.032	0.053
Hf/Nb			0.63	3.630

1- Johnson and Plank (1999)

2- Kogiso et al. (1997), Barth et al. (2001)

3- Zimmer et al. (1995)

4- see text for explanation

Table 3.3: Peridotite partition coefficients

**Partition coefficients for peridotite**

	olivine	orthopyroxene	clinopyroxene	garnet
Sm	0.0013	0.026	0.291	0.28
Yb	0.0015	0.141	0.43	3.3
Nb	0.01	0.00067	0.0077	0.03
Hf	0.01	0.048	0.256	0.68
Zr	0.007	0.022	0.1234	0.4

olivine: Hauri and Hart (1995) and McKenzie and O'Nions (1991)

orthopyroxene: Salters and Longhi (1999)

clinopyroxene: Hart and Dunn (1993)

garnet: van Westrenen (1999)

Table 3.4: Eclogite partition coefficients

<b>Partition coefficients for eclogite</b>		
	<b>clinopyroxene</b>	<b>garnet</b>
La	0.0039	0.0008
Sm	0.30	0.17
Yb	0.63	7.1
Nb	0.021	0.008
Hf	0.17	0.31
Zr	0.093	0.4
Sr	0.080	0.005

From Klemme et al. (2002)

## BIBLIOGRAPHY

- W. Abouchami, S. J. G. Galer, and A. W. Hofmann. High precision lead isotope systematics of lavas from the Hawaiian Scientific Drilling Project. *Chemical Geology*, 169:187–209, 2000.
- E. Aharonov, M. Spiegelman, and P. Kelemen. Three-dimensional flow and reaction in porous media: implications for the Earth's mantle and sedimentary basins. *Journal of Geophysical Research*, 102:14,821–14,833, 1997.
- F. Albarède. High-resolution geochemical stratigraphy of Mauna Kea flows from the Hawaii Scientific Drilling Project core. *Journal of Geophysical Research*, 101:11,841–11,843, 1996.
- J. F. Allan, R. O. Sack, and R. Batiza. Cr-rich spinels as petrogenetic indicators: MORB-type lavas from the Lamont seamount chain, eastern Pacific. *American Mineralogist*, 73: 741–753, 1988.
- N.-L. Anders and B. K. Nelson. Characteristics of the Hawaiian plume: correlations between intershield major element and isotopic compositions and the relation to the tholeiitic to alkalic basalt transition of Hawaiian volcanoes. *EOS, Transactions, AGU*, 77:F812, 1996.
- M. B. Baker and E. M. Stolper. Determining the composition of high-pressure mantle melts using diamond aggregates. *Geochimica et Cosmochimica Acta*, 58:2811–2827, 1994.
- K. E. Bargar and E. D. Jackson. Calculated volumes of individual shield volcanoes along the Hawaiian-Emperor chain. *Journal of Research of the U.S. Geological Survey*, 2:545–550, 1974.
- M. G. Barth, R. L. Rudnick, I. Horn, W. F. McDonough, M. J. Spicuzza, J. W. Valley, and S. E. Haggerty. Geochemistry of xenolithic eclogites from West Africa: Part I, a link between low MgO eclogites and Archean crust formation. *Geochimica et Cosmochimica Acta*, 65:1499–1527, 2001.
- A. R. Basu and B. E. Faggart Jr. Temporal isotopic variations in the hawaiian mantle plume: the Lanai anomaly, the Molokai Fracture Zone and a seawater-altered component in Hawaiian volcanism. In Asish Basu and Stan Hart, editors, *Earth Processes: Reading the Isotopic Code*, pages 149–159. American Geophysical Union, Washington, D.C., 1996.
- P. Beattie. Systematics and energetics of trace-element partitioning between olivine and silicate melts; implications for the nature of mineral/ melt partitioning. *Chemical Geology*, 117:57–71, 1994.
- H. Becker. Re-Os fractionation in eclogites and blueschists and the implications for recycling of oceanic crust into the mantle. *Earth and Planetary Science Letters*, 177:287–300, 2000.

- V. C. Bennett, T. M. Esat, and M. D. Norman. Two mantle-plume components in Hawaiian picrites inferred from correlated Os-Pb isotopes. *Nature*, 381:221-223, 1996.
- V. C. Bennett, M. D. Norman, and M. O. Garcia. Rhenium and platinum group element abundances corelated with mantle source components in Hawaiian picrites: sulphides in the plume. *Earth and Planetary Science Letters*, 183:513-526, 2000.
- J. Blichert-Toft and F. Albarède. Hf isotopic compositions of the Hawaii Scientific Drilling Project core and the source mineralogy of Hawaiian basalts. *Geophysical Research Letters*, 26:535-538, 1999.
- J. Blichert-Toft, C. Chauvel, and F. Albarède. Separation of Hf and Lu for high-precision isotope analysis of rock samples by magnetic sector-multiple collector ICP-MS. *Contributions to Mineralogy and Petrology*, 127:248-260, 1997.
- J. Blichert-Toft, F. A. Frey, and F. Albarède. Hf isotope evidence for pelagic sediments in the source of Hawaiian basalts. *Science*, 285:879-882, 1999.
- J. Blichert-Toft, D. Weis, C. Maerschalk, A. Agranier, and F. Albarède. Hawaiian hot spot dynamics as inferred from the Hf and Pb isotope evolution of Mauna Kea volcano. *Geochemistry Geophysics Geosystems*, 4:2002GC000340, 2003.
- J. Blusztajn, S. R. Hart, G. Ravizza, and H. J. B. Dick. Platinum-group elements and Os isotopic characteristics of the lower oceanic crust. *Chemical Geology*, 168:113-122, 2000.
- A. D. Brandon, J. E. Snow, R. J. Walker, J. W. Morgan, and T. D. Mock.  $^{190}\text{Pt}$ - $^{186}\text{Os}$  and  $^{187}\text{Re}$ - $^{187}\text{Os}$  systematics of abyssal peridotites. *Earth and Planetary Science Letters*, 177:319-335, 2000.
- J. R. Budahn and R. A. Schmitt. Petrogenetic modeling of hawaiian tholeiitic basalts; a geochemical approach. *Geochimica et Cosmochimica Acta*, 49:67-87, 1985.
- K. W. Burton, P. Schiano, J. L. Birck, and Claude J Allègre. Osmium isotope disequilibrium between mantle minerals in a spinel-lherzolite. *Earth and Planetary Science Letters*, 172:311-322, 1999.
- C. Chauvel and J. Blichert-Toft. A hafnium isotope and trace element perspective on melting of the depleted mantle. *Earth and Planetary Science Letters*, 190:137-151, 2001.
- C. Chauvel and C. Hémond. Melting of a complete section of recycled oceanic crust: trace element and Pb isotopic evidence from Iceland. *Geochemistry Geophysics Geosystems*, 1:1999GC000002, 2000.
- C.-H. Chen, D. C. Presnall, and R. J. Stern. Petrogenesis of ultramafic xenoliths from the 1800 Kaupulehu flow, Hualalai volcano, Hawaii. *Journal of Petrology*, 33:163-202, 1992.
- C.-Y. Chen. High-magnesium primary magmas from Haleakala Volcano, east Maui, Hawaii: petrography, nickel, and major-element constraints. *Journal of Volcanology and Geothermal Research*, 55:143-153, 1993.

- C.-Y. Chen and F. A. Frey. Trace element and isotopic geochemistry of lavas from Haleakala Volcano, East Maui, Hawaii: implications for the origin of Hawaiian basalts. *Journal of Geophysical Research*, 90:8743-8768, 1985.
- C.-Y. Chen, F. A. Frey, M. O. Garcia, G. B. Dalrymple, and S. R. Hart. The tholeiite to alkalic basalt transition at Haleakala Volcano, Maui, Hawaii. *Contributions to Mineralogy and Petrology*, 106:183-200, 1991.
- C.-Y. Chen, F. A. Frey, J. M. Rhodes, and R. M. Easton. Temporal geochemical evolution of Kilauea volcano: comparison of Hilina and Puna basalt. In Asish Basu and Stan Hart, editors, *Earth Processes: Reading the Isotopic Code*, pages 161-181. American Geophysical Union, Washington, D.C., 1996.
- D. A. Clague and C.-H. Chen. Ocean crust xenoliths from Hualalai Volcano, Hawaii. *Abstracts with Programs, Geological Society of America*, 18:565, 1986.
- D. A. Clague and F. A. Frey. Petrology and trace element geochemistry of the Honolulu Volcanics, Oahu: implications for the oceanic mantle below Hawaii. *Journal of Petrology*, 23:447-504, 1982.
- D. A. Clague, J. G. Moore, J. E. Dixon, and W. E. Freisen. Petrology of submarine lavas from Kilauea's Puna Ridge, Hawaii. *Journal of Petrology*, 36:299-349, 1995.
- J. D. Cocker, B. J. Griffin, K. Muehlenbachs, J. A. Miller, I. Cartwright, I. S. Buick, and A. C. Barnicoat. Oxygen and carbon isotope evidence for seawater-hydrothermal alteration of the Macquarie Island ophiolite. *Earth and Planetary Science Letters*, 61:112-122, 1982.
- R. A. Creaser, D. Papanastassiou, and G. J. Wasserburg. Negative thermal ion mass spectrometry of osmium, rhenium and iridium. *Geochimica et Cosmochimica Acta*, 55:397-401, 1991.
- J. H. Crocket, M. E. Fleet, and W. E. Stone. Implications of composition for experimental partitioning of platinum-group elements and gold between sulfide liquid and basalt melt: the significance of nickel content. *Geochimica et Cosmochimica Acta*, 61:4139-4149, 1997.
- D. J. DePaolo, J. G. Bryce, A. Dodson, D. L. Schuster, and B. M. Kennedy. Isotopic evolution of Mauna Loa and the chemical structure of the Hawaiian plume. *Geochemistry Geophysics Geosystems*, 2:2000GC000139, 2001.
- D. E. Diller. Contributions to the geology of West Maui Volcano. M.S. thesis, University of Hawaii, Honolulu, HI, 1982.
- N. M. du Vignaux and L. Fleitout. Stretching and mixing of viscous blobs in Earth's mantle. *Journal of Geophysical Research*, 106:30,893-30,908, 2001.
- M. Ducea, G. Sen, J. Eiler, and J. Fimbres. Melt depletion and subsequent metasomatism in the shallow mantle beneath Koolau volcano, Oahu (Hawaii). *Geochemistry, Geophysics, Geosystems*, 3:2001GC000184, 2002.



- S. M. Eggins. Petrogenesis of Hawaiian tholeiites: I, phase equilibria constraints. *Contributions to Mineralogy and Petrology*, 110:387–397, 1992.
- J. M. Eiler, A. Crawford, T. Elliott, K. A. Farley, J. W. Valley, and E. M. Stolper. Oxygen isotope geochemistry of oceanic-arc lavas. *Journal of Petrology*, 41:229–256, 2000a.
- J. M. Eiler, K. A. Farley, and E. M. Stolper. Correlated helium and lead isotope variations in Hawaiian lavas. *Geochimica et Cosmochimica Acta*, 62:1977–1984, 1998.
- J. M. Eiler, K. A. Farley, J. W. Valley, A. W. Hofmann, and E. M. Stolper. Oxygen isotope constraints on the sources of Hawaiian volcanism. *Earth and Planetary Science Letters*, 144:453–468, 1996.
- J. M. Eiler, P. Schiano, N. Kitchen, and E. M. Stolper. Oxygen-isotope evidence for recycled crust in the sources of mid-ocean-ridge basalts. *Nature*, 403:530–534, 2000b.
- J. Eisele, W. Abouchami, S. J. G. Galer, and A. W. Hofmann. The 320 kyr Pb isotope evolution of Mauna Kea lavas recorded in the HSDP-2 drill core. *Geochemistry, Geophysics, Geosystems*, 4:2002GC000339, 2003.
- C. G. Farnetani, B. Legras, and P. J. Tackley. Mixing and deformations in mantle plumes. *Earth and Planetary Science Letters*, 196:1–15, 2002.
- M. D. Feigenson, L. L. Bolge, M. J. Carr, and C. T. Herzberg. REE inverse modeling of HSDP2 basalts: evidence for multiple sources in the Hawaiian Plume. *Geochemistry, Geophysics, Geosystems*, 4:2001GC000271, 2003.
- M. D. Feigenson, L. C. Patino, and M. J. Carr. Constraints on partial melting imposed by rare earth element variations in Mauna Kea basalts. *Journal of Geophysical Research*, 101:11,815–11,829, 1996.
- M. E. Fleet, J. H. Crocket, and W. E. Stone. Partitioning of platinum-group elements (Os, Ir, Ru, Pt, Pd) and gold between sulfide liquid and basalt melt. *Geochimica et Cosmochimica Acta*, 60:2397–2412, 1996.
- R. V. Fodor, G. R. Bauer, R. S. Jacobs, and T. J. Bornhorst. Kahoolawe Island, Hawaii: tholeiitic, alkalic and unusual hydrothermal(?) 'enrichment' characteristics. *Journal of Volcanology and Geothermal Research*, 31:171–176, 1987.
- R. V. Fodor, F. A. Frey, G. R. Bauer, and D. A. Clague. Ages, rare-earth element enrichment, and petrogenesis of tholeiitic and alkalic basalts from Kahoolawe Island, Hawaii. *Contributions to Mineralogy and Petrology*, 110:442–462, 1992.
- F. A. Frey, M. O. Garcia, and M. F. Roden. Geochemical characteristics of Koolau Volcano: Implications of intershield geochemical differences among Hawaiian volcanoes. *Geochimica et Cosmochimica Acta*, 58:1441–1462, 1994.
- F. A. Frey, M. O. Garcia, W. S. Wise, A. Kennedy, P. Gurriet, and F. Albarède. The evolution of Mauna Kea volcano, Hawaii: petrogenesis of tholeiitic and alkalic basalts. *Journal of Geophysical Research*, 96:14,347–14,375, 1991.

- A. M. Gaffney, B. K. Nelson, and J. Blichert-Toft. Geochemical constraints on the role of oceanic lithosphere in intra-volcano heterogeneity at West Maui, Hawaii. *Journal of Petrology*, 45:in press, 2004.
- A. M. Gaffney, B. K. Nelson, L. Reisberg, and J. M. Eiler. Oxygen-osmium isotopic compositions of West Maui lavas and the link to oceanic lithosphere. *EOS, Transactions, AGU*, 84:F1598, 2003.
- M. O. Garcia, D. J. P. Foss, H. B. West, and J. J. Mahoney. Geochemical and isotopic evolution of Loihi volcano, Hawaii. *Journal of Petrology*, 36:1647–1674, 1995.
- M. O. Garcia, B. A. Jorgenson, J. J. Mahoney, E. Ito, and A. J. Irving. An evaluation of temporal geochemical evolution of Loihi summit lavas: results from Alvin submersible dives. *Journal of Geophysical Research*, 98:537–550, 1993.
- M. O. Garcia, A. J. Pietruszka, and J. M. Rhodes. A petrologic perspective of Kilauea Volcano's summit magma reservoir. *Journal of Petrology*, 44:2313–2339, 2003.
- M. O. Garcia, A. J. Pietruszka, J. M. Rhodes, and K. Swanson. Magmatic processes during the prolonged Pu'u 'O'o eruption of Kilauea Volcano, Hawaii. *Journal of Petrology*, 41: 967–990, 2000.
- M. O. Garcia, J. M. Rhodes, F. A. Trusdell, and A. J. Pietruszka. Petrology of lavas from the Puu Oo eruption of Kilauea Volcano: III. The Kupaianaha episode (1986-1992). *Bulletin of Volcanology*, 58:359–379, 1996.
- M. O. Garcia, J. M. Rhodes, E. W. Wolfe, G. E. Ulrich, and R. A. Ho. Petrology of lavas from episodes 2-47 of the Puu Oo eruption of Kilauea Volcano, Hawaii: evaluation of magmatic processes. *Bulletin of Volcanology*, 55:1–16, 1992.
- J. Geldmacher and K. Hoernle. The 72 Ma geochemical evolution of the Madeira hotspot (eastern North Atlantic): recycling of Paleozoic ( $\leq 500$  ma) oceanic lithosphere. *Earth and Planetary Science Letters*, 183:73–92, 2000.
- M. S. Ghiorso, M. M. Hirschmann, P. W. Reiners, and V. C. Kress. pMELTS: A revision of MELTS for improved calculation of phase relations and major element partitioning related to partial melting of the mantle to 3 GPa. *Geochemistry, Geophysics, Geosystems*, 3:2001GC000217, 2002.
- M. S. Ghiorso and R. O. Sack. Chemical Mass Transfer in Magmatic Processes IV. A revised and internally consistent thermodynamic model for the interpolation and extrapolation of liquid-solid equilibria in magmatic systems at elevated temperatures and pressures. *Contributions to Mineralogy and Petrology*, 119:197–212, 1995.
- D. H. Green and A. E. Ringwood. The genesis of basaltic magmas. *Contributions to Mineralogy and Petrology*, 15:103–190, 1967.

- R. T. Gregory and H. P. Taylor Jr. An oxygen isotope profile in a section of Cretaceous oceanic crust. Samail Ophiolite, Oman: evidence for  $\delta^{18}\text{O}$  buffering of the oceans by deep (>5 km) seawater-hydrothermal circulation at mid-ocean ridges. *Journal of Geophysical Research*, 86:2737–2755, 1981.
- T. H. Hansteen and V. R. Troll. Oxygen isotope composition of xenoliths from the oceanic crust and volcanic edifice beneath Gran Canaria (Canary Islands); consequences for crustal contamination of ascending magmas. *Chemical Geology*, 193:181–193, 2003.
- S. R. Hart. Heterogeneous mantle domains: signatures, genesis and mixing chronologies. *Earth and Planetary Science Letters*, 90:273–296, 1988.
- S. R. Hart, J. Blusztajn, H. J. B. Dick, P. S. Meyer, and K. Muehlenbachs. The fingerprint of seawater circulation in a 500-meter section of ocean crust gabbros. *Geochimica et Cosmochimica Acta*, 63:4059–4080, 1999.
- S. R. Hart and T. Dunn. Experimental cpx/melt partitioning of 24 trace elements. *Contributions to Mineralogy and Petrology*, 113:1–8, 1993.
- S. R. Hart and G. E. Ravizza. Os partitioning between phases in lherzolite and basalt. In Asish Basu and Stan Hart, editors, *Earth Processes: Reading the Isotopic Code*, pages 135–147. American Geophysical Union, Washington, D.C., 1996.
- E. H. Hauri. Major-element variability in the Hawaiian mantle plume. *Nature*, 382:415–419, 1996a.
- E. H. Hauri. Osmium isotope systematics of drilled lavas from Mauna Loa, Hawaii. *Journal of Geophysical Research*, 101:11,793–11,806, 1996b.
- E. H. Hauri. Melt migration and mantle chromatography, 2: a time-series Os isotope study of Mauna Loa volcano, Hawaii. *Earth and Planetary Science Letters*, 153:21–36, 1997.
- E. H. Hauri and S. R. Hart. Correction to “Constraints on melt migration from mantle plumes: a trace element study of peridotitic xenoliths from Savai’i, Western Samoa”. *Journal of Geophysical Research*, 100:2003, 1995.
- E. H. Hauri, J. A. Whitehead, and S. R. Hart. Fluid dynamic and geochemical aspects of entrainment in mantle plumes. *Journal of Geophysical Research*, 99:24,275–24,300, 1994.
- R. T. Helz and T. L. Wright. Differentiation and magma mixing on Kilauea’s east rift zone. *Bulletin of Volcanology*, 54:361–384, 1992.
- C. Herzberg and M. J. O’Hara. Plume-associated ultramafic magmas of Phanerozoic age. *Journal of Petrology*, 43:1857–1883, 2002.
- M. M. Hirschmann, T. Kogiso, M. B. Baker, and E. M. Stolper. Alkalic magmas generated by partial melting of garnet pyroxenite. *Geology*, 31:481–484, 2003.

- M. M. Hirschmann and E. M. Stolper. A possible role for garnet pyroxenite in the origin of the 'garnet signature' in MORB. *Contributions to Mineralogy and Petrology*, 124:185-208, 1996.
- S. E. Hoffman, M. Wilson, and D. S. Stakes. Inferred oxygen isotope profile of Archaean oceanic crust, Onverwacht Group, South Africa. *Nature*, 321:55-58, 1986.
- A. W. Hofmann, W. Abouchami, J. Eisele, K. P. Jochum, A. V. Sobolev, and S. J. G. Galer. Anatomy of the Hawaiian Plume: heterogeneity on many scales. *Geochimica et Cosmochimica Acta*, 66:336, 2002.
- A. W. Hofmann and K. P. Jochum. Source characteristics derived from very incompatible trace elements in Mauna Loa and Mauna Kea basalts, Hawaii Scientific Drilling Project. *Journal of Geophysical Research*, 101:11,831-11,839, 1996.
- A. W. Hofmann and W. M. White. Mantle plumes from ancient oceanic crust. *Earth and Planetary Science Letters*, 57:421-436, 1982.
- A. W. Hofmann, M. D. Feigenson, and I. Raczek. Case studies on the origin of basalt: III. Petrogenesis of the Mauna Ulu eruption, Kilauea, 1969-1971. *Contributions to Mineralogy and Petrology*, 88:24-35, 1984.
- S. Huang and F. A. Frey. Trace element abundances of Mauna Kea basalt from phase 2 of the Hawaii Scientific Drilling Project: petrogenetic implications of correlations with major element content and isotopic ratios. *Geochemistry, Geophysics, Geosystems*, 4: 2002GD000322, 2003.
- E. D. Jackson, E. A. Silver, and G. B. Dalrymple. Hawaiian-Emperor chain and its relation to Cenozoic circumpacific tectonics. *Geological Society of America Bulletin*, 83:601-617, 1972.
- M. C. Jackson, F. A. Frey, M. O. Garcia, and R. A. Wilmoth. Geology and geochemistry of basaltic lava flows and dikes from the Trans-Koolau tunnel, Oahu, Hawaii. *Bulletin of Volcanology*, 60:381-401, 1999.
- D. M. Johnson, P. R. Hooper, and R. M. Conrey. XRF analysis of rocks and minerals for major and trace elements on a single low dilution Li-tetraborate fused bead. *Advances in X-Ray Analysis*, 41:843-867, 1999.
- M. C. Johnson and T. Plank. Dehydration and melting experiments constrain the fate of subducted sediments. *Geochemistry, Geophysics, Geosystems*, 1:1999GC000014, 1999.
- P. B. Kelemen, J. A. Whitehead, E. Aharonov, and K. A. Jordahl. Experiments on flow focusing in soluble porous media, with applications to melt extraction from the mantle. *Journal of Geophysical Research*, 100:475-496, 1995.
- A. J. King, D. G. Wagoner, and M. O. Garcia. Geochemistry and petrology of basalts from Leg 136, Central Pacific Ocean. In *Proceedings of the Ocean Drilling Program, Scientific Results*, volume 136, pages 107-118. Ocean Drilling Program, 1993.

- S. Klemme, J. D. Blundy, and B. J. Wood. Experimental constraints on major and trace element partitioning during partial melting of eclogite. *Geochimica et Cosmochimica Acta*, 66:3109–3123, 2002.
- T. Kogiso, K. Hirose, and E. Takahashi. Melting experiments on homogeneous mixtures of peridotite and basalt; application to the genesis of ocean island basalts. *Earth and Planetary Science Letters*, 162:45–61, 1998.
- T. Kogiso, M. M. Hirschmann, and D. J. Frost. High-pressure partial melting of garnet pyroxenite: possible mafic lithologies in the source of ocean island basalts. *Earth and Planetary Science Letters*, 216:603–617, 2003.
- T. Kogiso, M. M. Hirschmann, and P. W. Reiners. Length scales of mantle heterogeneities and their relationship to ocean island basalt geochemistry. *Geochimica et Cosmochimica Acta*, 68:345–360, 2004.
- T. Kogiso, Y. Tatsumi, and S. Nakano. Trace element transport during dehydration processes in the subducted oceanic crust: 1, experiments and implications for the origin of ocean island basalts. *Earth and Planetary Science Letters*, 148:193–205, 1997.
- M. D. Kurz, J. Curtice, D. E. Lott III, and A. Solow. Rapid helium isotopic variability in Mauna Kea shield lavas from the Hawaiian Scientific Drilling Project. *Geochemistry, Geophysics, Geosystems*, 5:2002GC000439, 2004.
- M. D. Kurz, M. O. Garcia, F. A. Frey, and P. A. O'Brien. Temporal helium isotopic variations within Hawaiian volcanoes; basalts from Mauna Loa and Haleakala. *Geochimica et Cosmochimica Acta*, 51:2905–2914, 1987.
- M. D. Kurz, W. J. Jenkins, S. R. Hart, and D. A. Clague. Helium isotopic variations in volcanic rocks from Loihi Seamount and the island of Hawaii. *Earth and Planetary Science Letters*, 66:388–406, 1983.
- M. D. Kurz, T. C. Kenna, D. P. Kammer, J. M. Rhodes, and M. O. Garcia. Isotopic evolution of Mauna Loa Volcano; a view from the submarine southwest rift zone. In J. M. Rhodes and J. P. Lockwood, editors, *Mauna Loa Revealed: Structure, Composition, History and Hazards*, pages 289–306. American Geophysical Union, Washington, D.C., 1995.
- G. B. Lanphere, M. A. Dalrymple, and D. Clague. Rb-sr systematics of basalts from the Hawaiian-Emperor volcanic chain. In J. Shambach, E. D. Jackson, I. Koizumi, G. Avdeiko, A. Butt, D. Clague, G. B. Dalrymple, H. G. Greene, A. M. Karpoff, R. J. Kirkpatrick, M. Kono, Y. L. Hsin, J. McKenzie, J. Morgan, and T. Takayama, editors, *Initial reports of the Deep Sea Drilling Project covering Leg 55 of the cruises of the drilling vessel Glomar Challenger, Honolulu, Hawaii to Yokohama, Japan; July-September 1977.*, volume 55 of *Initial Reports of the Deep Sea Drilling Project*, pages 695–706. Texas A & M University, Ocean Drilling Program, College Station, TX, United States, 1980.

- J. C. Lassiter. Rhenium volatility in subaerial lavas: constraints from subaerial and submarine portions of the HSDP-2 Mauna Kea drillcore. *Earth and Planetary Science Letters*, pages 311–325, 2003.
- J. C. Lassiter, D. J. DePaolo, and M. Tatsumoto. Isotopic evolution of Mauna Kea volcano: results from the initial phases of the Hawaii Scientific Drilling Project. *Journal of Geophysical Research*, 101:11, 769–11,780, 1996.
- J. C. Lassiter and E. H. Hauri. Osmium-isotope variations in Hawaiian lavas: evidence for recycled oceanic lithosphere in the Hawaiian plume. *Earth and Planetary Science Letters*, 164:483–496, 1998.
- J. C. Lassiter, E. H. Hauri, P. W. Reiners, and M. O. Garcia. Generation of Hawaiian post-erosional lavas by melting of a mixed lherzolite/pyroxenite source. *Earth and Planetary Science Letters*, 178:269–284, 2000.
- W. P. Leeman, D. C. Gerlach, M. O. Garcia, and H. B. West. Geochemical variation in lavas from Kahoolawe volcano, Hawaii: evidence for open system evolution of plume-derived magmas. *Contributions to Mineralogy and Petrology*, 116:66–72, 1994.
- G. A. Macdonald and T. Katsura. Chemical composition of Hawaiian lavas. *Journal of Petrology*, 5:82–133, 1964.
- C. E. Martin, R. W. Carlson, S. B. Shirey, F. A. Frey, and C.-Y. Chen. Os isotopic variation in basalts from Haleakala Volcano, Maui, Hawaii: A record of magmatic processes in oceanic mantle and crust. *Earth and Planetary Science Letters*, 128:287–301, 1994.
- J. A. Mavrogenes and H. St. C. O'Neill. The relative effects of pressure, temperature and oxygen fugacity on the solubility of sulfide in mafic magmas. *Geochimica et Cosmochimica Acta*, 63:1173–1180, 1999.
- I. McDougall. Potassium-argon ages from lavas of the Hawaiian Islands. *Geological Society of America Bulletin*, 75:107–128, 1964.
- D. McKenzie and R. K. O'Nions. Partial melt distributions from inversion of rare earth element concentrations. *Journal of Petrology*, 32:1021–1091, 1991.
- T. Meisel, R. J. Walker, A. J. Irving, and J. P. Lorand. Osmium isotopic compositions of mantle xenoliths; a global perspective. *Geochimica et Cosmochimica Acta*, 65:1311–1323, 2001.
- T. Meisel, R. J. Walker, and J. W. Morgan. The osmium isotopic composition of the Earth's primitive upper mantle. *Nature*, 383:517–520, 1996.
- J. A. Miller, I. Cartwright, I. S. Buick, and A. C. Barnicoat. An O-isotope profile through the HP-LT Corsican ophiolite, France and its implications for fluid flow during subduction. *Chemical Geology*, 178:43–69, 2001.

- C. Montierth, A. D. Johnston, and K. V. Cashman. An empirical glass-composition-based geothermometer for Mauna Loa lavas. In J. M. Rhodes and J. P. Lockwood, editors. *Mauna Loa Revealed: Structure, Composition, History and Hazards*, pages 207–217. American Geophysical Union, Washington, D.C., 1995.
- S. Mukhopadhyay, J. C. Lassiter, K.A. Farley, and S. W. Bougue. Geochemistry of Kauai shield-stage lavas: implications for the chemical evolution of the Hawaiian plume. *Geochemistry, Geophysics, Geosystems*, 4:2002GC000342, 2003.
- J. E. Mungall. Kinetic controls on the partitioning of trace elements between silicate and sulfide liquids. *Journal of Petrology*, 43:749–768, 2002.
- J. J. Naughton, G. A. Macdonald, and V. A. Greenberg. Some additional potassium-argon ages of Hawaiian rocks: the Maui volcanic complex of Molokai, Maui, Lanai and Kahoolawe. *Journal of Volcanology and Geothermal Research*, 7:339–355, 1980.
- B. K. Nelson. Fluid flow in subduction zones: evidence from neodymium and strontium isotope variations in metabasalts of the Franciscan Complex, California. *Contributions to Mineralogy and Petrology*, 119:247–262, 1995.
- M. D. Norman and M. O. Garcia. Primitive magmas and source characteristics of the Hawaiian plume: petrology and geochemistry of shield picrites. *Earth and Planetary Science Letters*, 168:27–44, 1999.
- M. D. Norman, M. O. Garcia, V. S. Kamenetsky, and R. L. Nielsen. Olivine-hosted melt inclusions in Hawaiian picrites; equilibration, melting, and plume source characteristics. *Chemical Geology*, 183:143–168, 2002.
- O. Okano and M. Tatsumoto. Petrogenesis of ultramafic xenoliths from Hawaii inferred from Sr, Nd, and Pb isotopes. In Asish Basu and Stan Hart, editors, *Earth Processes: Reading the Isotopic Code*, pages 135–147. American Geophysical Union, Washington, D.C., 1996.
- M. Pertermann and M. M. Hirschmann. Anhydrous partial melting experiments on MORB-like eclogite: phase relations, phase compositions and mineral-melt partitioning of major elements at 2–3 GPa. *Journal of Petrology*, 44:2173–2201, 2003a.
- M. Pertermann and M. M. Hirschmann. Partial melting experiments on a morb-like pyroxenite between 2 and 3 GPa: constraints on the presence of pyroxenite in basalt source regions from solidus location and melting rate. *Journal of Geophysical Research*, 108: doi:10.1029/2000JP000118, 2003b.
- B. Peucker-Ehrenbrink, W. Bach, S. R. Hart, J. S. Blusztajn, and T. Abbruzzese. Rhenium-osmium isotope systematics and platinum group element concentrations in oceanic crust from DSDP/ODP Sites 504 and 417/418. *Geochemistry, Geophysics, Geosystems*, 4: 2002GC000414, 2003.

- A. J. Pietruszka and M. O. Garcia. A rapid fluctuation in the mantle source and melting history of Kilauea volcano inferred from the geochemistry of its historical summit lavas (1790-1982). *Journal of Petrology*, 40:1321-1342, 1999.
- R. P. Rapp, N. Shimizu, M. D. Norman, and G. S. Applegate. Reaction between slab-derived melts and peridotite in the mantle wedge; experimental constraints at 3.8 GPa. *Chemical Geology*, 160:335-356, 1999.
- P. W. Reiners and B. K. Nelson. Temporal-compositional-isotopic trends in rejuvenated magmas of Kauai, Hawaii, and implications for mantle melting processes. *Geochimica et Cosmochimica Acta*, 62:2347-2368, 1998.
- L. Reisberg, C. France-Lanord, and A.-C. Pierson-Wickmann. Os isotopic compositions of leachates and bulk sediments from the Bengal Fan. *Earth and Planetary Science Letters*, 150:117-127, 1997.
- J. M. Rhodes. Geochemical stratigraphy of lava flows sampled by the Hawaii Scientific Drilling Project. *Journal of Geophysical Research*, 101:11,729-11,746, 1996.
- M. F. Roden, T. Trull, S. R. Hart, and F. A. Frey. New He, Nd, Pb, and Sr isotopic constraints on the constitution of the Hawaiian plume: Results from Koolau Volcano, Oahu, Hawaii, USA. *Geochimica et Cosmochimica Acta*, 58:1431-1440, 1994.
- M. Roy-Barman and C. J. Allègre.  $^{187}\text{Os}/^{188}\text{Os}$  ratios of mid-ocean ridge basalts and abyssal peridotites. *Geochimica et Cosmochimica Acta*, 58:5043-5054, 1994.
- M. Roy-Barman and C. J. Allègre.  $^{187}\text{Os}/^{188}\text{Os}$  in oceanic island basalts: tracing oceanic crust recycling in the mantle. *Earth and Planetary Science Letters*, 129:145-161, 1995.
- M. Roy-Barman, G. J. Wasserburg, D. A. Papanastassiou, and M. Chaussidon. Osmium isotopic compositions and Re-Os concentrations in sulfide globules from basaltic glasses. *Earth and Planetary Science Letters*, 154:331-347, 1998.
- L. Sachs. *Applied statistics: a handbook of techniques*. Springer-Verlag, New York, 1984.
- V. J. Salters and A. Zindler. Extreme  $^{176}\text{Hf}/^{177}\text{Hf}$  in the sub-oceanic mantle. *Earth and Planetary Science Letters*, 129:13-30, 1995.
- V. J. M. Salters and J. Longhi. Trace element partitioning during the initial stages of melting beneath mid-ocean ridges. *Earth and Planetary Science Letters*, 1999.
- P. Schiano, J.-L. Birck, and C. Allègre. Osmium-strontium-neodymium-lead isotopic co-variations in mid-ocean ridge basalt glasses and the heterogeneity of the upper mantle. *Earth and Planetary Science Letters*, 150:363-379, 1997.
- C. C. Schnetzler and J. A. Philpotts. Partition coefficients of rare-earth elements between igneous matrix material and rock-forming mineral phenocrysts; II. *Geochimica et Cosmochimica Acta*, 34:331-340, 1970.



- G. Sen. Xenoliths associated with the hawaiian hotspot. In P. H. Nixon, editor, *Mantle Xenoliths*, pages 359-375. John Wiley and Sons, Ltd., 1987.
- G. Sen, H.-J. Yang, and M. Ducea. Anomalous isotopes and trace element zoning in plagioclase peridotite xenoliths of Oahu (Hawaii); implications for the Hawaiian Plume. *Earth and Planetary Science Letters*, 207:23-38, 2003.
- S. B. Shirey and R. J. Walker. Carius tube digestion for low-blank rhenium-osmium analysis. *Analytical Chemistry*, 67:2136-2141, 1995.
- K. W. W. Sims, D. J. DePaolo, M. T. Murrell, W. S. Baldrige, S. Goldstein, D. Clague, and M. Jull. Porosity of the melting zone and variations in the solid mantle upwelling rate beneath Hawaii: Inferences from  $^{238}\text{U}$ - $^{230}\text{Th}$ - $^{226}\text{Ra}$  and  $^{235}\text{U}$ - $^{231}\text{Pa}$  disequilibria. *Geochimica et Cosmochimica Acta*, 63:4119-4138, 1999.
- K. W. W. Sims, D. J. DePaolo, M. T. Murrell, W. S. Baldrige, S. J. Goldstein, and D. A. Clague. Mechanisms of magma generation beneath Hawaii and mid-ocean ridges: uranium/thorium and samarium/neodymium isotopic evidence. *Science*, 267:508-511, 1995.
- A. C. Skovgaard, M. Storey, J. Baker, J. Blusztajn, and S. R. Hart. Osmium-oxygen isotopic evidence for a recycled and strongly depleted component in the Iceland mantle plume. *Earth and Planetary Science Letters*, 194:259-275, 2001.
- A. V. Sobolev, A. W. Hofmann, and I. K. Nikogosian. Recycled oceanic crust observed in 'ghost plagioclase' within the source of Mauna Loa lavas. *Nature*, 404:986-989, 2000.
- M. Spiegelman, P. B. Kelemen, and E. Aharonov. Causes and consequences of flow organization during melt transport: the reaction infiltration instability in compactible media. *Journal of Geophysical Research*, 106:2061-2077, 2001.
- D. S. Stakes. Oxygen and hydrogen isotope compositions of oceanic plutonic rocks: high-temperature deformation and metamorphism of oceanic layer 3. In H. P. Taylor Jr., J. R. O'Neil, and I. R. Kaplan, editors, *Stable Isotope Geochemistry: A Tribute to Samuel Epstein*, pages 77-90. The Geochemical Society, 1991.
- H. Staudigel, G. R. Davies, S. R. Hart, K. M. Marchant, and B. M. Smith. Large scale isotopic Sr, Nd and O isotopic anatomy of altered oceanic crust: DSDP/ODP sites 417/418. *Earth and Planetary Science Letters*, 130:169-185, 1995.
- H. Staudigel, A. Zindler, S. R. Hart, T. Leslie, C. Y. Chen, and D. A. Clague. The isotope systematics of a juvenile intraplate volcano; Pb, Nd, and Sr isotope ratios of basalts from Loihi Seamount, Hawaii. *Earth and Planetary Science Letters*, 69:13-29, 1984.
- H. T. Stearns and G. M. Macdonald. Geology and ground-water resources of the Island of Maui, Hawaii. Division of Hydrography Bulletin 7, 1942.
- P. Stille, D. M. Unruh, and M. Tatsumoto. Pb, Sr, Nd and Hf isotopic evidence of multiple sources for Oahu, Hawaii basalts. *Nature*, 304:25-29, 1983.

- P. Stille, D. M. Unruh, and M. Tatsumoto. Pb, Sr, Nd, and Hf isotopic constraints on the origin of Hawaiian basalts and evidence for a unique mantle source. *Geochimica et Cosmochimica Acta*, 50:2303–2319, 1986.
- E. M. Stolper, D. J. DePaolo, and D. M. Thomas. Introduction to special section; Hawaii Scientific Drilling Project. *Journal of Geophysical Research*, 101:11,593–11,598, 1996.
- A. Stracke, M. Bizimis, and V. J. M. Salters. Recycling oceanic crust: quantitative constraints. *Geochemistry Geophysics Geosystems*, 4:2001GC000223, 2003.
- A. Stracke and K. W. W. Sims. Assessing the presence of garnet-pyroxenite in the mantle sources of basalts through combined hafnium-neodymium-thorium isotope systematics. *Geochemistry Geophysics Geosystems*, 1:1999GC000013, 1999.
- S.-s. Sun and W. F. McDonough. Chemical and isotopic systematics of oceanic basalts: implications for mantle composition and processes. In A. D. Saunders and M. J. Norry, editors, *Magmatism in the Ocean Basins*, pages 313–345. The Geological Society, 1989.
- T. Tagami, Y. Nishimitsu, and D. R. Sherrod. Rejuvenated-stage volcanism after 0.6-m.y. of quiescence at West Maui volcano, Hawaii: new evidence from K-Ar ages and chemistry of Lahaina Volcanics. *Journal of Volcanology and Geothermal Research*, 120:207–214, 2003.
- E. Takahashi. Melting of a dry peridotite KLB-1 up to 14 GPa; implications on the origin of peridotitic upper mantle. *Journal of Geophysical Research*, 91:9367–9382, 1986.
- E. Takahashi and K. Nakajima. Melting process in the Hawaiian Plume: an experimental study. In E. Takahashi, P. W. Lipman, M. O. Garcia, J. Naka, and S. Aramaki, editors, *Hawaiian volcanoes; deep underwater perspectives*, pages 403–418. American Geophysical Union, Washington, DC, 2002.
- R. Tanaka, E. Nakamura, and E. Takahashi. Geochemical evolution of Koolau Volcano, Hawaii. In E. Takahashi, P. W. Lipman, M. O. Garcia, J. Naka, and S. Aramaki, editors, *Hawaiian volcanoes; deep underwater perspectives*, pages 311–332. American Geophysical Union, Washington, D.C., 2002.
- M. Tatsumoto, E. Hegner, and D. M. Unruh. Origin of the West Maui volcanic rocks inferred from Pb, Sr, and Nd isotopes and a multicomponent model for oceanic basalt. In *Volcanism in Hawaii*, pages 723–744. US Geological Survey, 1987. Professional Paper 1350.
- R. N. Thompson. Primary basalts and magma genesis; I, Skye, north-west Scotland. *Contributions to Mineralogy and Petrology*, 45:317–341, 1974.
- R. N. Thompson. Primary basalts and magma genesis; II, Snake River Plain, Idaho, U.S.A. *Contributions to Mineralogy and Petrology*, 52:213–232, 1975.
- R. I. Tilling, T. L. Wright, and H. T. Millard Jr. Trace-element chemistry of Kilauea and Mauna Loa in space and time: a reconnaissance. In *Volcanism in Hawaii*, pages 641–689. US Geological Survey, 1987. Professional Paper 1350.

- W. Todt, R. A. Cliff, A. Hanser, and A. W. Hofmann. Evaluation of a  $^{202}\text{Pb}$ - $^{205}\text{Pb}$  double spike for high-precision lead isotope analysis. In Asish Basu and Stan Hart, editors. *Earth Processes: Reading the Isotopic Code*, pages 429–437. American Geophysical Union, Washington, D.C., 1996.
- P. van Keken and S. Zhong. Mixing in a 3D spherical model of present-day mantle convection. *Earth and Planetary Science Letters*, 171:533–547, 1999.
- W. van Westrenen, J. Blundy, and B. Wood. Crystal-chemical controls on trace element partitioning between garnet and anhydrous silicate melt. *American Mineralogist*, 84: 838–847, 1999.
- W. van Westrenen, J. D. Blundy, and B. J. Wood. High field strength element/rare earth element fractionation during partial melting in the presence of garnet: implications for identification of mantle heterogeneities. *Geochemistry, Geophysics, Geosystems*, 2:2000GC000133, 2001.
- J. Volkening, T. Walczyk, and K. G. Heumann. Osmium isotope determinations by negative thermal ionization mass spectrometry. *International Journal of Mass Spectrometry and Ion Physics*, 105:147–159, 1991.
- T. P. Wagner, D. A. Clague, E. H. Hauri, and T. L. Grove. Trace element abundances of high-MgO glasses from Kilauea, Mauna Loa and Haleakala volcanoes, Hawaii. *Contributions to Mineralogy and Petrology*, 131:13–21, 1998.
- T. P. Wagner and T. L. Grove. Melt-harzburgite reaction in the petrogenesis of tholeiitic magma from Kilauea Volcano, Hawaii. *Contributions to Mineralogy and Petrology*, 131: 1–12, 1998.
- P. Wallace and I. S. E. Carmichael. Sulfur in basaltic magmas. *Geochimica et Cosmochimica Acta*, 56:1863–1874, 1992.
- Z. Wang, N. E. Kitchen, and J. M. Eiler. Oxygen isotope geochemistry of the second HSDP core. *Geochemistry, Geophysics, Geosystems*, 4:2002GC000406, 2003.
- H. B. West, M. O. Garcia, D. C. Gerlach, and J. Romano. Geochemistry of tholeiites from Lanai, Hawaii. *Contributions to Mineralogy and Petrology*, 112:520–542, 1992.
- H. B. West, D. C. Gerlach, W. P. Leeman, and M. O. Garcia. Isotopic constraints on the origin of Hawaiian lavas from the Maui Volcanic Complex, Hawaii. *Nature*, 330:216–220, 1987.
- H. B. West and W. P. Leeman. Isotopic evolution of lavas from Haleakala Crater, Hawaii. *Earth and Planetary Science Letters*, 84:211–225, 1987.
- W. M. White, F. Albarède, and P. Télouk. High-precision analysis of Pb isotope ratios by multi-collector ICP-MS. *Chemical Geology*, 167:257–270, 2000.

- B. J. Wood and J. D. Blundy. A predictive model for rare earth element partitioning between clinopyroxene and anhydrous silicate melt. *Contributions to Mineralogy and Petrology*, 129:166-181, 1997.
- T. L. Wright. Origin of Hawaii tholeiite: a metasomatic model. *Journal of Geophysical Research*, 89:3233-3252, 1984.
- H.-J. Yang, F. A. Frey, M. O. Garcia, and D.A. Clague. Submarine lavas from Mauna Kea Volcano, Hawaii: implications for Hawaiian shield stage processes. *Journal of Geophysical Research*, 99:15,577-15,594, 1994.
- H.-J. Yang, F. A. Frey, J. M. Rhodes, and M. O. Garcia. Evolution of Mauna Kea volcano: Inferences from lava compositions recovered in the Hawaii Scientific Drilling Project. *Journal of Geophysical Research*, 101:11,747-11,767, 1996.
- G. M. Yaxley and D. H. Green. Reactions between eclogite and peridotite; mantle refertilisation by subduction of oceanic crust. *Schweizerische Mineralogische und Petrographische Mitteilungen*, 78:243-255, 1998.
- M. Zimmer, A. Kröner, K. P. Jochum, T. Reischmann, and W. Todt. The Gabal Gerf Complex; a Precambrian N-MORB ophiolite in the Nubian Shield, NE Africa. *Chemical Geology*, 123:29-51, 1995.
- A. Zindler and S. Hart. Chemical geodynamics. *Annual Reviews in Earth and Planetary Science*, 14:493-571, 1986.

## Appendix A

## SAMPLE LOCATIONS

Most of the breadth-reaching samples we collected either on ridges that closely represent original flow surfaces [Stearns and Macdonald, 1942] or at stream level in traverses of deep canyons that dissect the volcano. Taking into account distance from caldera, depth within volcanic edifice and local dips of flows, we have divided these samples into two groups: 'deep' and 'shallow'. This terminology describes collection depth of a given sample relative to the surface of the volcano. In most of the canyons that we traversed, lavas are dipping more steeply than the canyon floor, such that samples collected farther inland are older than samples collected closer to the coast. Therefore, within each canyon, we were able to assign relative ages to the samples. Correlating relative ages between canyon traverses is more difficult, because it requires making assumptions about the volcano morphology, eruption frequency and distance traveled by individual flows, relative to the caldera and rift zones as mapped by Stearns and Macdonald [1942] and Diller [1982], and therefore is not strictly quantifiable in the absence of actual ages. Thus, although the transition from deep to shallow should be gradational, we are not able to specifically define this gradational transition in the composite stratigraphy of the volcano. In general, the same thickness of stratigraphic section represents more absolute time the farther away it is from the caldera. As a guideline, at 2 km away from the caldera, we use 300 m as the dividing depth between deep and shallow, and at 10 km from the caldera, we use 75 m as the dividing depth. Based on these guidelines, the deep and shallow categories show some geochemical distinction, and we use this terminology in geochemical discussion. Table 1A gives geographic coordinates, distance from caldera and depth within volcanic edifice for all samples.

Table A.1: West Maui sample locations

	Latitude	Longitude	Distance to caldera rim (km)	Depth in edifice (m)
<i>Papaiaua Gulch Section</i>				
UP50	20° 48' 37" N	156° 34' 33" W	1.4	5
UP47	20° 48' 37" N	156° 34' 33" W	1.4	38
UP46	20° 48' 37" N	156° 34' 33" W	1.4	58
UP43	20° 48' 37" N	156° 34' 33" W	1.4	79
UP41	20° 48' 37" N	156° 34' 33" W	1.4	91
UP40	20° 48' 37" N	156° 34' 33" W	1.4	100
UP39	20° 48' 37" N	156° 34' 33" W	1.4	102
UP37	20° 48' 37" N	156° 34' 33" W	1.4	107
LP16	20° 48' 23" N	156° 34' 33" W	2.2	121
LP14	20° 48' 23" N	156° 34' 33" W	2.2	144
LP13	20° 48' 23" N	156° 34' 33" W	2.2	155
LP11	20° 48' 23" N	156° 34' 33" W	2.2	170
LP10	20° 48' 23" N	156° 34' 33" W	2.2	181
LP05	20° 48' 23" N	156° 34' 33" W	2.2	236
LP03	20° 48' 23" N	156° 34' 33" W	2.2	248
LP01	20° 48' 23" N	156° 34' 33" W	2.2	260

Table A.1, continued:

	Latitude	Longitude	Distance to caldera rim (km)	Depth in edifice (m)
<b><i>Mahinahina Well Section</i></b>				
<b>MA30</b>	20° 57' 08" N	156° 39' 36" W	10.1	9
<b>MA50</b>	20° 57' 08" N	156° 39' 36" W	10.1	15
<b>MA100</b>	20° 57' 08" N	156° 39' 36" W	10.1	30
<b>MA120</b>	20° 57' 08" N	156° 39' 36" W	10.1	36
<b>MA150</b>	20° 57' 08" N	156° 39' 36" W	10.1	45
<b>MA190</b>	20° 57' 08" N	156° 39' 36" W	10.1	58
<b>MA210</b>	20° 57' 08" N	156° 39' 36" W	10.1	64
<b>MA240</b>	20° 57' 08" N	156° 39' 36" W	10.1	73
<b>MA270</b>	20° 57' 08" N	156° 39' 36" W	10.1	82
<b>MA320</b>	20° 57' 08" N	156° 39' 36" W	10.1	97
<b>MA330</b>	20° 57' 08" N	156° 39' 36" W	10.1	100
<b>MA390</b>	20° 57' 08" N	156° 39' 36" W	10.1	118
<b>MA410</b>	20° 57' 08" N	156° 39' 36" W	10.1	124
<b>MA460</b>	20° 57' 08" N	156° 39' 36" W	10.1	139
<b>MA490</b>	20° 57' 08" N	156° 39' 36" W	10.1	148
<b>MA520</b>	20° 57' 08" N	156° 39' 36" W	10.1	158
<b>MA560</b>	20° 57' 08" N	156° 39' 36" W	10.1	170
<b>MA600</b>	20° 57' 08" N	156° 39' 36" W	10.1	182
<b>MA650</b>	20° 57' 08" N	156° 39' 36" W	10.1	197
<b>MA670</b>	20° 57' 08" N	156° 39' 36" W	10.1	203
<b>MA800</b>	20° 57' 08" N	156° 39' 36" W	10.1	242
<b>MA840</b>	20° 57' 08" N	156° 39' 36" W	10.1	255
<b>MA865</b>	20° 57' 08" N	156° 39' 36" W	10.1	262
<b>MA895</b>	20° 57' 08" N	156° 39' 36" W	10.1	271
<b>MA910</b>	20° 57' 08" N	156° 39' 36" W	10.1	276
<b>MA945</b>	20° 57' 08" N	156° 39' 36" W	10.1	286
<b>MA965</b>	20° 57' 08" N	156° 39' 36" W	10.1	292
<b>MA970</b>	20° 57' 08" N	156° 39' 36" W	10.1	294
<b>MA1020</b>	20° 57' 08" N	156° 39' 36" W	10.1	309
<b>MA1135</b>	20° 57' 08" N	156° 39' 36" W	10.1	344

Table A.1, continued:

	Latitude	Longitude	Distance to caldera rim (km)	Depth in edifice (m)
<i>'Breadth' samples - shallow</i>				
LT18	20° 30' 17" N	156° 33' 09" W	3.9	surface
LT21	20° 30' 17" N	156° 33' 17" W	3.9	surface
LT22	20° 30' 16" N	156° 33' 18" W	3.8	surface
LT24	20° 30' 02" N	156° 33' 37" W	4.0	surface
LT27	20° 30' 00" N	156° 33' 48" W	3.9	surface
OL29 *	20° 50' 11" N	156° 35' 40" W	2.3	764
WA05	21° 00' 52" N	156° 34' 51" W	8.9	surface
WA13	20° 48' 48" N	156° 31' 10" W	5.7	91
WA14	20° 48' 53" N	156° 31' 42" W	4.8	212
WA16	20° 49' 03" N	156° 32' 06" W	3.8	255
WA17	20° 57' 41" N	156° 35' 12" W	2.6	339
WA19	20° 57' 58" N	156° 35' 27" W	3.2	345
<i>'Breadth' samples - deep</i>				
OL28	20° 50' 19" N	156° 35' 37" W	1.9	812
OL30	20° 50' 08" N	156° 35' 49" W	2.4	703
OL31	20° 50' 04" N	156° 35' 54" W	2.6	667
OL32	20° 50' 04" N	156° 35' 54" W	2.6	667
OL33A	20° 49' 56" N	156° 36' 00" W	2.6	582
OL34	20° 49' 57" N	156° 36' 02" W	2.6	582
WA09	20° 50' 04" N	156° 35' 55" W	2.6	667
WA10	20° 51' 19" N	156° 32' 18" W	3.0	667
WA12	20° 51' 19" N	156° 32' 31" W	2.6	782
WA18	20° 57' 21" N	156° 35' 12" W	2.1	436
WA21	20° 51' 15" N	156° 36' 44" W	2.3	533
WA22	20° 51' 24" N	156° 36' 14" W	1.4	702
<i>Transitional</i>				
WA03	21° 01' 15" N	156° 37' 38" W	10.6	surface
WA04	21° 01' 08" N	156° 36' 32" W	9.4	surface
WA06	20° 46' 36" N	156° 31' 47" W	7.2	surface

\* Sample OL29 is a columnar jointed flow with minimal lateral extent. We interpret it as a flow that has filled in a lava tube and is therefore younger than other flows at the same elevation. Based upon this observation and the isotopic composition of this sample, we have grouped it with the shallow samples.



## Appendix B

## MAUI NUI DATA SOURCES

Data presented in Chapter 3 come from the following sources:

**East Molokai**

Anders and Nelson [1996]

B. K. Nelson and J. Blichert-Toft, unpublished data

**West Maui**

Gaffney et al. [2003]

Gaffney et al. [2004]

**Lanai**

Budahn and Schmitt [1985]

West et al. [1987]

West et al. [1992]

Basu and Faggart Jr. [1996]

B. K. Nelson and J. Blichert-Toft, unpublished data

**Kahoolawe**

Fodor et al. [1987]

West et al. [1987]

Fodor et al. [1992]

Leeman et al. [1994]

Blichert-Toft et al. [1999]

**Haleakala**

Chen and Frey [1985]

West et al. [1987]

Chen et al. [1991]

Wagner et al. [1998]

Blichert-Toft et al. [1999]

## VITA

Amy Gaffney was born in Bellevue, WA. She earned her B.A. in Geology from Colorado College in 1996. In 1999, she received an M.S. in Geological Sciences from University of Washington. She was awarded a Ph.D. in Geological Sciences from the University of Washington in 2004.